1-1-2008

Development of modular and reconfigurable robot with multiple working modes

Xiaojia He
Ryerson University

DEVELOPMENT OF MODULAR AND RECONFIGURABLE ROBOT WITH MULTIPLE WORKING MODES

by

Xiaojia He
Master of Science in Mechanical Engineering
Xi'an Jiaotong University, China, May 1992

A THESIS
PRESENTED TO RYERSON UNIVERSITY
IN PARTIAL FULFILLMENT OF THE
REQUIREMENTS FOR THE DEGREE OF

MASTER OF APPLIED SCIENCE

IN THE PROGRAM OF

MECHANICAL EGINEERING

TORONTO, ONTARIO, CANADA, 2008

Author's Declaration

I hereby declare that I am the sole author of this thesis. I authorize Ryerson University to lend this thesis or dissertation to other institutions or individuals for the purpose of scholarly research.

Xiaojia He

I further authorize Ryerson University to reproduce this thesis by photocopying or by other means, in total or in part, at the request of other institutions or individuals for the purpose of scholarly research.

Xiaojiă He

Development of Modular and Reconfigurable Robot
with Multiple Working Modes

Masters of Applied Science
In the Program of
Mechanical Engineering
2008

Xiaojia He

School of Graduate Studies
Ryerson University

Abstract

A modular and reconfigurable robot (MRR) with multiple working modes for performing manipulation in uncontrolled environments is developed in this thesis. In the proposed MRR design, each joint module can independently work in active mode or passive mode. Major contributions of this thesis include the development of the passive mode with a unique friction compensation method and the use of force control in manipulation, such as door opening. In order to implement force control, the kinematics model and Jacobian matrix of the manipulator are derived by using the twist and wrench method, which is superior to the common D-H method, and the complete force analysis of the spherical wrist is presented as well. As a case study, the door opening process using force control is investigated by simulation and experiments. Door opening is successfully demonstrated using the developed MRR with multiple working modes.

Acknowledgements

The author would like to offer his sincere thanks to his advisor, Dr. G. Liu, who offered technical support throughout the entire process. Thanks are also offered to the Modular and Reconfigurable Robot (MRR) group at Ryerson, including Sajan Abdul and Jing Yuan for helping set up the experiment.

This research would not have been possible without the financial support from the Natural Sciences and Engineering Research Council (NSERC) of Canada and Engineering Services Inc. (ESI). The technical support staff of the Department of Aerospace Engineering, Mr. Peter Bradley, provided helpful technical assistance.

The author is also grateful to Dr. Yugang Liu for the helpful discussions.

Table of Contents

Author's Declaration.....ii
Abstract.....iii
Acknowledgements.....iv
Table of Contents.....v
List of Figures.....vii
List of Tables.....ix
Nomenclature.....x
Chapter1 Introduction.....1
1.1 Manipulation in Uncontrolled Environments.....1
1.2 MRR Manipulator and Multiple Working Modes.....2
1.3 Thesis Objectives and Contributions.....4
1.3.1 Problem Statement.....4
1.3.2 Multiple Working Modes.....5
1.3.3 Force Controlled Dexterous Manipulation.....5
1.3.4 Spherical Wrist Design and Force Analysis.....6
1.3.5 Door Opening Case Study and Experiment.....6
1.4 Thesis Layout.....7
Chapter 2 Modular Joint and Multiple Working Modes.....9
2.1 Design of the MRR Modules.....9
2.1.1 MRR Joint Modules.....9
2.1.2 Control System Architecture of MRR.....13
2.2 Passive Working Mode.....14
2.2.1 Friction Model and Compensation.....14
2.2.2 Experimental Validation.....17
2.3 Working Modes Switch.....18
Chapter 3 Manipulator Modeling, Analysis and Design.....19
3.1 Mobile Manipulator.....19
3.2 Manipulator Kinematics.....21
3.2.1 Wrenches and Screw Coordinates.....21

3.2.2 Forward Kinematics....24
3.3 Jacobian Matrix.... 34
3.3.1 Velocity and Jacobian Matrix.... 34
3.3.2 Jacobian Matrix.... 36
Chapter 4 Anthropomorphic Wrist Design and Analysis....43
4.1 Mechanism Structure and Motion Analysis....43
4.2 DAUJ Wrist Position Analysis....47
4.3 DAUJ Wrist Force Analysis and Torque Relationship....51
Chapter 5 Robot Manipulation and Door Opening Case Study 55
5.1 Door Opening Task Study 55
5.1.1 Literature Review and Research Status....55
5.1.2 Door Opening Requirement and Process Analysis.... 59
5.2 Passive Mode Control and Force Control.... 60
5.3 6 DOF Manipulator Door Opening Process 63
5.3.1 Process Analysis and Force Control....63
5.3.2 Door Opening Simulation 65
5.4 Gravity Compensation and Initial Position Effects 69
5.4.1 Gravity Compensation 69
5.4.2 Initial Position Effects....70
Chapter 6 Dexterous Manipulation Experiment....77
6.1 Experimental Set up....77
6.1.1 Experiment Set up and Software Platform 77
6.1.2 Experimental Control System 78
6.1.3 Sensors and Power system 78
6.2 Position Control Manipulation.... 79
6.3 Friction Compensation and Passive Joint Experiment 81
6.4 Door Open Experiment.... 82
Chapter 7 Conclusions and future work.... 84
Appendix....87
Reference....98

List of Figures

Figure 2-1: Schematic diagram of an MRR module.....9
Figure 2-2: Hardware architecture of an MRR module 10
Figure 2-3: Control system architecture of an MRR module.....10
Figure 2-4: One MRR module.....11
Figure 2-5: Two MRR modules.....12
Figure 2-6: MRR arm with three modules.....12
Figure 2-7: Control system architecture of MRR.....13
Figure 2-8: Plots of two friction models.....15
Figure 2-9: Constant part of friction 16
Figure 2-10: Friction after compensation of the constant part.....17

Figure 3-1: Developed Modular Elbow Manipulator..... 20
Figure 3-2: LMA Mobile Robot (ESI, Canada).....20
Figure 3-3: With an industrial arm.....21
Figure 3-4: Special designed arm..... 21
Figure 3-5: Elbow manipulator with spherical wrist.....25

Figure 4-1: Swiveling of index finger and anthropomorphic motion.....43
Figure 4-2: 3D view of DAUJ Joint with Pitch and Yaw motions.....44
Figure 4-3: Structure of DAUJ Joint Assembly.....44
Figure 4-4: Anthropomorphic Joint with link.....45
Figure 4-5: Kinematic diagram.....45
Figure 4-6: Workspace of DAUJ.....46
Figure 4-7: Kinematic parameters and frame assignments.....48
Figure 4-8: Generalized coordinate frame assignment for DAUJ.....50
Figure 4-9: Assembled DAUJ Wrist 54

Figure 5-1: Service robot HomBot for door opening (2004).....58

Figure 5-2: A planar model of door opening.....61
Figure 5-3: Door opening procedure with two passive joints and one active joint.....62
Figure 5-4: Door opening process and coordinate relation.....63
Figure 5-5: Simulation for door opening process (T1=0).....66
Figure 5-6: X-Z Projected Vision (T1=0).....67
Figure 5-7: X-Y Projected Vision (T1=0).....67
Figure 5-8: Joint angles in door opening process (T1=0).....68
Figure 5-9: Torque output of each joint without gravity compensation (T1=0).....68
Figure 5-10: Gravity compensation for the elbow manipulator.....69
Figure 5-11: Torque output of each joint with gravity compensation (T1=0).....70
Figure 5-12: Different initial condition and its effect in door opening (T1=+30).....71
Figure 5-13: X-Z Projected Vision (T1=+30).....72
Figure 5-14: X-Y Projected Vision (T1=+30).....72
Figure 5-15: Joint angles in door opening process (T1=+30).....73
Figure 5-16: Torque output of each joint in door opening process (T1=+30).....73
Figure 5-17: Different initial condition and its effect in door opening (T1=-30).....74
Figure 5-18: X-Z Projected Vision (T1=-30).....74
Figure 5-19: X-Y Projected Vision (T1=-30).....75
Figure 5-20: Joint angles in door opening process (T1=-30).....75
Figure 5-21: Torque output of each joint in door opening process (T1=-30).....76

Figure 6-1: MRR2 module manipulator with spherical wrist.....77
Figure 6-2: Experimental System 78
Figure 6-3: The joint angle position in a three DOF motion control.....79
Figure 6-4: Three MRR motion control demonstration.....80
Figure 6-5: Torque sensor output in passive joint experiment.....81
Figure 6-6: Door opening experiment with multiple working modes.....83

List of Tables

Table 2-1: External Torque for MRR Joint in Passive Mode.....17

Table 6-1: External Torque for MRR Joint in Passive Mode with friction model.....81

Nomenclature

Roman

Ad_g - Adjoint transformation

b - Viscous friction coefficient

f_c - Coulomb friction

f_s - Static friction coefficient

f_τ - Stribeck friction coefficient

f - The vector of force acting on the end-effector

F – Friction

G - The gravity

G_e - The equivalent gravity

J_i - The *i-th* joint in the wrist

J_d - The moment of inertia of the door

J^T - The transpose of Jacobian matrix of the manipulator

J_{st}^{s} - Spatial Jacobian Matrix

L_i - The *i-th* link in the wrist

M_i - The *i-th* motor in the wrist

M_f - The minimum moment caused by friction

$\dot{q}$ - The relative velocity of the contact surfaces

r - The radius of the door between the pivot and the knob

v - Velocity

V^s - Spatial velocity

V^b - Body velocity

Greek

α - Longitudinal angles

β - Latitudinal angles

δ - Pitch angle

φ - Universal joint axis angle

γ - Yaw angle

θ_d - The rotated angle of the door

θ_i - Joint angle

θ - Rotation angle

τ_1 - The 1st motor torque

τ_3 - The 3rd motor torque

τ_δ - The outer universal link torque along pitch rotation

τ_γ - The outer universal link torque along yaw rotation

τ - The vector of joint torques of the manipulator

υ - Pure translation

$\hat{\omega}$ - Pure rotation

$\hat{\xi}$ - Twist Coordinates

Chapter 1

Introduction

The purpose of this chapter is to provide background information, and to introduce some underlying materials pertinent to the subject of the thesis. Furthermore, it presents the objective and contributions of the thesis work. At the end of this chapter, an organization outline for the remainder of the thesis is presented.

1.1 Manipulation in Uncontrolled Environments

Robots are growing out of industrial plants into businesses, homes, fields and space, performing versatile tasks for service, security, rescue and space exploration, among other areas of application. A mobile manipulator has many advantages over a fixed base manipulator in terms of either larger workspace or more dexterous manipulation capability. Such robots are required to have the abilities to carry out manipulations in uncontrolled environments, similar to humans, such as opening a door or even cooperating tasks with human beings.

To date, robots have been very successful at manipulation in controlled environments such as factories. Outside of controlled environments, robots still have difficulty to perform sophisticated manipulation tasks. In the mobile manipulator literature, attempts have been made to integrate traditional robot manipulators with mobile platforms. However, traditional robot manipulators are position controlled, with a fixed configuration and joints working in a single active mode. These characteristics of traditional robots substantially limit the application of mobile manipulators. Within controlled environments, the world can be adapted to the capabilities of the robot [1]. In uncontrolled environments, the robot has to adapt to the world consisting of only partially known or unknown objects and tasks, and real-time constraints.

Up till now, there are still many challenges to develop robots for working in uncontrolled environments or human environments [1]. A typical example is that opening a door is still a difficult task for mobile manipulators. To open a general door, an active mode is necessary for a

robot manipulator to approach the door knob. After the gripper gets hold of the knob, if only the active mode and position control were used, it would be very difficult for regular robot manipulator to finish this task. The reason is that the robot needs to know the radius distance from the door knob to the pivot and precisely trace the space curve (circular); if the position error is greater than a certain value, the internal force of the manipulator could break the joint or link. In the published papers, online estimation of the radius is needed. To prevent damage of the robot joints, a force compliance control or a Remote Center Compliance (RCC) device must be employed. All of the above make the robot control system complicated and difficult to use in practice. A more detailed literature review in this area will be provided in Chapter 5 of this thesis.

When carefully examining the human beings' behaviour and actions during the door opening process, one can see that the human hand follows the trace of the door knob. People can close their eyes and pull the door open. That means no vision guided position feedback is required, and the human being joint control is not position control. The joint control could be force control; sometimes the joint is in the passive mode. It is desirable for the manipulator to have the passive mode to follow the unknown door knob trajectory. In the active mode, on-line switching between position control and force control will be helpful during the door opening process. The development of Modular and Reconfigurable Robot (MRR) with multiple working modes is aimed to tackle such challenges in uncontrolled environments or human environments. The newly developed modular robot is expected to operate on a mobile platform to work in a large working area.

1.2 MRR Manipulator and Multiple Working Modes

Modular and Reconfigurable Robot aims to provide a solution in situations where the configuration and/or task changes. MRR manipulators are composed of similar/identical modules that can be assembled in various configurations to form a new system, enabling new functionalities. For MRR manipulators, the modules can be divided into two general types: joint modules and link modules. The previous one includes rotary joints, prismatic joints, multiple DOF joints and gripper module, while the latter has links with fixed dimension and flexible dimension. By using several modules and links, users can reconfigure MRR into PUMA, SCARA, STANDFORD manipulators or any other structures to perform welding, assembling, or

grinding tasks, etc. A modular and reconfigurable mobile robot can change its shape from a snake-like robot into caterpillar, 4-legged spider robot or a loop robot and thus surpass obstacles. Through the practice in last two decades, MRR shows the promise of great versatility, flexibility, simplicity and robustness, and keeping itself active in research and market as well.

Nowadays, the research subjects for the MRR are mainly about the following issues:

1. Compact modular mechanical design and mechatronics integration to achieve high power density
2. Configuration-independent kinematics and dynamics analysis methodology
3. Optimal configuration computation method based on given tasks
4. Control scheme that can adapt to robot configuration

The above issues have been studied at the System and Control Lab at Ryerson University for several years [2] [3] [4]. To meet the requirement of modularity and re-configurability, a distributed architecture is more suitable for MRR. In reference [2], the control system architecture of MRR manipulator was developed. In reference [3], the distributed control of MRR with torque sensing was investigated. Also in reference [4], genetic algorithm was used in the control algorithm study to estimate the parameters. All the experiments above have been done on a self-made MRR electro-mechanical joint.

In order to adapt various tasks, sometimes the robot joint should be in a passive mode. In the published relevant literature, passive joints are used in the cooperation control of multiple manipulators [5]~[7]. In reference [6], the motion planning and control of mobile manipulators are greatly simplified with using the exchangeable active/passive joints; the positioning error of the mobile manipulator can be absorbed passively and detected as the angular information of the passive joints. Relatively complex tasks are executed without the use of external sensors such as vision or a wrist force sensor.

Robot arms with passive impedance based on mechanical compliance have been investigated by many researchers. Design of robot joints with programmable passive impedance using antagonistic nonlinear springs and binary dampers was studied in reference [8]. Passive impedance control using viscoelastic material and a passive trunk mechanism was developed in reference [9]. A mechanical impedance adjuster was reported in reference [10] and [11], where a variable spring and damper adjusted by an electromagnetic brake were used for the passive compliant joint.

A recent hybrid joint was developed in references [5], [12] and [13], which introduces an electromagnetic clutch between the motor and the output shaft. The hybrid joint has passive and active working modes. When the clutches are released, the joints are free and passively controlled by the coupling forces of the manipulator. The joint is capable of compliantly adapting to external force and motion by switching between the active and passive modes, depending on the requirement of a given task. The hybrid joint needs a recovering algorithm to resume the joint position.

All of the hybrid active/passive joints or passive mechanisms mentioned above have to be specially designed, which leads to extra weight and volume due to the additional components. In some cases, passive joints can help reduce power consumption, increase flexibility, and improve safety. It is desirable to be able to switch a normal robot joint to a passive operation mode without changing the existing joint mechanism or electronics system. This thesis will focus on the topic of developing joint with multiple working modes, which includes both normal active mode and passive mode. In the later door opening case study, the passive mode will play an important role.

1.3 Thesis Objectives and Contributions

1.3.1 Problem Statement

In the mobile manipulator literature, attempts have been made to integrate traditional robot manipulators with mobile platforms. However, traditional robot manipulators are position controlled, with a fixed configuration and joints working in a single active mode. To tackle the challenges for robot manipulation in human environments or uncontrolled environments, the manipulator must have multiple working modes for different working requirements. In order to perform various tasks, a robot joint should be able to work in both active and passive working modes.

In the active mode, the joint could be in position control or force control. When the manipulator interacts with environments, force control should be employed. In the passive mode, the joint becomes free with no torque. Some other working modes could be more suitable for certain specific applications. In contrast, traditional robots still work in the active mode and keep consuming electrical energy.

The goal of this research work is to develop an MRR joint with multiple working modes in order to achieve the manipulation tasks in uncontrolled environments. A friction compensation passive working mode is proposed and implemented. In the active working mode, force control instead of position control is investigated and used in the case study of door opening task as an example. A compact spherical wrist is designed in this thesis for final dextrous manipulation experiment in uncontrolled environments.

1.3.2 Contribution I: Multiple Working Modes

First and foremost, it is desired to develop MRR manipulators with multiple working modes. The working modes should include both active and passive modes. A new MRR modular joint with passive working modes has been implemented and reported in this thesis.

With the electronics embedded in the link modules, the MRR joint modules are compact. The active and passive working modes have been implemented under a federated control system architecture, which enables distributed module control with multiple working modes and centralized supervisory control. A unique feature of the developed MRR robot joint is the implementation of both active and passive working modes on the same MRR module.

The research works include: (A) a simple and effective method to execute the switch between active and passive modes is proposed. The method is easy to apply in practice without altering the original mechanical structure of the joint. The proposed method involves joint friction compensation based on the motion trend of the joint. (B) The MRR joints have been successfully assembled, tested and used to perform multiple working modes and a door opening experiment.

1.3.3 Contribution II: Force Controlled Dexterous Manipulation

In the developed MRR, there are torque sensors installed in joints to meet the force feedback control. The contribution of this thesis is to study the force control methodology using the developed MRR manipulator. Unlike a traditional industrial robot, which has a fixed configuration arm and its joints in a position control active mode, the 6 DOF manipulator with force control active mode is modeled, designed, and analyzed in this thesis.

The modeling of the MRR manipulator is a key task to implement a force control. The MRR manipulator consists of one waist joint, two elbow joints and one spherical wrist. The modeling of the MRR manipulator consists of the forward kinematics analysis, inverse kinematics analysis

and Jacobian matrix. The Denavit-Hartenberg (D-H) method is widely used for modeling a traditional industrial manipulator. If the D-H method is used to get the Jacobian matrix, it is tedious and complicated. In addition, when the number of robot's DOF is greater than five, it becomes difficult to obtain a Jacobian matrix. In this thesis, the twist & wrench method is used instead. The two significant advantages of this new method are: avoidance of sophisticated differential calculation; the correctness of the result can be easily checked for use. This thesis provides the kinematics model and Jacobian matrix of the 6DOF MRR manipulator for the final force control.

1.3.4 Contribution III: Spherical Wrist Design and Force Analysis

In order to build a complete manipulator, an anthropomorphic wrist is designed for this project. The Double Active Universal Joint (DAUJ) anthropomorphic wrist is the one of the most compact spherical wrists [14] which is very suitable for a mobile manipulator. The spherical wrist can rotate in two directions: pitch and yaw. The output link is prepared for the future roll movement.

The wrist design work in this thesis includes: (A) search of papers and patents; (B) definition of the specifications; (C) concept design and SolidWorks COSMOSmotion simulation; (D) position control algorithm simulation; (E) final assembly and test.

In order to use the wrist in force control or friction compensation, a complete force analysis is presented in this thesis. The force relationship between the torques of the pitch and yaw and the torques of the applied two motors is also provided for practical use. All above analysis have been used for the final force control.

1.3.5 Contribution IV: Door Opening Case Study and Experiment

Door opening is a typical manipulation task in the uncontrolled environment. Up to now, opening a door is still a difficult task for robots [1], [15], [16]. To open a door, a position control in the active mode is necessary for approaching the door knob. After the gripper holds on the door knob, a force control should be applied. Different from using traditional position control, the robot does not need to know the radius of the door, or use online estimation, or use compliance control and RCC device. The force control manipulation for opening a door is analyzed and simulated. The simulations combine the inverse kinematics analysis of the manipulator and the door's position analysis. The final torque of each joint is provided. The

gravity compensation and initial position of the mobile platform are considered and discussed in the simulation.

Using the passive mode is a unique method to open a door. In the final door opening experiment, the manipulator can open the doors with different radii. During a space door opening process demonstration, only one elbow MRR joint is in the active mode and controlled. Another MRR joint and the spherical wrist are in the passive mode, and the MRR joint in the passive mode is implemented by the friction compensation method. The developed MRR joints with multiple working modes successfully finished the door opening task in a 3D space uncontrolled environment.

1.4 Thesis Layout

This thesis is organized in the following manner. Detailed literature reviews are given in every chapter for different issues. Chapter 2 focuses on the topic of modular joint and multiple working modes. It includes two sections: design of MRR module and passive working mode. In the first section, the mechanical and electronics design of the developed joint module is shown; the hybrid control system architecture is presented. In the second section, passive working mode control is proposed. The friction model and compensation method are analyzed. The friction compensation experiment for a passive joint has been done for validation. Chapter 3 deals with the manipulator modeling and analysis. A manipulator with spherical wrist is presented. The wrenches and screw coordinates method is used for analyzing the kinematics and Jacobian matrix instead of the normal D-H method. The sophisticated differential calculation of the manipulator is avoided and all results are correctly checked. These results will be used in the later proposed force control for door opening. Chapter 4 provides the anthropomorphic wrist design and analysis. A DUAJ joint is described and designed is the first section. The position analysis is given in the 2nd section. The force analysis is provided in the 3rd section, and a useful force relationship between the two motor torques and the outer universal link torques is presented. Chapter 5 details the door opening case and the dexterous manipulation analysis and simulation. The first section includes door opening literature review and the door opening requirement. The 2nd section describes the former designed passive joint and force control method. The 3rd presents the whole door opening process simulation, which combines the contents provided in former chapters. The 4th section considers the effects of the initial position

and the gravity compensation. The simulations demonstrate not only the feasibility of the control method, but also a roadmap for the experiments. Chapter 6 presents the final experimental setup, MRR manipulator position control experiment, passive mode joint implementation through the friction compensation method, door opening experiments for adapting different radii and door opening demonstration in 3D space. Final conclusions and proposed future research are provided in Chapter 7.

Chapter 2

Modular Joint and Multiple Working Modes

2.1 Design of the MRR Modules

2.1.1 Joint Modules

The MRR robot joint has been studied at Ryerson University for several years. A schematic diagram of the developed MRR joint module is shown in Figure 2-1 [3]. The joint consists of a brushless DC motor and driver, a harmonic drive with an integrated torque sensor and amplifier, an encoder, a brake, and homing and limit sensors [2]. The hardware architecture is shown in Figure 2-2 [2].

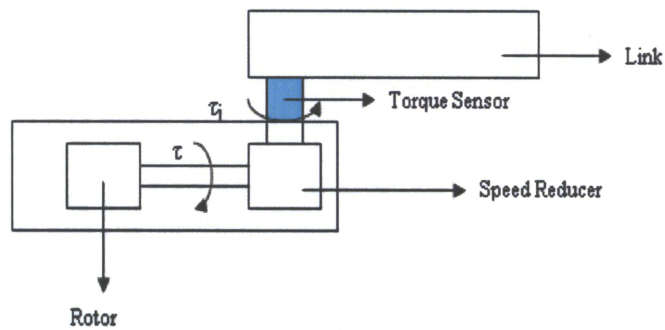

Figure 2-1: Schematic diagram of an MRR module

By using a DSP controller, the hardware architecture supports multiple control modes of the joint module such as the torque control mode and position control mode, which is illustrated in Figure 2-3 [2].

There are several layers in this architecture. The first layer, communication layer, is realized by the CAN Bus and its protocol. The decision layer is a command interpreter which decodes the commands according to the communication protocol and then determines the working mode and

task to perform, such as homing, position control, and torque control. The action layer includes various tasks such as calibrating, homing, and determining limits.

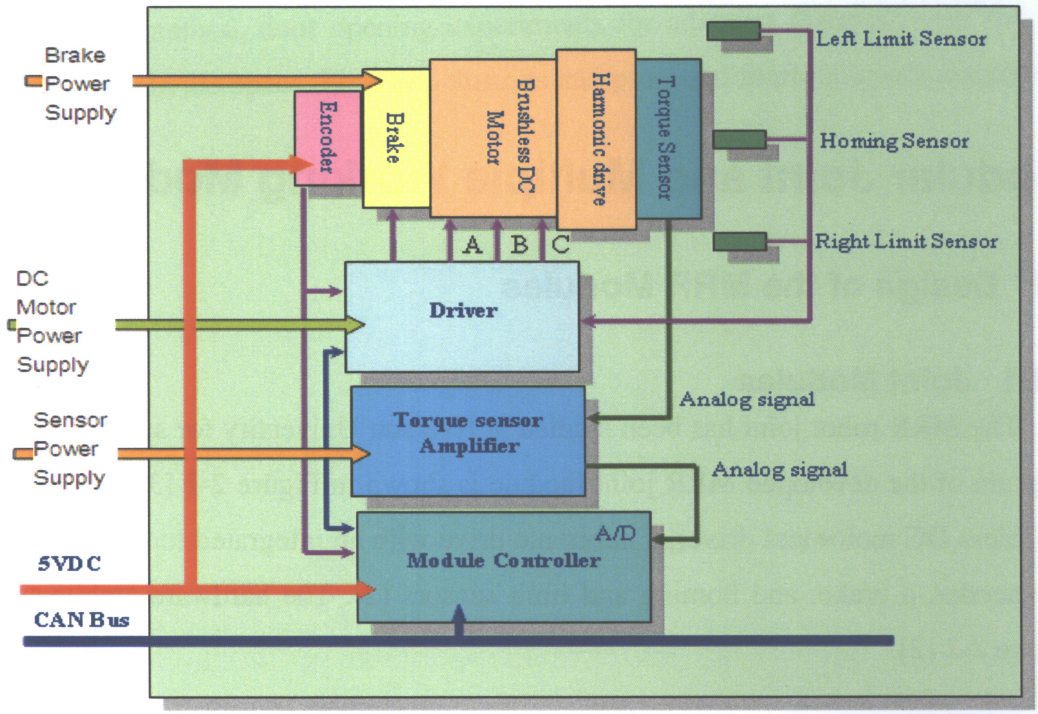

Figure 2-2: Hardware architecture of an MRR module

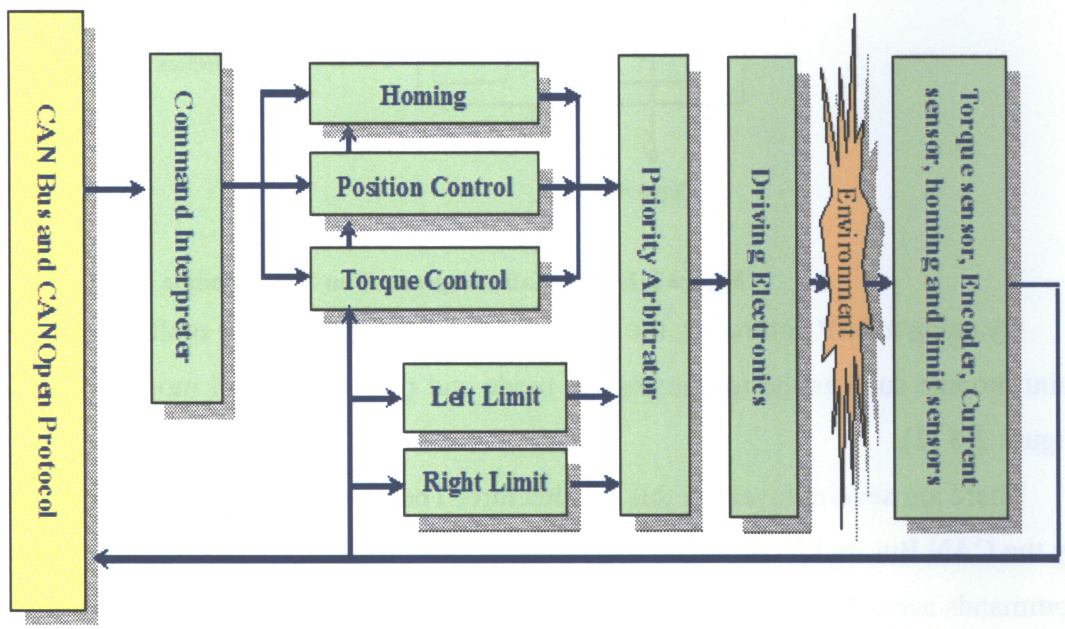

Figure 2-3: Control system architecture of an MRR module

In the motor drive, the homing and limiting procedures are the pre-programmed sub-routines and have pre-set priorities, and what the users need to do is to activate these functions. The drive electronics in the execution layer outputs power signals (PWM) to drive the motor. The sensing layer includes torque sensor, encoder, current sensor, homing and limit sensors and their amplifiers or signal conditioning circuits. These sensors provide feedback to the module controller, and also to the supervisor controller through the communication layer for on-line planning.

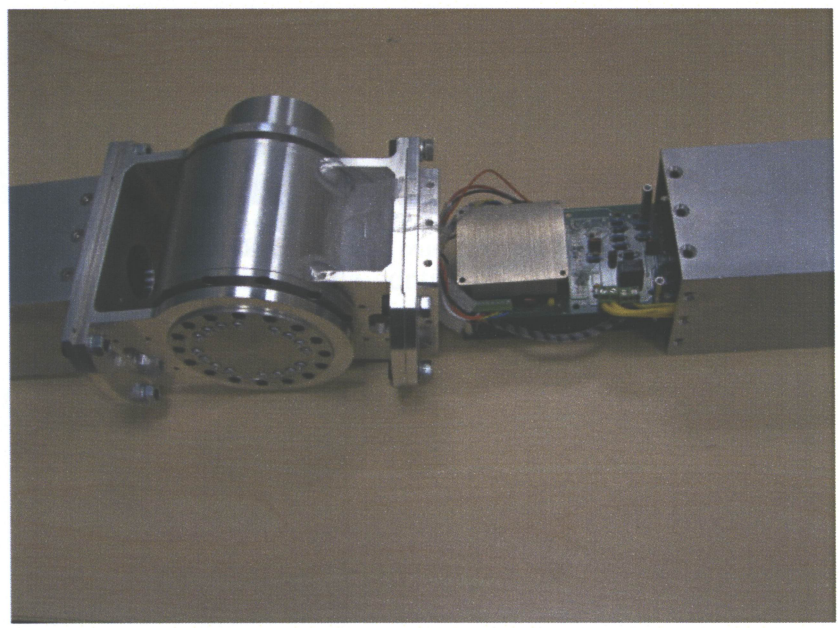

Figure 2-4: One MRR module

Two types of joint modules have been developed recently at Ryerson University group using the TMS320F2812 DSP controller, and they are shown in Figure 2-4 and Figure 2-5. Two compact modules are assembled with electronics and cables embedded in the tube link. All can be reconfigured at the interface between the joint and its link.

Another type module has been developed as well, which has two interfaces with power and communication connectors for connecting the base support to reconfiguration. An elbow arm assembled with three module configuration is shown in Figure 2-6.

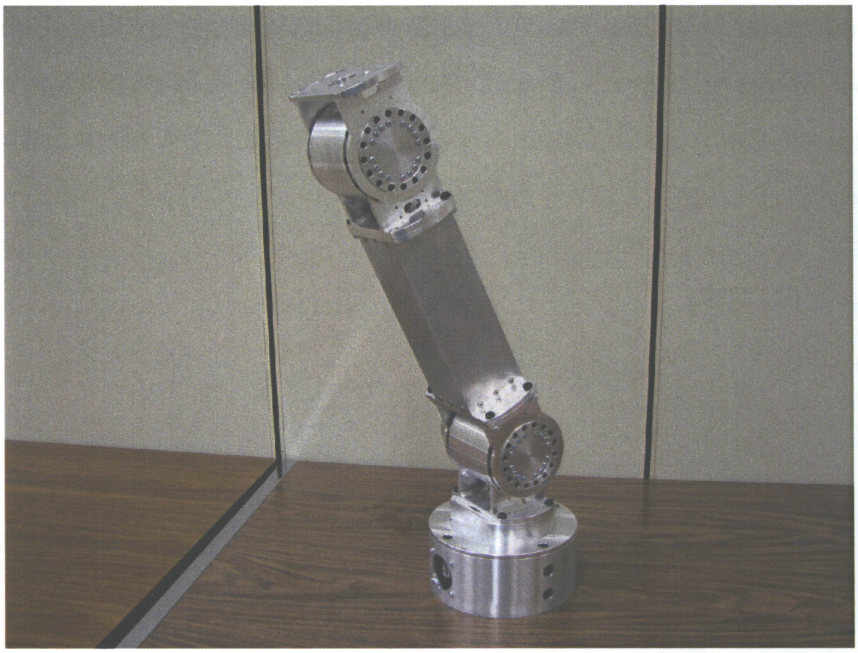

Figure 2-5: Two MRR modules

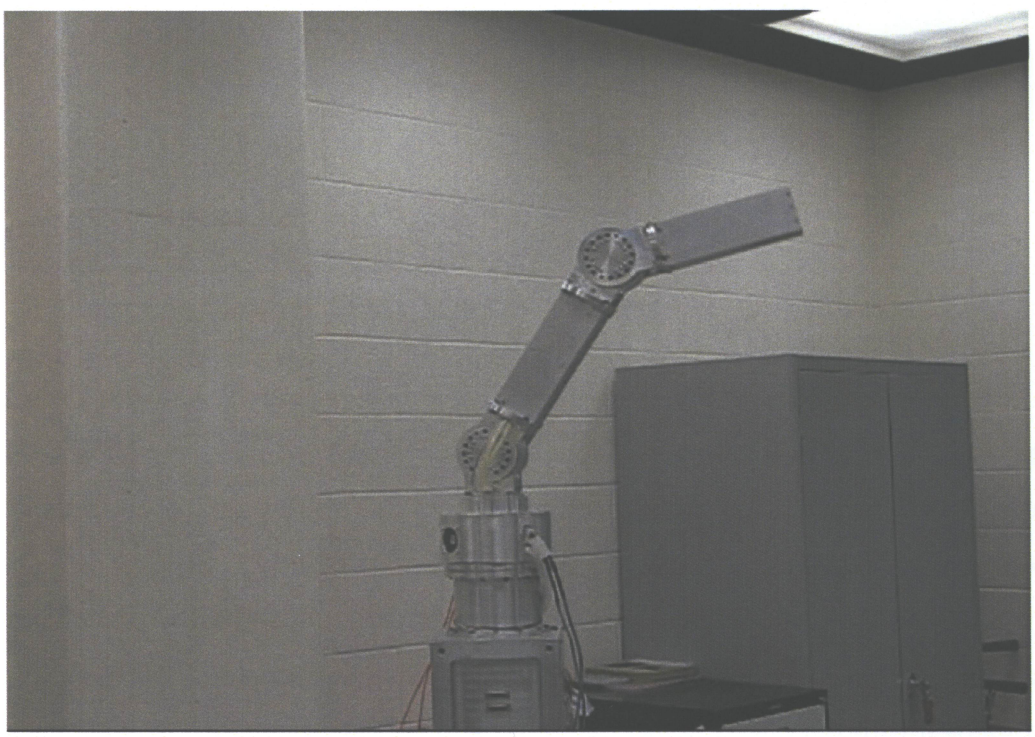

Figure 2-6: MRR arm with three modules

2.1.2 Control System Architecture of MRR

The overall MRR control system architecture is shown in Figure 2-7. The architecture is the overall organization of the MRR control system, specifically the inter-relatedness of components within the system. It determines the execution sequence of the individual components and defines the flow of information among them. Traditional robot control system architectures are centralized, usually with a single processor managing all the computations and controls all robot components. One major merit of a centralized control system is that it is easier to achieve a global optimal solution for some tasks than other architectures, such as coordinated control and global trajectory planning. However, for a modular and re-configurable robot, the module control tasks, including module's position control, torque/force control, friction compensation, homing, limit detection and control, should be distributed to the module in order to achieve modularity and satisfy the self-contained requirement [3]. However, not all of the tasks of an MRR manipulator can be distributed to the module controller, and centralized processing is essential for tasks such as on-line trajectory planning, task space control, and coordinating control of multiple modular joints. The working mode of each module is determined by the supervisory controller as required to carry out particular tasks, which is transmitted through the CAN bus and interpreted by the command interpreter at each module. The proposed federated architecture shown in Figure 2-7 has been developed to serve all the purposes [2].

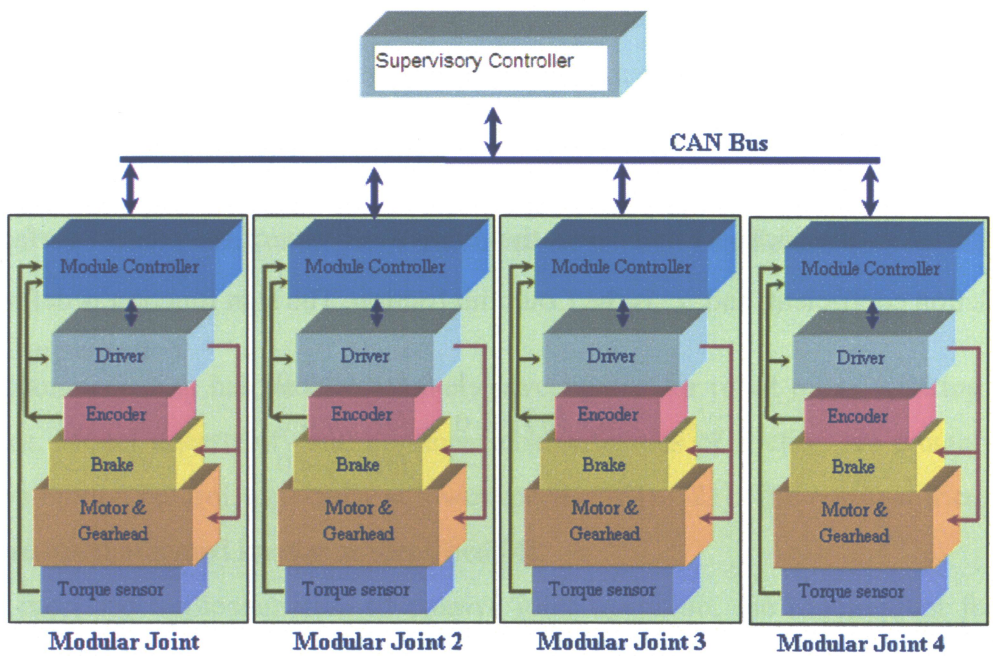

Figure 2-7: Control system architecture of MRR

2.2 Passive Working Mode

In this section, a proposed method to implement passive mode control of an MRR joint with friction compensation is presented. In friction compensation, the friction model or the motion trend of the joint should be known. Normally, the motion trend of a robot joint is known or predictable. For instance, when a mobile manipulator is to open a door, the direction of the door's movement is known, and the motion trend of the robot can be predicted. Based on the motion trend of each passive joint, a feed forward torque is applied to compensate the friction at the joint, which is the key to implement passive operation mode of the joint without introducing extra mechanisms. If the friction is compensated, the output shaft of the joint can be moved freely and work in a passive mode. The proposed method does not need a clutch to separate the output shaft from the motor and gear. Also, as the actuation chain is never disconnected, the joint can be switched back to an active working mode any time at any position without the need to recover from a disconnection.

2.2.1 Friction Model and Compensation

In the friction modeling and compensation literature, there have been many friction models reported [17]. The following two models are well known simple friction models. The curves in Figure2-8 show the two friction models graphically.

1) Coulomb and Viscous Model

A Coulomb and viscous model can be expressed as:

$$F(\dot{q}) = \left[f_c \operatorname{sgn}(\dot{q}) + b\dot{q} \right] \tag{2-1}$$

where F is the friction force, $\dot{q}$ is the relative velocity of the contact surfaces, b is the viscous friction coefficient, and f_C is the Coulomb friction. The sign function is defined as:

$$\operatorname{sgn}(\dot{q}) = \begin{cases} 1 & for \quad \dot{q} > 0 \\ 0 & for \quad \dot{q} = 0 \\ -1 & for \quad \dot{q} < 0 \end{cases} \tag{2-2}$$

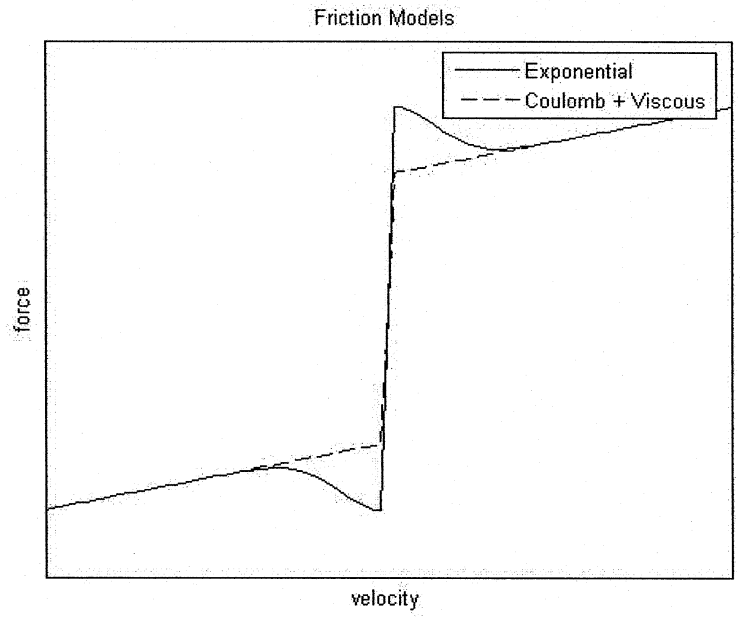

Figure 2-8: Plots of two friction models

2) Static and Stribeck Model

The model in Equation (2-1) does not accurately reflect what takes place at low speeds in real systems. It is known that when two objects are in contact, it takes an initial force to push them apart. This force is often referred to as the break away force and the phenomenon is described as static friction or "stiction". What follows is a nonlinear region between the break away force and the viscous friction. This region is referred to as the Stribeck region. The following model describes this behaviour:

$$F(\dot{q}) = \left[f_c + (f_s - f_c) e^{-\left|\frac{\dot{q}}{f_\tau}\right|^{\delta}} \right] \mathrm{sgn}(\dot{q}) + b\dot{q} \qquad (2\text{-}3)$$

where f_τ and f_s are the Stribeck coefficient and the static friction coefficient, respectively [17].

3) Friction Compensation

Friction compensation has been extensively investigated for robot joints working in active control modes. Model uncertainty and nonlinear characteristics of friction are crucial issues in high precision motion control, especially at lower speeds [18] ~ [21]. The nominal friction model parameters are often assumed known or identified [4].

For the proposed implementation of passive joint operation, the requirement for friction compensation is fundamentally different from that for precise tracking control. In order for the

joint to work in a passive mode, the joint friction only needs to be compensated such that the external torque can rotate the joint. In other words, the uncompensated friction should be much smaller compared to the magnitude of the external torque.

As shown in Figure2-9, friction can be separated into two parts: a constant part and a variable part, and the magnitude of the constant friction part often dominate the overall magnitude of the total friction at lower speeds. The constant part of friction, *fm,* is less than the static friction f_s and has the same sign as f_s. The sign is determined by the trend of the relative movement. In many situations, the trend can be predicted by kinematics analysis or measured by a toque sensor. For example, when a manipulator is used to open a door, after the gripper holds the door knob, the moving direction of the door is known, and the trend of motion of the robot joints can be predicted.

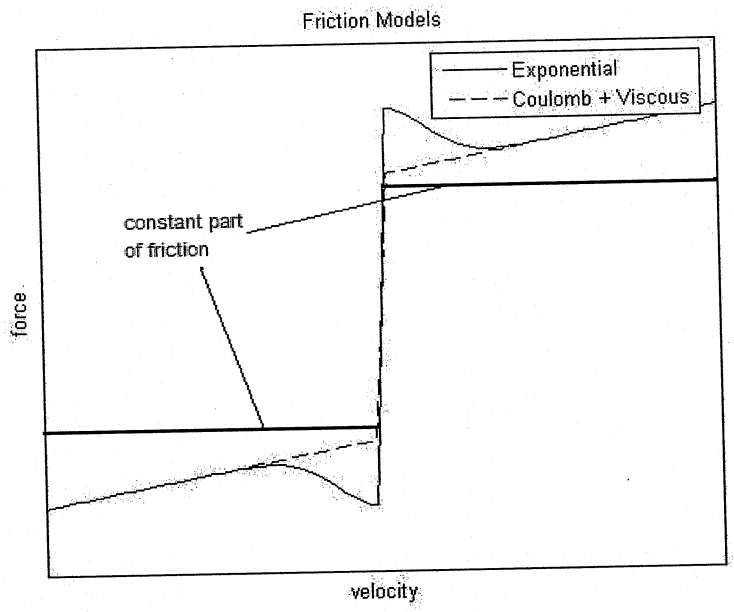

Figure 2-9: Constant part of friction

After compensating the constant part, the friction models (1) and (3) become

$$\begin{aligned}\Delta F(\dot{q}) &= F(\dot{q}) - f_m \operatorname{sgn}(\dot{q}) \\ &= (f_c - f_m)\operatorname{sgn}(\dot{q}) + b\dot{q}\end{aligned} \tag{2-4}$$

and

$$\begin{aligned}\Delta F(\dot{q}) &= F(\dot{q}) - f_m \operatorname{sgn}(\dot{q}) \\ &= \left[(f_c - f_m) + (f_s - f_c)e^{-\left|\frac{\dot{q}}{f_\tau}\right|^\delta}\right]\operatorname{sgn}(\dot{q}) + b\dot{q}\end{aligned} \tag{2-5}$$

respectively, and are shown in Figure 2-10.

The compensation of the constant friction part is achieved by setting the module to torque control mode and sending a constant current command to the motor drive based on the motion trend of the joint.

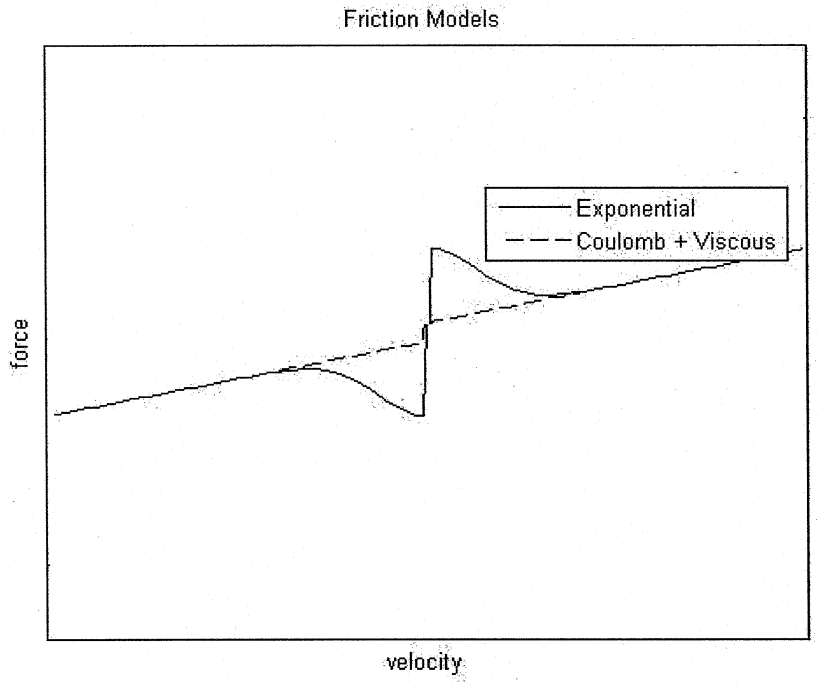

Figure 2-10: Friction after compensation of the constant part

2.2.2 Experimental Validation

The idea for implementing passive working mode with friction compensation has been tested experimentally using the base module shown in Figure 2-6. For the larger MMR joint (the maximum output torque is 150 Nm), the compensation currents are: -1.5 A for the positive direction and +1.2 A for the negative direction. With and without friction compensation, the external torques required to rotate the MRR joint in the passive mode in two different directions are measured and given in Table 2-1.

Table 2-1: External Torque for MRR Joint in Passive Mode

Rotate Direction	**Positive** (0~360 deg)	**Negative** (0 ~ -360 deg)
Torque without compensation(a)	36.3 Nm	36.2 Nm
Torque with compensation(b)	7.6 Nm	5.7 Nm
Ratio (b/a)	21 %	16 %

From Table 2-1, with the simple friction compensation, the required external torque to rotate the joint has been greatly reduced, by 79% in the positive direction and 84% in the negative direction. Such results have been adequate for many applications. Friction compensation using a more complete friction model or the torque sensor feedback can reduce the friction further if necessary.

In Chapter 6, the final experiments used the friction model based method proposed by Liu et al. in reference [20] [21], which successfully reduced the friction by 85% and are convenient to use in practice.

2.3 Working Modes Switch

The working mode switch can be used for various tasks and the posture adjustment. The following procedure gives an example for door opening.

(1) Mode switch for position control and force control: when the mobile manipulator is close to the door knob, each joint is in active mode, and the control system could be a visual guided position control system. The position and orientation of the gripper can be measured. After the gripper holds the knob, one or more MRR joint will be switched to passive mode, and the control system becomes force control. The door is pulled open, while the vision system does not work.

(2) Mode switch for the posture adjustment: (I) First, it is to set the wrist joint angle. For example, set the 3rd joint and the 2nd joint in Figure 2-6 in passive mode and set the 1st joint in active mode; change the mobile platform's position to modify the wrist angle. Or another method is to lock the 1st and 2nd angles, then move the platform position around the passive wrist center. (II) Second, it is about how to set the 2nd angle: lock the settled 3rd angle, and set the elbow and shoulder in passive mode; move the platform position until the 2nd angle is obtained. Or another method is to lock the 1st angle, and move the platform position around the passive elbow center. (III) Third, it is to set 1st angle: lock the settled 2nd and 3rd joints, and set the 1st joint in passive mode; move the platform position around the passive shoulder center. In summary, the setting order is from 3rd, 2nd to 1st joint. From the viewpoint of kinematics, this order reduces the effects of coupling. For example, if the 1st joint is settled, it would affect the 2nd and the 3rd. The above procedure also demonstrates the important role of the joint passive mode, which greatly improves the flexibility of the MRR manipulator.

Chapter 3

Manipulator Modeling, Analysis and Design

3.1 Mobile Manipulator

A mobile manipulator has many advantages over a fixed base manipulator either in larger workspace or in more dexterous manipulation capability. Such robots are required to have the abilities to carry out manipulations in uncontrolled environments, similarly as human beings open a door or finish the cooperative tasks. In the mobile manipulator literature, attempts have been made to integrate traditional robot manipulators with mobile platforms. In the mobile manipulator literature, attempts have been made to integrate traditional robot manipulators with mobile platforms. However, traditional robot manipulators are position controlled, with a fixed configuration and joints working in a single active mode. These characteristics of traditional robots substantially limit the application of mobile manipulators. Within controlled environments, the world can be adapted to the capabilities of the robot [1]. In uncontrolled environments, the robot has to adapt to the world consisting of only partially known or unknown objects and tasks, and real-time constraints. To date, there are still many challenges to develop robots for working in such uncontrolled environments or human environments [1].

Up to now, as a typical example, opening a door is still a difficult task for robots. When to open a door, position control active mode is necessary for a manipulator to approach the door knob. After the gripper holds on the knob, the passive mode is desirable for the manipulator to follow the unknown door knob trajectory. On-line switching between position and force control are necessary during the door opening process. The present work is aimed to tackle such challenges by developing MRR manipulators with multiple working modes on mobile platforms.

The manipulator consists of one MRR waist joint, two MMR elbow joints and one spherical wrist joint. Each MRR joint includes multiple working modes. The first three joints construct the

arm of the manipulator, which is shown in Figure 2-6. The final manipulator with a spherical wrist is demonstrated in Figure 3-1, which is a Solidworks model.

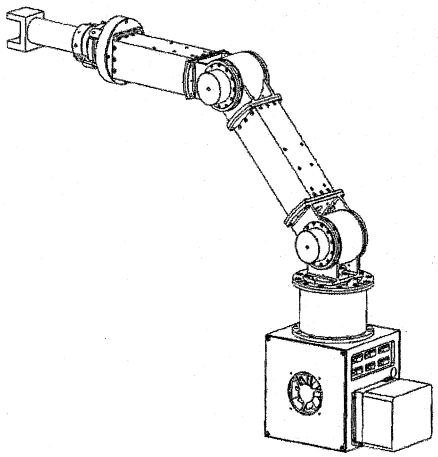

Figure 3-1: Developed Modular Elbow Manipulator

The mobile platform could be a wheeled cart or a trucked cart according to the application aim. The trucked cart can move on a bump field or even stairs, which greatly enlarges the mobile working area and its functions for uncontrolled environments. The selected trucked mobile platform in the research group at Ryerson University is the L-LMA made by ESI Inc, Toronto, which is shown in the Figure 3-2, its size parameters are used for later simulations.

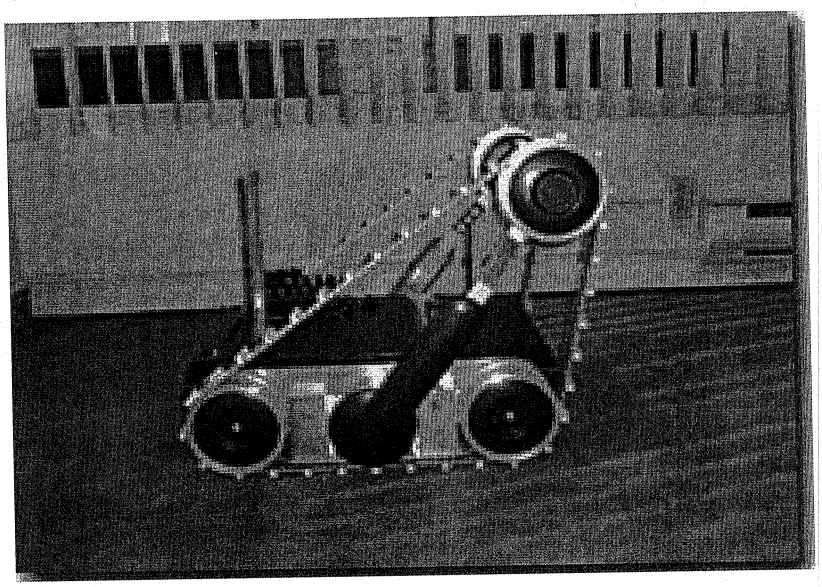

Figure 3-2: LMA Mobile Robot (ESI, Canada)

Up to now, a typical commercial mobile manipulator can be found in Figure 3-3, which is a wheeled platform plus an industrial arm (Mitsubishi PA-10), and a special designed non-modular manipulator (Hombot_1) is shown in Figure 3-4.

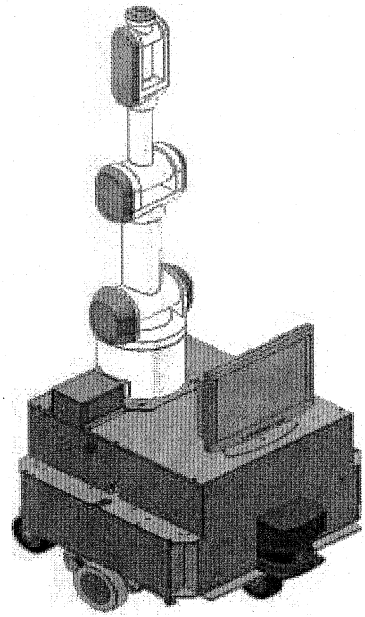

Figure 3-3: Industrial arm (Mitsubishi PA-10)

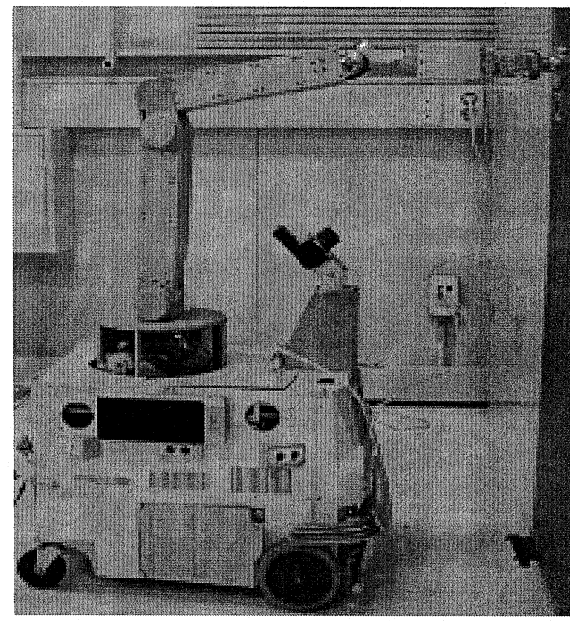

Figure 3-4: Special designed arm (Hombot_1)

The new designed MRR manipulator could be an optional choice for flexible assembled manipulator in different types or functions. The multiple modes will show significant advantages over a traditional arm. The path planning task of the mobile platform becomes simple as well. In the following sections, the model of the manipulator will be presented and analyzed; the spherical wrist also will be analyzed and designed in Chapter 4. The final whole manipulator used for opening a door is analyzed and simulated in Chapter 5.

3.2 Manipulator Kinematics

3.2.1 Wrenches and Screw Coordinates

The screw theory is applied to the description of the manipulator in this thesis. There are two advantages to use screws, twists and wrenches to describe the rigid body kinematics [22] [23]. The first is that they allow a global description of rigid body motion which does not suffer from singularities due to the use of local coordinates. Such singularities are inevitable when one chooses to represent rotation via Euler angles, for example. The second advantage is that screw

theory provides a very geometric description of rigid motion which greatly simplifies the analysis of mechanisms. The use of the geometry of screws is extended in this thesis. In the following kinematics analysis, the above advantages are significant. The following provide some basic key concepts on this topic, more details can be found in reference [22] and [23].

1. The *configuration* of a rigid body is represented as an element $g \in SE(3)$. An element $g \in SE(3)$ may also be viewed as a mapping g: $R^3 \to R^3$ which preserves distances and angles between points. In homogeneous coordinates, we write

$$g = \begin{bmatrix} R & p \\ 0 & 1 \end{bmatrix} \qquad R \in SO(3)\ ;\ p \in R^3$$

The same representation can also be used for a rigid body transformation between two coordinate frames.

2. *Rigid body transformations* can be represented as the exponentials of twists:

$$g = \exp(\hat{\xi}\theta), \qquad \hat{\xi} = \begin{bmatrix} \hat{\omega} & \upsilon \\ 0 & 0 \end{bmatrix}, \quad \hat{\omega} \in SO(3),\ \upsilon \in R^3,\ \theta \in R$$

The twist coordinates of $\hat{\xi}$ are $\xi = (\upsilon, \omega) \in R^6$.

3. A twist $\xi = (\upsilon, \omega) \in R^6$ is associated with a *screw* motion having attributes

Pitch: $$h = \frac{\omega^T \upsilon}{\|\omega\|^2}$$

Axis: $$l = \begin{cases} \left\{ \dfrac{\omega \times \upsilon}{\|\omega\|^2} + \lambda\omega : \lambda \in R \right\}, if\ \omega \neq 0 \\ \{0 + \lambda\upsilon : \lambda \in R\}, if\ \omega = 0; \end{cases}$$

Magnitude: $$M = \begin{cases} \|\omega\|, if\ \omega \neq 0 \\ \|\upsilon\|, if\ \omega = 0. \end{cases}$$

Conversely, given a screw we can write the associated twist. Two special cases are *pure rotation* about axis $l = \{q + \lambda\omega\}$ by an amount θ and *pure translation* along an axis $l = \{0 + \lambda\upsilon\}$:

$$\xi = \begin{bmatrix} -\omega \times \upsilon \\ \omega \end{bmatrix} \theta \quad (\textit{pure}\ \text{rotation}) \qquad \xi = \begin{bmatrix} \upsilon \\ 0 \end{bmatrix} \theta \quad (\textit{pure}\ \text{translation})$$

4. The *velocity* of a rigid motion $g \in SE(3)$ can be specified in two ways. The *spatial velocity* $V^s = Ad_g V^b$, is a twist which gives the velocity of the rigid body as measured by an observer at the origin of the reference frame. The *body velocity* $\hat{V}^b = g^{-1}\dot{g}$, is the velocity of the object in the instantaneous body frame. These velocities are related by the *adjoint* transformation.

$$\hat{V}^b = g^{-1}\dot{g}, \qquad Ad_g = \begin{bmatrix} R & \hat{p}R \\ 0 & R \end{bmatrix}$$

which maps $R^6 \to R^6$. To transform velocities between coordinate frames, we use the relations

$$V^s_{ac} = V^s_{ab} + Ad_{g_{ab}} V^s_{bc}$$

$$V^b_{ac} = Ad_{g^{-1}_{bc}} V^b_{ab} + V^b_{bc}$$

where the V^s_{ab} is the spatial velocity of coordinate frame B relative to frame A and V^b_{ab} is the body velocity.

5. *Wrenches*

A generalized force acting on a rigid body consists of a linear component (pure force) and an angular component (pure moment) acting at a point. We can represent this generalized force as a vector in R^6:

$$F = \begin{bmatrix} f \\ \tau \end{bmatrix} \qquad \tau \in R^3 \text{ linear component, } \tau \in R^3 \text{ rotational component}$$

We will refer to a force/moment pair as a *wrench*

If B is a coordinate frame attached to a rigid body, then we write $F_b = (f_b, \tau_b)$ for a wrench applied at origin of B, with f_b and τ_b specified with respect to the B coordinate frame. If C is a second coordinate frame, then we can write $F_b = (f_b, \tau_b)$ as an equivalent wrench applied at C:

$$F_c = Ad^T_{g_{bc}} F_b .$$

For a rigid body with configuration g_{ab}, $F^s := F_a$ is called the spatial wrench and $F^b := F_b$ is called the body wrench.

6. A wrench $F = (f, \tau)$ is associated with a *screw* having attributes

Pitch: $h = \dfrac{f^T \tau}{\|f\|^2}$

Axis: $l = \begin{cases} \left\{ \dfrac{f \times \tau}{\|f\|^2} + \lambda f : \lambda \in R \right\}, f \neq 0 \\ \{0 + \lambda \tau : \lambda \in R\}, f = 0; \end{cases}$

Magnitude: $M = \begin{cases} \|f\|, f \neq 0 \\ \|\tau\|, f = 0. \end{cases}$

7. A wrench F and a twist V are reciprocal if FV=0. Two screws S1and S2 are reciprocal if the twist V1 about S1 and the wrench F2 along S2 are reciprocal. The reciprocal product between two screws is given by

$$S_1 \odot S_2 = V_1 \bullet F_2 = V_1 \odot V_2 = \upsilon_1 \bullet \omega_2 + \upsilon_2^T \omega_1$$

Where the Vi represents the twist associated with the screw Si. Two screws are reciprocal if the reciprocal product between the screws is zero.

8. A system of screws $\{S_1,...,S_k\}$ describes the vector space of all linear combinations of the screws $\{S_1,...,S_k\}$. A reciprocal screw system is the set of all screws which are reciprocal to S_i , the dimensions of a screw system and its reciprocal system sum to 6 (in $SE(3)$).

3.2.2 Forward Kinematics

Given a base frame S and a tool frame T, the coordinates of the twists corresponding to each joint of a robot manipulator provide a complete parameterization of the kinematics of the manipulator. This method is very different with the normal D-H method. The D-H parameters are available for standard industrial robots and are used by most commercial robot simulation and programming system.

One of the most attractive features of the product of exponential formula is its usage of only two coordinates, a base frame S and a tool frame T, This property, combined with the geometric significance of the twists, makes the product of exponentials representation a superior alternative to the use of D-H parameters. In later section, it will be found this method is so convenient to derive the manipulator Jacobian for analyzing the toques (forces) of each joints.

The developed manipulator is shown in Figure 3-1 and its model is demonstrated in Figure 3-5, which is from reference [22]. This model will be used to derive the forward kinematics and Jacobian matrix. The mechanism consists of two intersecting axes at the shoulder, elbow, and a spherical wrist which is modeled as three intersecting axes. The reference configuration ($\theta = 0$) is fully extended, as shown.

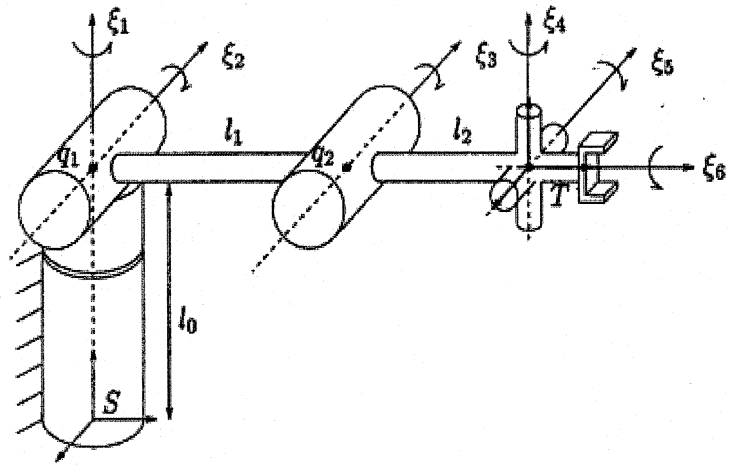

Figure 3-5: Elbow manipulator with spherical wrist

The forward kinematics is computed by calculating the individual twist motions for each joint. The transformation between the tool and the base frames at $\theta = 0$ is given by

$$g_{st}(0) = \begin{bmatrix} I & \begin{pmatrix} 0 \\ l_1 + l_2 \\ l_0 \end{pmatrix} \\ 0 & 1 \end{bmatrix} = \begin{bmatrix} I & p_0 \\ 0 & 1 \end{bmatrix} \tag{3-1}$$

For the joint twists, the general representation is:

$$\xi_i = \begin{bmatrix} -\omega_i \times q_i \\ \omega_i \end{bmatrix} = \begin{bmatrix} v_i \\ \omega_i \end{bmatrix} \quad \text{(i=1…6)} \tag{3-2}$$

The directions are:

$$\omega_1 = \begin{bmatrix} 0 \\ 0 \\ 1 \end{bmatrix} \quad \omega_2 = \begin{bmatrix} -1 \\ 0 \\ 0 \end{bmatrix} \quad \omega_3 = \begin{bmatrix} -1 \\ 0 \\ 0 \end{bmatrix} \quad \omega_4 = \begin{bmatrix} 0 \\ 0 \\ 1 \end{bmatrix} \quad \omega_5 = \begin{bmatrix} -1 \\ 0 \\ 0 \end{bmatrix} \quad \omega_6 = \begin{bmatrix} 0 \\ 1 \\ 0 \end{bmatrix} \tag{3-3}$$

For the first two joints, the twists pass through the points $q_1 = q_2 = \begin{bmatrix} 0 \\ 0 \\ l_0 \end{bmatrix}$ and point in the directions ω_1 and ω_2, so the 1st and the 2nd twists are,

$$\xi_1 = \begin{bmatrix} -\begin{pmatrix} 0 \\ 0 \\ 1 \end{pmatrix} \times \begin{pmatrix} 0 \\ 0 \\ l_0 \end{pmatrix} \\ \begin{pmatrix} 0 \\ 0 \\ 1 \end{pmatrix} \end{bmatrix} = \begin{bmatrix} 0 \\ 0 \\ 0 \\ 0 \\ 0 \\ 1 \end{bmatrix} \tag{3-4}$$

$$\xi_2 = \begin{bmatrix} -\begin{pmatrix} -1 \\ 0 \\ 0 \end{pmatrix} \times \begin{pmatrix} 0 \\ 0 \\ l_0 \end{pmatrix} \\ \begin{pmatrix} -1 \\ 0 \\ 0 \end{pmatrix} \end{bmatrix} = \begin{bmatrix} 0 \\ -l_0 \\ 0 \\ -1 \\ 0 \\ 0 \end{bmatrix} \tag{3-5}$$

Similarly, the points are:

$$q_3 = \begin{bmatrix} 0 \\ l_1 \\ l_0 \end{bmatrix} \qquad q_4 = q_5 = q_6 = \begin{bmatrix} 0 \\ l_1 + l_2 \\ l_0 \end{bmatrix}$$

Other twists are calculated as the following,

$$\xi_3 = \begin{bmatrix} -\begin{pmatrix} -1 \\ 0 \\ 0 \end{pmatrix} \times \begin{pmatrix} 0 \\ l_1 \\ l_0 \end{pmatrix} \\ \begin{pmatrix} -1 \\ 0 \\ 0 \end{pmatrix} \end{bmatrix} = \begin{bmatrix} 0 \\ -l_0 \\ l_1 \\ -1 \\ 0 \\ 0 \end{bmatrix} \tag{3-6}$$

$$\xi_4 = \begin{bmatrix} -\begin{pmatrix} 0 \\ 0 \\ 1 \end{pmatrix} \times \begin{pmatrix} 0 \\ l_1 + l_2 \\ l_0 \end{pmatrix} \\ \begin{pmatrix} 0 \\ 0 \\ 1 \end{pmatrix} \end{bmatrix} = \begin{bmatrix} l_1 + l_2 \\ 0 \\ 0 \\ 0 \\ 0 \\ 1 \end{bmatrix} \tag{3-7}$$

$$\xi_5 = \begin{bmatrix} -\begin{pmatrix} -1 \\ 0 \\ 0 \end{pmatrix} \times \begin{pmatrix} 0 \\ l_1 + l_2 \\ l_0 \end{pmatrix} \\ \begin{pmatrix} -1 \\ 0 \\ 0 \end{pmatrix} \end{bmatrix} = \begin{bmatrix} 0 \\ -l_0 \\ l_1 + l_2 \\ -1 \\ 0 \\ 0 \end{bmatrix} \tag{3-8}$$

$$\xi_6 = \begin{bmatrix} -\begin{pmatrix} 0 \\ 1 \\ 0 \end{pmatrix} \times \begin{pmatrix} 0 \\ l_1 + l_2 \\ l_0 \end{pmatrix} \\ \begin{pmatrix} 0 \\ 1 \\ 0 \end{pmatrix} \end{bmatrix} = \begin{bmatrix} -l_0 \\ 0 \\ 0 \\ 0 \\ 1 \\ 0 \end{bmatrix} \tag{3-9}$$

Then we get the following relations:

$$v_1 = \begin{bmatrix} 0 \\ 0 \\ 0 \end{bmatrix} \quad \omega_1 \times v_1 = \begin{bmatrix} 0 \\ 0 \\ 0 \end{bmatrix}; \qquad v_2 = \begin{bmatrix} 0 \\ -l_0 \\ 0 \end{bmatrix} \quad \omega_2 \times v_2 = \begin{bmatrix} 0 \\ 0 \\ l_0 \end{bmatrix}$$

$$v_3 = \begin{bmatrix} 0 \\ -l_0 \\ l_1 \end{bmatrix} \quad \omega_3 \times v_3 = \begin{bmatrix} 0 \\ l_1 \\ l_0 \end{bmatrix}; \qquad v_4 = \begin{bmatrix} l_1 + l_2 \\ 0 \\ 0 \end{bmatrix} \quad \omega_4 \times v_4 = \begin{bmatrix} 0 \\ l_1 + l_2 \\ 0 \end{bmatrix} \tag{3-10}$$

$$v_5 = \begin{bmatrix} 0 \\ -l_0 \\ l_1 + l_2 \end{bmatrix} \quad \omega_5 \times v_5 = \begin{bmatrix} 0 \\ l_1 + l_2 \\ 0 \end{bmatrix}; \quad v_6 = \begin{bmatrix} -l_0 \\ 0 \\ 0 \end{bmatrix} \quad \omega_6 \times v_5 = \begin{bmatrix} 0 \\ 0 \\ l_0 \end{bmatrix}$$

When $\omega \neq 0$, generally we have,

$$e^{\hat{\xi}\theta} = \begin{bmatrix} e^{\hat{\omega}\theta} & (I - e^{\hat{\omega}\theta})(\omega \times v) + \omega\omega^T v\theta \\ o & 1 \end{bmatrix} = \begin{bmatrix} R & p \\ 0 & 1 \end{bmatrix} \tag{3-11}$$

where
$$e^{\hat{\omega}\theta} = I + \hat{\omega}\sin\theta + \hat{\omega}^2(1 - \cos\theta) \tag{3-12}$$

and
$$\hat{\omega} = \begin{bmatrix} 0 & -\omega 3 & \omega 2 \\ \omega 3 & 0 & -\omega 1 \\ -\omega 2 & \omega 1 & 0 \end{bmatrix} \text{ if } \omega = \begin{bmatrix} \omega 1 \\ \omega 2 \\ \omega 3 \end{bmatrix} \tag{3-13}$$

and
$$\omega \times v = \begin{bmatrix} \omega 2 v 3 - \omega 3 v 2 \\ \omega 3 v 1 - \omega 1 v 3 \\ \omega 1 v 2 - \omega 2 v 1 \end{bmatrix} \text{ if } \omega = \begin{bmatrix} \omega 1 \\ \omega 2 \\ \omega 3 \end{bmatrix} \text{ and } v = \begin{bmatrix} v 1 \\ v 2 \\ v 3 \end{bmatrix} \tag{3-14}$$

In Equation (3-11),

$$e^{\hat{\omega}\theta} = R \tag{3-15}$$

$$(I - e^{\hat{\omega}\theta})(\omega \times v) + \omega\omega^T v\theta = p \tag{3-16}$$

Define
$$c_i = \cos\theta_i \text{ and } s_i = \sin\theta_i \tag{3-18}$$

In later sections, also
$$c_{ij} = \cos(\theta_i + \theta_j) \text{ and } s_{ij} = \sin(\theta_i + \theta_j) \tag{3-19}$$

For $\omega_1 = \begin{bmatrix} 0 \\ 0 \\ 1 \end{bmatrix}$, we have $\hat{\omega}_1 = \begin{bmatrix} 0 & -1 & 0 \\ 1 & 0 & 0 \\ 0 & 0 & 0 \end{bmatrix}$.

and
$$e^{\hat{\omega}_1\theta_1} = \begin{bmatrix} c_1 & -s_1 & 0 \\ s_1 & c_1 & 0 \\ 0 & 0 & 1 \end{bmatrix} = R_1 \tag{3-20}$$

From Equation (3-10) $\upsilon_1 = \begin{bmatrix} 0 \\ 0 \\ 0 \end{bmatrix}$ and $\omega_1 \times \upsilon_1 = \begin{bmatrix} 0 \\ 0 \\ 0 \end{bmatrix}$

$$p_1 = (I - e^{\hat{\omega}_1\theta_1})(\omega_1 \times \upsilon_1) + \omega_1\omega_1^T\upsilon_1\theta_1 = \begin{bmatrix} 0 \\ 0 \\ 0 \end{bmatrix} \tag{3-21}$$

Finally,

$$e^{\hat{\xi}_1\theta_1} = \begin{bmatrix} R_1 & p_1 \\ 0 & 1 \end{bmatrix} = \begin{bmatrix} \begin{bmatrix} c_1 & -s_1 & 0 \\ s_1 & c_1 & 0 \\ 0 & 0 & 1 \end{bmatrix} & \begin{bmatrix} 0 \\ 0 \\ 0 \end{bmatrix} \\ 0 \quad 0 \quad 0 & 1 \end{bmatrix} \tag{3-22}$$

Similarly, for $\omega_2 = \begin{bmatrix} -1 \\ 0 \\ 0 \end{bmatrix}$, we have $\hat{\omega}_2 = \begin{bmatrix} 0 & 0 & 0 \\ 0 & 0 & 1 \\ 0 & -1 & 0 \end{bmatrix}$

and
$$e^{\hat{\omega}_2\theta_2} = \begin{bmatrix} 1 & 0 & 0 \\ 0 & c_2 & s_2 \\ 0 & -s_2 & c_2 \end{bmatrix} = R_2 \tag{3-23}$$

$$p_2 = (I - e^{\hat{\omega}_2\theta_2})(\omega_2 \times \upsilon_2) + \omega_2\omega_2^T\upsilon_2\theta_2 = \begin{bmatrix} 0 \\ -l_0 s_2 \\ l_0 - l_0 c_2 \end{bmatrix} \tag{3-24}$$

$$e^{\hat{\xi}_2\theta_2} = \begin{bmatrix} \begin{bmatrix} 1 & 0 & 0 \\ 0 & c_2 & s_2 \\ 0 & -s_2 & c_2 \end{bmatrix} & \begin{bmatrix} 0 \\ -l_0 s_2 \\ l_0 - l_0 c_2 \end{bmatrix} \\ 0 \quad 0 \quad 0 & 1 \end{bmatrix} \tag{3-25}$$

For $\omega_3 = \begin{bmatrix} -1 \\ 0 \\ 0 \end{bmatrix}$, we have $\hat{\omega}_3 = \begin{bmatrix} 0 & 0 & 0 \\ 0 & 0 & 1 \\ 0 & -1 & 0 \end{bmatrix}$,

and
$$e^{\hat{\omega}_3 \theta_3} = \begin{bmatrix} 1 & 0 & 0 \\ 0 & c_3 & s_3 \\ 0 & -s_3 & c_3 \end{bmatrix} = R_3 \tag{3-26}$$

$$p_3 = (I - e^{\hat{\omega}_3 \theta_3})(\omega_3 \times v_3) + \omega_3 \omega_3^T v_3 \theta_3 = \begin{bmatrix} 0 \\ -l_0 s_3 + l_1 - l_1 c_3 \\ l_0 - l_0 c_3 + l_1 s_3 \end{bmatrix} \tag{3-27}$$

$$e^{\hat{\xi}_3 \theta_3} = \begin{bmatrix} \begin{bmatrix} 1 & 0 & 0 \\ 0 & c_3 & s_3 \\ 0 & -s_3 & c_3 \end{bmatrix} & \begin{bmatrix} 0 \\ -l_0 s_3 + l_1 - l_1 c_3 \\ l_0 - l_0 c_3 + l_1 s_3 \end{bmatrix} \\ 0 \quad 0 \quad 0 & 1 \end{bmatrix} \tag{3-28}$$

For $\omega_4 = \begin{bmatrix} 0 \\ 0 \\ 1 \end{bmatrix}$, we have $\hat{\omega}_4 = \begin{bmatrix} 0 & -1 & 0 \\ 1 & 0 & 0 \\ 0 & 0 & 0 \end{bmatrix}$.

and
$$e^{\hat{\omega}_4 \theta_4} = \begin{bmatrix} c_4 & -s_4 & 0 \\ s_4 & c_4 & 0 \\ 0 & 0 & 1 \end{bmatrix} = R_4 \tag{3-29}$$

From Equation (3-10) $v_4 = \begin{bmatrix} l_1 + l_2 \\ 0 \\ 0 \end{bmatrix}$ and $\omega_4 \times v_4 = \begin{bmatrix} 0 \\ l_1 + l_2 \\ 0 \end{bmatrix}$

$$p_4 = (I - e^{\hat{\omega}_4 \theta_4})(\omega_4 \times v_4) + \omega_4 \omega_4^T v_4 \theta_4 = \begin{bmatrix} (l_1 + l_2) s_4 \\ (l_1 + l_2)(1 - c_4) \\ 0 \end{bmatrix} \tag{3-30}$$

$$e^{\hat{\xi}_4 \theta_4} = \begin{bmatrix} R_4 & p_4 \\ 0 & 1 \end{bmatrix} = \begin{bmatrix} \begin{bmatrix} c_4 & -s_4 & 0 \\ s_4 & c_4 & 0 \\ 0 & 0 & 1 \end{bmatrix} & \begin{bmatrix} (l_1 + l_2) s_4 \\ (l_1 + l_2)(1 - c_4) \\ 0 \end{bmatrix} \\ 0 \quad 0 \quad 0 & 1 \end{bmatrix} \tag{3-31}$$

For $\omega_5 = \begin{bmatrix} -1 \\ 0 \\ 0 \end{bmatrix}$, we have $\hat{\omega}_5 = \begin{bmatrix} 0 & 0 & 0 \\ 0 & 0 & 1 \\ 0 & -1 & 0 \end{bmatrix}$

and
$$e^{\hat{\omega}_5 \theta_5} = \begin{bmatrix} 1 & 0 & 0 \\ 0 & c_5 & s_5 \\ 0 & -s_5 & c_5 \end{bmatrix} = R_5 \tag{3-32}$$

$$p_5 = (I - e^{\hat{\omega}_5 \theta_5})(\omega_5 \times v_5) + \omega_5 \omega_5^T v_5 \theta_5 = \begin{bmatrix} 0 \\ -l_0 s_5 + (l_1 + l_2) - (l_1 + l_2) c_5 \\ l_0 - l_0 c_5 + (l_1 + l_2) s_5 \end{bmatrix} \tag{3-33}$$

$$e^{\hat{\xi}_5 \theta_5} = \begin{bmatrix} \begin{bmatrix} 1 & 0 & 0 \\ 0 & c_5 & s_5 \\ 0 & -s_5 & c_5 \end{bmatrix} & \begin{bmatrix} 0 \\ -l_0 s_5 + (l_1 + l_2) - (l_1 + l_2) c_5 \\ l_0 - l_0 c_5 + (l_1 + l_2) s_5 \end{bmatrix} \\ 0 \quad 0 \quad 0 & 1 \end{bmatrix} \tag{3-34}$$

For $\omega_6 = \begin{bmatrix} 0 \\ 1 \\ 0 \end{bmatrix}$ and $v_6 = \begin{bmatrix} -l_0 \\ 0 \\ 0 \end{bmatrix}$, we have $\omega_6 \times v_5 = \begin{bmatrix} 0 \\ 0 \\ l_0 \end{bmatrix}$, $\hat{\omega}_6 = \begin{bmatrix} 0 & 0 & 1 \\ 0 & 0 & 0 \\ -1 & 0 & 0 \end{bmatrix}$.

Then
$$e^{\hat{\omega}_6 \theta_6} = \begin{bmatrix} c_6 & 0 & s_6 \\ 0 & 1 & 0 \\ -s_6 & 0 & c_6 \end{bmatrix} = R_6 \tag{3-35}$$

$$p_5 = (I - e^{\hat{\omega}_6 \theta_6})(\omega_6 \times v_6) + \omega_6 \omega_6^T v_6 \theta_6 = \begin{bmatrix} l_0 s_6 \\ 0 \\ l_0 - l_0 c_6 \end{bmatrix} \tag{3-36}$$

$$e^{\hat{\xi}_6 \theta_6} = \begin{bmatrix} \begin{bmatrix} c_6 & 0 & s_6 \\ 0 & 1 & 0 \\ -s_6 & 0 & c_6 \end{bmatrix} & \begin{bmatrix} l_0 s_6 \\ 0 \\ l_0 - l_0 c_6 \end{bmatrix} \\ 0 \quad 0 \quad 0 & 1 \end{bmatrix} \tag{3-37}$$

From above Equations (3-1), (3-22), (3-25), (3-28), (3-31), (3-34) and (3-37), we obtain the full forward kinematics.

$$g_{st}(\theta) = e^{\hat{\xi}_1\theta_1}...e^{\hat{\xi}_6\theta_6} g_{st}(0) = \begin{bmatrix} R & p \\ 0 & 1 \end{bmatrix} \tag{3-38}$$

where

$$g_{st}(\theta) = e^{\hat{\xi}_1\theta_1}...e^{\hat{\xi}_6\theta_6} g_{st}(0)$$

$$= \begin{bmatrix} R_1 & p_1 \\ 0 & 1 \end{bmatrix}\begin{bmatrix} R_2 & p_2 \\ 0 & 1 \end{bmatrix}...\begin{bmatrix} R_5 & p_5 \\ 0 & 1 \end{bmatrix}\begin{bmatrix} R_6 & p_6 \\ 0 & 1 \end{bmatrix}\begin{bmatrix} I & p_0 \\ 0 & 1 \end{bmatrix}$$

$$= \begin{bmatrix} R_1 & p_1 \\ 0 & 1 \end{bmatrix}\begin{bmatrix} R_2 & p_2 \\ 0 & 1 \end{bmatrix}...\begin{bmatrix} R_5 & p_5 \\ 0 & 1 \end{bmatrix}\begin{bmatrix} R_6 & R_6p_0 + p_6 \\ 0 & 1 \end{bmatrix}$$

$$= \begin{bmatrix} R_1 & p_1 \\ 0 & 1 \end{bmatrix}\begin{bmatrix} R_2 & p_2 \\ 0 & 1 \end{bmatrix}...\begin{bmatrix} R_5 & p_5 \\ 0 & 1 \end{bmatrix}\begin{bmatrix} R_6 & \begin{bmatrix} 0 \\ l_1 + l_2 \\ l_0 \end{bmatrix} \\ 0 & 1 \end{bmatrix}$$

$$= \begin{bmatrix} R_1 & p_1 \\ 0 & 1 \end{bmatrix}\begin{bmatrix} R_2 & p_2 \\ 0 & 1 \end{bmatrix}...\begin{bmatrix} R_5 & p_5 \\ 0 & 1 \end{bmatrix}\begin{bmatrix} R_6 & p_0 \\ 0 & 1 \end{bmatrix}$$

$$= \begin{bmatrix} R_1 & p_1 \\ 0 & 1 \end{bmatrix}\begin{bmatrix} R_2 & p_2 \\ 0 & 1 \end{bmatrix}...\begin{bmatrix} R_4 & p_4 \\ 0 & 1 \end{bmatrix}\begin{bmatrix} R_5R_6 & R_5p_0 + p_5 \\ 0 & 1 \end{bmatrix}$$

$$= \begin{bmatrix} R_1 & p_1 \\ 0 & 1 \end{bmatrix}\begin{bmatrix} R_2 & p_2 \\ 0 & 1 \end{bmatrix}...\begin{bmatrix} R_4 & p_4 \\ 0 & 1 \end{bmatrix}\begin{bmatrix} R_5R_6 & p_0 \\ 0 & 1 \end{bmatrix}$$

$$= \begin{bmatrix} R_1 & p_1 \\ 0 & 1 \end{bmatrix}\begin{bmatrix} R_2 & p_2 \\ 0 & 1 \end{bmatrix}\begin{bmatrix} R_3 & p_3 \\ 0 & 1 \end{bmatrix}\begin{bmatrix} R_4R_5R_6 & R_4p_0 + p_4 \\ 0 & 1 \end{bmatrix}$$

$$= \begin{bmatrix} R_1 & p_1 \\ 0 & 1 \end{bmatrix}\begin{bmatrix} R_2 & p_2 \\ 0 & 1 \end{bmatrix}\begin{bmatrix} R_3 & p_3 \\ 0 & 1 \end{bmatrix}\begin{bmatrix} R_4R_5R_6 & p_0 \\ 0 & 1 \end{bmatrix}$$

$$= \begin{bmatrix} R_1 & p_1 \\ 0 & 1 \end{bmatrix}\begin{bmatrix} R_2 & p_2 \\ 0 & 1 \end{bmatrix}\begin{bmatrix} R_3R_4R_5R_6 & R_3p_0 + p_3 \\ 0 & 1 \end{bmatrix}$$

$$= \begin{bmatrix} R_1 & p_1 \\ 0 & 1 \end{bmatrix} \begin{bmatrix} R_2 & p_2 \\ 0 & 1 \end{bmatrix} \begin{bmatrix} R_3R_4R_5R_6 & \begin{bmatrix} 0 \\ l_1 + l_2c_3 \\ l_0 - l_2s_3 \end{bmatrix} \\ 0 & 1 \end{bmatrix}$$

$$= \begin{bmatrix} R_1 & p_1 \\ 0 & 1 \end{bmatrix} \begin{bmatrix} R_2R_3R_4R_5R_6 & R_2 \begin{bmatrix} 0 \\ l_1 + l_2c_3 \\ l_0 - l_2s_3 \end{bmatrix} + p_2 \\ 0 & 1 \end{bmatrix}$$

$$= \begin{bmatrix} R_1 & p_1 \\ 0 & 1 \end{bmatrix} \begin{bmatrix} R_2R_3R_4R_5R_6 & \begin{bmatrix} 0 \\ l_1c_2 + l_2c_{23} \\ l_0 - l_1s_2 - l_2s_{23} \end{bmatrix} \\ 0 & 1 \end{bmatrix}$$

$$= \begin{bmatrix} R_1R_2R_3R_4R_5R_6 & R_1 \begin{bmatrix} 0 \\ l_1c_2 + l_2c_{23} \\ l_0 - l_1s_2 - l_2s_{23} \end{bmatrix} + p_1 \\ 0 & 1 \end{bmatrix}$$

$$= \begin{bmatrix} R_1R_2R_3R_4R_5R_6 & \begin{bmatrix} -s_1(l_1c_2 + l_2c_{23}) \\ c_1(l_1c_2 + l_2c_{23}) \\ l_0 - l_1s_2 - l_2s_{23} \end{bmatrix} \\ 0 & 1 \end{bmatrix} \qquad (3\text{-}39)$$

where $R(\theta) = R_1R_2R_3R_4R_5R_6 = \begin{bmatrix} r_{11} & r_{12} & r_{13} \\ r_{21} & r_{22} & r_{23} \\ r_{31} & r_{32} & r_{33} \end{bmatrix}$,

and $p(\theta) = \begin{bmatrix} -s_1(l_1c_2 + l_2c_{23}) \\ c_1(l_1c_2 + l_2c_{23}) \\ l_0 - l_1s_2 - l_2s_{23} \end{bmatrix}$

$$r_{11} = c_6(c_1c_4 - s_1s_4c_{23}) + s_6(s_1c_5s_{23} + s_5(c_1s_4 + s_1c_4c_{23}))$$

$$r_{12} = -c_5(c_1s_4 + s_1c_4c_{23}) + s_1s_5s_{23}$$

$$r_{13} = s_6(c_1c_4 - s_1s_4c_{23}) - c_6(s_1c_5s_{23} + s_5(c_1s_4 + s_1c_4c_{23}))$$

$$r_{21} = c_6(s_1c_4 + c_1s_4c_{23}) - s_6(c_1c_5s_{23} + s_5(-s_1s_4 + c_1c_4c_{23}))$$

$$r_{22} = c_5(-s_1s_4 + c_1c_4c_{23}) - c_1s_5s_{23}$$

$$r_{23} = s_6(s_1c_4 + c_1s_4c_{23}) + c_6(c_1c_5s_{23} + s_5(-s_1s_4 + c_1c_4c_{23}))$$

$$r_{31} = -s_4c_6s_{23} - s_6(c_5c_{23} - c_4s_5s_{23})$$

$$r_{32} = -s_5c_{23} - c_4c_5s_{23}$$

$$r_{33} = -s_4s_6s_{23} + c_6(c_5c_{23} - c_4s_5s_{23})$$

3.3 Jacobian Matrix

3.3.1 Velocity and Jacobian Matrix

Traditionally, one describes the Jacobian for a manipulator by differencing the forward kinematics map. This works when the forward kinematics is represented as a mapping $g : R^n \to R^p$, in which case the Jacobian is the linear map $\frac{\partial g}{\partial \theta} : R^n \to R^p$. However, if the forward kinematics is more completely represented as $g : R^n \to SE(3)$, the Jacobian is not easily obtained. The problem is that $\frac{\partial g}{\partial \theta}$ is not a natural quantity since g is a matrix-valued function. Of course, one could always choose coordinates for *SE(3)* , but this description only holds locally. More importantly, choosing a local parameterization for *SE(3)* destroys the natural geometric structure of rigid body motion.

Using the Jacobian forward kinematics map in terms of twists can correct this problem. We shall see that the product of exponentials formula leads to a very natural and explicit description

of the manipulator Jacobian, which highlights the geometry of the mechanism and has none of the drawbacks of a local representation.

End-effector velocity

Let $g_{st}: Q \to SE(3)$ be the forward kinematics map for a manipulator. If the joints move along a path $\theta(t) \in Q$, then the end-effector traverses a path $g_{st}(\theta(t)) \in SE(3)$. The instantaneous spatial velocity of the end-effector is given by the twist

$$\hat{V}_{st}^{s} = \dot{g}_{st}(\theta) g_{st}^{-1}(\theta) \tag{3-40}$$

Applying the chain rule,

$$\hat{V}_{st}^{s} = \sum_{i=1}^{n} (\frac{\partial g_{st}}{\partial \theta_i} \dot{\theta}_i) g_{st}^{-1}(\theta) = \sum_{i=1}^{n} (\frac{\partial g_{st}}{\partial \theta_i} g_{st}^{-1}(\theta)) \dot{\theta}_i \tag{3-41}$$

The end-effector velocity is linearly related to the velocity of the individual joints. In twist coordinates, Equation (3-41) can be written as

$$V_{st}^{s} = J_{st}^{s}(\theta) \dot{\theta},$$

where

$$J_{st}^{s}(\theta) = \left[(\frac{\partial g_{st}}{\partial \theta_i} g_{st}^{-1})^{\vee} ..... \quad (\frac{\partial g_{st}}{\partial \theta_i} g_{st}^{-1})^{\vee} \right] \tag{3-42}$$

The matrix $J_{st}^{s}(\theta) \in R^{6 \times n}$ is the spatial manipulator Jacobian. At each configuration θ, it maps the joint velocity vector into the corresponding velocity of the end-effecter.

Using the former forward kinematics,

$$g_{st}(\theta) = e^{\hat{\xi}_1 \theta_1} ... e^{\hat{\xi}_6 \theta_6} g_{st}(0)$$

$$(\frac{\partial g_{st}}{\partial \theta_i}) g_{st}^{-1} = e^{\hat{\xi}_1 \theta_1} \ldots e^{\hat{\xi}_{i-1} \theta_{i-1}} \frac{\partial}{\partial \theta_i} (e^{\hat{\xi}_i \theta_i}) e^{\hat{\xi}_{i+1} \theta_{i+1}} \ldots e^{\hat{\xi}_n \theta_n} \; g_{st}(0) \; g_{st}^{-1}$$

$$= e^{\hat{\xi}_1 \theta_1} \ldots e^{\hat{\xi}_{i-1} \theta_{i-1}} \; (\hat{\xi}_i) \; e^{\hat{\xi}_i \theta_i} \ldots e^{\hat{\xi}_n \theta_n} \; g_{st}(0) \; g_{st}^{-1}$$

$$= e^{\hat{\xi}_1 \theta_1} \ldots e^{\hat{\xi}_{i-1} \theta_{i-1}} \; (\hat{\xi}_i) \; e^{-\hat{\xi}_{i-1} \theta_{i-1}} \ldots e^{-\hat{\xi}_1 \theta_1}$$

and convert to twist coordinates,

$$(\frac{\partial g_{st}}{\partial \theta_i} g_{st}^{-1})^{\vee} = Ad_{(e^{\hat{\xi}_1 \theta_1} ..... e^{\hat{\xi}_{i-1} \theta_{i-1}})} \xi_i \tag{3-43}$$

where $$Ad_g = \begin{bmatrix} R & \hat{p}R \\ 0 & R \end{bmatrix} \tag{3-44}$$

and twist operators: $$\hat{\xi} = \begin{bmatrix} v \\ \omega \end{bmatrix}^{\wedge} = \begin{bmatrix} \hat{\omega} & v \\ 0 & 0 \end{bmatrix}$$

$$\begin{bmatrix} \hat{\omega} & v \\ 0 & 0 \end{bmatrix}^{\vee} = \begin{bmatrix} v \\ \omega \end{bmatrix} \tag{3-45}$$

The spatial manipulator Jacobian becomes,

$$J_{st}^{s}(\theta) = \begin{bmatrix} \xi_1 & \xi_2' \ldots\ldots \xi_n' \end{bmatrix} \tag{3-46}$$

$$\xi_i' = Ad_{(e^{\hat{\xi}_1\theta_1}\ldots\ldots e^{\hat{\xi}_{i-1}\theta_{i-1}})}\xi_i \tag{3-47}$$

By virtue of the definition ξ_i', the i-th column of the Jacobian depends only on $\theta_1,\ldots,\theta_{i-1}$. And the i-th column of the Jacobian, $\xi_i' = Ad_{(e^{\hat{\xi}_1\theta_1}\ldots\ldots e^{\hat{\xi}_{i-1}\theta_{i-1}})}\xi_i$, corresponds to the i-th joint twist, ξ_i, transformed by the rigid transformation $\exp(\hat{\xi}_1\theta_1)\ldots\exp(\hat{\xi}_{i-1}\theta_{i-1})$. This is precisely the rigid body transformation which takes the i-th joint frame from its reference configuration to the current configuration of the manipulator. Thus, the i-th column of the spatial Jacobian is the i-th joint twist, transformed to the current manipulator. This powerful structure property means that we can calculate $J_{st}^{s}(\theta)$ "by inspection".

3.3.2 Jacobian Matrix

Following the forward kinematics of Elbow manipulator in the former section, we know the following relations.

$$\omega_1 = \begin{bmatrix} 0 \\ 0 \\ 1 \end{bmatrix} \quad \omega_2 = \begin{bmatrix} -1 \\ 0 \\ 0 \end{bmatrix} \quad \omega_3 = \begin{bmatrix} -1 \\ 0 \\ 0 \end{bmatrix} \quad \omega_4 = \begin{bmatrix} 0 \\ 0 \\ 1 \end{bmatrix} \quad \omega_5 = \begin{bmatrix} -1 \\ 0 \\ 0 \end{bmatrix} \quad \omega_6 = \begin{bmatrix} 0 \\ 1 \\ 0 \end{bmatrix} \tag{3-51}$$

$$\xi_1 = \begin{bmatrix} 0 \\ 0 \\ 0 \\ 0 \\ 0 \\ 1 \end{bmatrix} \quad \xi_2 = \begin{bmatrix} 0 \\ -l_0 \\ 0 \\ -1 \\ 0 \\ 0 \end{bmatrix} \quad \xi_3 = \begin{bmatrix} 0 \\ -l_0 \\ l_1 \\ -1 \\ 0 \\ 0 \end{bmatrix} \quad \xi_4 = \begin{bmatrix} l_1 + l_2 \\ 0 \\ 0 \\ 0 \\ 0 \\ 1 \end{bmatrix} \quad \xi_5 = \begin{bmatrix} 0 \\ -l_0 \\ l_1 + l_2 \\ -1 \\ 0 \\ 0 \end{bmatrix} \quad \xi_6 = \begin{bmatrix} -l_0 \\ 0 \\ 0 \\ 0 \\ 1 \\ 0 \end{bmatrix} \tag{3-52}$$

$$q_1 = q_2 = \begin{bmatrix} 0 \\ 0 \\ l_0 \end{bmatrix} \quad q_3 = \begin{bmatrix} 0 \\ l_1 \\ l_0 \end{bmatrix} \quad q_4 = q_5 = q_6 = \begin{bmatrix} 0 \\ l_1 + l_2 \\ l_0 \end{bmatrix} \tag{3-53}$$

Define the following elementary rotations about *x*-, *y*- and *z*- axes:

$$R_X(\phi) = e^{\hat{X}\phi} = \begin{bmatrix} 1 & 0 & 0 \\ 0 & \cos\phi & -\sin\phi \\ 0 & \sin\phi & \cos\phi \end{bmatrix} \tag{3-54a}$$

$$R_Y(\beta) = e^{\hat{Y}\beta} = \begin{bmatrix} \cos\beta & 0 & \sin\beta \\ 0 & 1 & 0 \\ -\sin\beta & 0 & \cos\beta \end{bmatrix} \tag{3-54b}$$

$$R_Z(\alpha) = e^{\hat{Z}\alpha} = \begin{bmatrix} \cos\alpha & -\sin\alpha & 0 \\ \sin\alpha & \cos\alpha & 0 \\ 0 & 0 & 1 \end{bmatrix} \tag{3-54c}$$

The directions of the joint twists are:

$$\omega_2' = e^{\hat{Z}\theta_1}\,\omega_2 = \begin{bmatrix} c_1 & -s_1 & 0 \\ s_1 & c_1 & 0 \\ 0 & 0 & 1 \end{bmatrix} \begin{bmatrix} -1 \\ 0 \\ 0 \end{bmatrix} = \begin{bmatrix} -c_1 \\ -s_1 \\ 0 \end{bmatrix} \tag{3-55}$$

$$\omega_3' = e^{\hat{Z}\theta_1}\, e^{-\hat{X}\theta_2}\,\omega_3 = \begin{bmatrix} c_1 & -s_1 & 0 \\ s_1 & c_1 & 0 \\ 0 & 0 & 1 \end{bmatrix} \begin{bmatrix} 1 & 0 & 0 \\ 0 & c_2 & s_2 \\ 0 & -s_2 & c_2 \end{bmatrix} \begin{bmatrix} -1 \\ 0 \\ 0 \end{bmatrix} = \begin{bmatrix} -c_1 \\ -s_1 \\ 0 \end{bmatrix} \tag{3-56}$$

$$\omega_4' = e^{\hat{Z}\theta_1}\, e^{-\hat{X}\theta_2}\, e^{-\hat{X}\theta_3}\, \omega_4 = \begin{bmatrix} c_1 & -s_1c_2 & -s_1s_2 \\ s_1 & c_1c_2 & c_1s_2 \\ 0 & -s_2 & c_2 \end{bmatrix} \begin{bmatrix} 1 & 0 & 0 \\ 0 & c_3 & s_3 \\ 0 & -s_3 & c_3 \end{bmatrix} \begin{bmatrix} 0 \\ 0 \\ 1 \end{bmatrix}$$

$$= \begin{bmatrix} c_1 & -s_1c_{23} & -s_1s_{23} \\ s_1 & c_1c_{23} & c_1s_{23} \\ 0 & -s_{23} & c_{23} \end{bmatrix} \begin{bmatrix} 0 \\ 0 \\ 1 \end{bmatrix} = \begin{bmatrix} -s_1s_{23} \\ c_1s_{23} \\ c_{23} \end{bmatrix} \tag{3-57}$$

$$\omega_5' = e^{\hat{Z}\theta_1}\, e^{-\hat{X}\theta_2}\, e^{-\hat{X}\theta_3}\, e^{\hat{Z}\theta_4}\, \omega_5 = \begin{bmatrix} c_1 & -s_1c_{23} & -s_1s_{23} \\ s_1 & c_1c_{23} & c_1s_{23} \\ 0 & -s_{23} & c_{23} \end{bmatrix} \begin{bmatrix} c_4 & -s_4 & 0 \\ s_4 & c_4 & 0 \\ 0 & 0 & 1 \end{bmatrix} \begin{bmatrix} -1 \\ 0 \\ 0 \end{bmatrix}$$

$$= \begin{bmatrix} c_1 & -s_1c_{23} & -s_1s_{23} \\ s_1 & c_1c_{23} & c_1s_{23} \\ 0 & -s_{23} & c_{23} \end{bmatrix} \begin{bmatrix} -c_4 \\ -s_4 \\ 0 \end{bmatrix} = \begin{bmatrix} -c_1c_4 + s_1s_4c_{23} \\ -s_1c_4 - c_1s_4c_{23} \\ s_4s_{23} \end{bmatrix} \tag{3-58}$$

$$\omega_6' = e^{\hat{Z}\theta_1}\, e^{-\hat{X}\theta_2}\, e^{-\hat{X}\theta_3}\, e^{\hat{Z}\theta_4}\, e^{-\hat{X}\theta_5}\, \omega_6 = \begin{bmatrix} c_1 & -s_1c_{23} & -s_1s_{23} \\ s_1 & c_1c_{23} & c_1s_{23} \\ 0 & -s_{23} & c_{23} \end{bmatrix} \begin{bmatrix} c_4 & -s_4 & 0 \\ s_4 & c_4 & 0 \\ 0 & 0 & 1 \end{bmatrix} \begin{bmatrix} 1 & 0 & 0 \\ 0 & c_5 & s_5 \\ 0 & -s_5 & c_5 \end{bmatrix} \begin{bmatrix} 0 \\ 1 \\ 0 \end{bmatrix}$$

$$= \begin{bmatrix} c_1 & -s_1c_{23} & -s_1s_{23} \\ s_1 & c_1c_{23} & c_1s_{23} \\ 0 & -s_{23} & c_{23} \end{bmatrix} \begin{bmatrix} c_4 & -s_4 & 0 \\ s_4 & c_4 & 0 \\ 0 & 0 & 1 \end{bmatrix} \begin{bmatrix} 0 \\ c_5 \\ -s_5 \end{bmatrix} = \begin{bmatrix} c_1 & -s_1c_{23} & -s_1s_{23} \\ s_1 & c_1c_{23} & c_1s_{23} \\ 0 & -s_{23} & c_{23} \end{bmatrix} \begin{bmatrix} -s_4c_5 \\ c_4c_5 \\ -s_5 \end{bmatrix}$$

$$= \begin{bmatrix} -c_1s_4c_5 - s_1c_4c_5c_{23} + s_1s_5s_{23} \\ -s_1s_4c_5 + c_1c_4c_5c_{23} - c_1s_5s_{23} \\ -c_4c_5s_{23} - s_5c_{23} \end{bmatrix} \tag{3-59}$$

For the first two points, $q_1' = q_2' = q_1 = q_2 = \begin{bmatrix} 0 \\ 0 \\ l_0 \end{bmatrix}$ (3-60)

For the 3rd point, $q_3' = \begin{bmatrix} 0 \\ 0 \\ l_0 \end{bmatrix} + e^{\hat{Z}\theta_1}\, e^{-\hat{X}\theta_2} \begin{bmatrix} 0 \\ l_1 \\ 0 \end{bmatrix} = \begin{bmatrix} 0 \\ 0 \\ l_0 \end{bmatrix} + \begin{bmatrix} c_1 & -s_1c_2 & -s_1s_2 \\ s_1 & c_1c_2 & c_1s_2 \\ 0 & -s_2 & c_2 \end{bmatrix} \begin{bmatrix} 0 \\ l_1 \\ 0 \end{bmatrix}$

$$= \begin{bmatrix} -l_1 s_1 c_2 \\ l_1 c_1 c_2 \\ l_0 - l_1 s_2 \end{bmatrix} \tag{3-61}$$

$$q_4' = q_5' = q_6' = q_w' = \begin{bmatrix} -l_1 s_1 c_2 \\ l_1 c_1 c_2 \\ l_0 - l_1 s_2 \end{bmatrix} + e^{\hat{Z}\theta_1} \; e^{-\hat{X}\theta_2} \; e^{-\hat{X}\theta_3} \begin{bmatrix} 0 \\ l_2 \\ 0 \end{bmatrix} = \begin{bmatrix} -l_1 s_1 c_2 \\ l_1 c_1 c_2 \\ l_0 - l_1 s_2 \end{bmatrix} + \begin{bmatrix} c_1 & -s_1 c_{23} & -s_1 s_{23} \\ s_1 & c_1 c_{23} & c_1 s_{23} \\ 0 & -s_{23} & c_{23} \end{bmatrix} \begin{bmatrix} 0 \\ l_2 \\ 0 \end{bmatrix}$$

$$= \begin{bmatrix} -l_1 s_1 c_2 - l_2 s_1 c_{23} \\ l_1 c_1 c_2 + l_2 c_1 c_{23} \\ l_0 - l_1 s_2 - l_2 s_{23} \end{bmatrix} = \begin{bmatrix} -s_1 (l_1 c_2 + l_2 c_{23}) \\ c_1 (l_1 c_2 + l_2 c_{23}) \\ l_0 - l_1 s_2 - l_2 s_{23} \end{bmatrix} \tag{3-62}$$

By inspection, the spherical wrist centre obviously equals to $p(\theta)$ in Equation (3-39).

For the first two joints which pass through the point $q_1' = q_2' = \begin{bmatrix} 0 \\ 0 \\ l_0 \end{bmatrix}$

$$\xi_1 = \begin{bmatrix} -\omega_1 \times q_1' \\ \omega_1 \end{bmatrix} = \begin{bmatrix} 0 \\ 0 \\ 0 \\ 0 \\ 0 \\ 1 \end{bmatrix} \tag{3-63}$$

$$\xi_2' = \begin{bmatrix} -\omega_2' \times q_2' \\ \omega_2' \end{bmatrix} = \begin{bmatrix} l_0 s_1 \\ -l_0 c_1 \\ 0 \\ -c_1 \\ -s_1 \\ 0 \end{bmatrix} \tag{3-64}$$

$$\xi_3^{'} = \begin{bmatrix} -\omega_3^{'} \times q_3^{'} \\ \omega_3^{'} \end{bmatrix} = \begin{bmatrix} s_1(l_0 - l_1 s_2) \\ -c_1(l_0 - l_1 s_2) \\ l_1 c_2 \\ -c_1 \\ -s_1 \\ 0 \end{bmatrix} = \begin{bmatrix} s_1 l_0 - s_1 s_2 l_1 \\ -c_1 l_0 - c_1 s_2 l_1 \\ l_1 c_2 \\ -c_1 \\ -s_1 \\ 0 \end{bmatrix} \tag{3-65}$$

$$\xi_4^{'} = \begin{bmatrix} -\omega_4^{'} \times q_4^{'} \\ \omega_4^{'} \end{bmatrix} = \begin{bmatrix} -c_1(l_0 - l_1 s_2)s_{23} + l_1 c_1 c_2 + l_2 c_1 \\ -s_1(l_0 - l_1 s_2)s_{23} + l_1 s_1 c_2 c_{23} + l_2 s_1 \\ 0 \\ -s_1 s_{23} \\ c_1 s_{23} \\ c_{23} \end{bmatrix}$$

$$= \begin{bmatrix} -c_1 s_{23} l_0 + (c_1 s_2 s_{23} + c_1 c_2 c_{23}) l_1 + c_1 l_2 \\ -s_1 s_{23} l_0 + (s_1 c_2 c_{23} + s_1 s_2 s_{23}) l_1 + s_1 l_2 \\ 0 \\ -s_1 s_{23} \\ c_1 s_{23} \\ c_{23} \end{bmatrix} \tag{3-66}$$

$$\xi_5^{'} = \begin{bmatrix} -\omega_5^{'} \times q_5^{'} \\ \omega_5^{'} \end{bmatrix} = \begin{bmatrix} (s_1 c_4 + c_1 s_4 c_{23})(l_0 - l_1 s_2) + l_1 c_1 c_2 s_4 s_{23} \\ -l_2 s_1 c_4 s_{23} \\ -(c_1 c_4 - s_1 s_4 c_{23})(l_0 - l_1 s_2) + l_1 s_1 c_2 s_4 c_{23} \\ +l_2 c_1 c_4 s_{23} \\ l_1 c_2 c_4 + l_2 c_4 c_{23} \\ -c_1 c_4 + s_1 s_4 c_{23} \\ -s_1 c_4 - c_1 s_4 c_{23} \\ s_4 s_{23} \end{bmatrix}$$

$$= \begin{bmatrix} (s_1c_4 + c_1s_4c_{23})l_0 - (s_1s_2c_4 + c_1s_2s_4c_{23} - c_1c_2s_4s_{23})l_1 \\ -s_1c_4s_{23}l_2 \\ \\ -(c_1c_4 - s_1s_4c_{23})l_0 + (c_1s_2c_4 - s_1s_2s_4c_{23} + s_1c_2s_4s_{23})l_1 \\ +c_1c_4s_{23}l_2 \\ \\ c_2c_4l_1 + c_4c_{23}l_2 \\ \\ -c_1c_4 + s_1s_4c_{23} \\ \\ -s_1c_4 - c_1s_4c_{23} \\ \\ s_4s_{23} \end{bmatrix} \qquad (3\text{-}67)$$

$$\xi_6' = \begin{bmatrix} -\omega_6' \times q_6' \\ \omega_6' \end{bmatrix} = \begin{bmatrix} -(c_1c_4c_5c_{23} - s_1s_4c_5 - c_1s_5s_{23})(l_0 - l_1s_2) - \\ (c_1c_2c_4c_5s_{23} + c_1c_2s_5c_{23})l_1 - (c_1s_5 + s_1s_4c_5s_{23})l_2 \\ \\ -(s_1c_4c_5c_{23} + c_1s_4c_5 - s_1s_5s_{23})(l_0 - l_1s_2) - \\ (s_1c_2c_4c_5s_{23} + s_1c_2s_5c_{23})l_1 - (s_1s_5 - c_1s_4c_5s_{23})l_2 \\ \\ s_4c_5(l_1c_2 + l_2c_{23}) \\ \\ -c_1s_4c_5 - s_1c_4c_5c_{23} + s_1s_5s_{23} \\ \\ -s_1s_4c_5 + c_1c_4c_5c_{23} - c_1s_5s_{23} \\ \\ -c_4c_5s_{23} - s_5c_{23} \end{bmatrix}$$

$$= \begin{bmatrix} -(c_1c_4c_5c_{23} - s_1s_4c_5 - c_1s_5s_{23})l_0 - (c_1s_5 + s_1s_4c_5s_{23})l_2 \\ -(c_1c_2c_4c_5s_{23} - c_1s_2c_4c_5c_{23} + s_1s_2s_4c_5 + c_1c_2s_5c_{23} + c_1s_2s_5c_{23})l_1 \\ \\ -(s_1c_4c_5c_{23} + c_1s_4c_5 - s_1s_5s_{23})l_0 - (s_1s_5 - c_1s_4c_5s_{23})l_2 \\ -(s_1c_2c_4c_5s_{23} - s_1s_2c_4c_5c_{23} + c_1s_2s_4c_5 + s_1c_2s_5c_{23} - s_1s_2s_5s_{23})l_1 \\ \\ c_2s_4c_5l_1 + s_4c_5c_{23}l_2 \\ \\ -c_1s_4c_5 - s_1c_4c_5c_{23} + s_1s_5s_{23} \\ \\ -s_1s_4c_5 + c_1c_4c_5c_{23} - c_1s_5s_{23} \\ \\ -c_4c_5s_{23} - s_5c_{23} \end{bmatrix} \quad (3\text{-}68)$$

$$J_{st}^{s}(\theta) = \begin{bmatrix} \xi_1 & \xi_2^{'} \cdots\cdots \xi_n^{'} \end{bmatrix} \quad (3\text{-}69)$$

$$J_{st}^{s}(\theta) = \begin{bmatrix} 0 & -\omega_2^{'} \times q_2^{'} & -\omega_3^{'} \times q_3^{'} & -\omega_4^{'} \times q_w^{'} & -\omega_5^{'} \times q_w^{'} & -\omega_6^{'} \times q_w^{'} \\ \omega_1 & \omega_2^{'} & \omega_3^{'} & \omega_4^{'} & \omega_5^{'} & \omega_6^{'} \end{bmatrix} \quad (3\text{-}70)$$

The above Equations (3-63) ~ (3-70) provide the Jacobian Matrix of Elbow manipulator.

For a check, the following relationship should be satisfied.

$$(J_{st}^{s}\dot{\theta})^{\wedge} p(\theta) = \dot{p}(\theta) \quad (3\text{-}71)$$

All above equations have been rechecked and are correct.

As the number of the elements in a Jacobian matrix usually is huge, the expressions become complicated. The above method shows significant advantage to avoid the differential operation from the forward kinematics and the expressions are guaranteed for use. The detailed check process is provided in Appendix A. (Jacobian Matrix Check) of this thesis.

Chapter 4

Anthropomorphic Wrist Design and Torque Analysis

In our new mobile manipulator, a DUAJ Anthropomorphic Joint is designed and used. The wrist will perform the 4th yaw and 5th pitch motions in Figure 3-5. The 6th roll motion will be on the gripper. The DUAJ wrist has the advantages of gaining high weight-to-force ratio and one of the most compact structures [14]. It is able to ensure complete free-of-rolling motion that is the fundamental requirements for the anthropomorphic motions and it has some additional advantageous characteristic features [14] [16]. Up to now normal robot hands reported do not seem to satisfy the requirements for the humanlike motion. The DAUJ joint makes it possible to generate humanlike two-degree of freedom motions with coupled non-orthogonal actuation [14] [24] [25].

4.1 Mechanism Structure and Motion Analysis

Figure 4-1 shows the anthropomorphic motion. The 3D view, structure and assembly of the designed DUAJ wrist are respectively shown in Figure 4-2, Figure 4-3 and Figure 4-4.

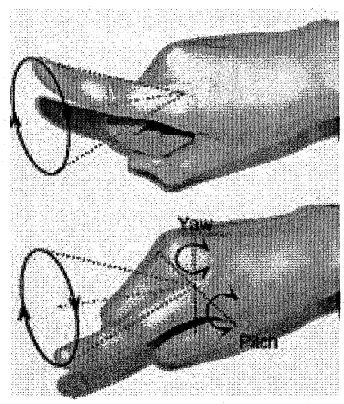

Figure 4-1: Swiveling of index finger and anthropomorphic motion*

****Notes: for position analysis and force analysis in later sections, the symbols and the figures: Figures 4-1, Figure 4-5 to Figure 4-8 are from references [14] [24] [25].***

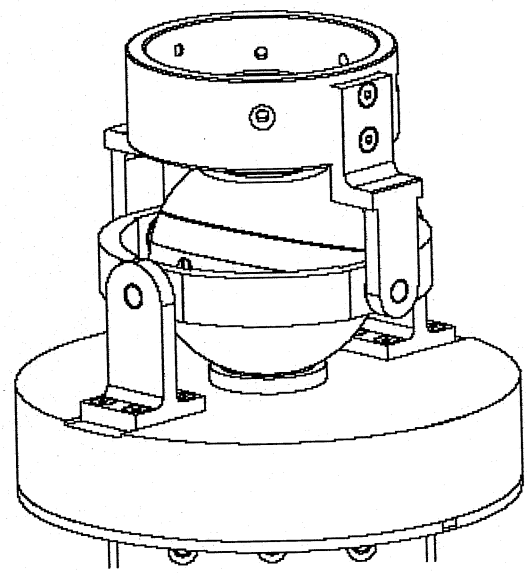

Figure 4-2: 3D view of DAUJ Joint with Pitch and Yaw motions

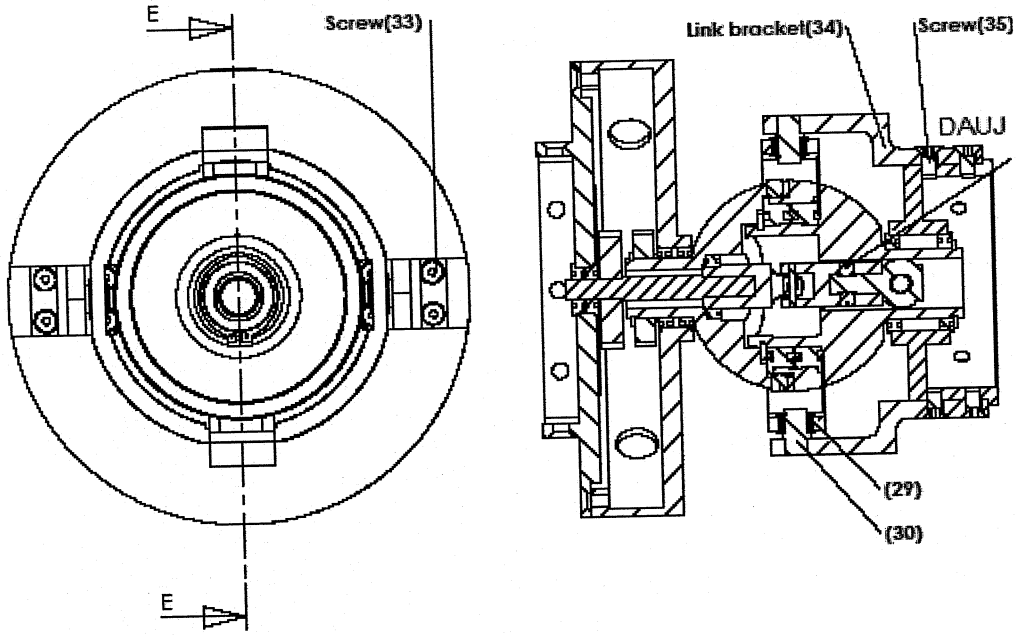

Figure 4-3: Structure of DAUJ Joint Assembly

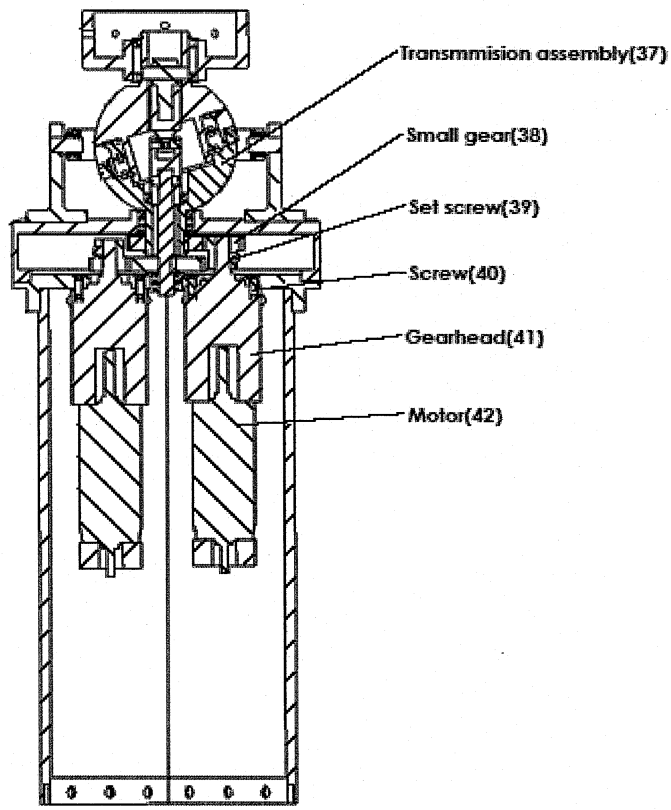

Figure 4-4: Anthropomorphic Joint with link

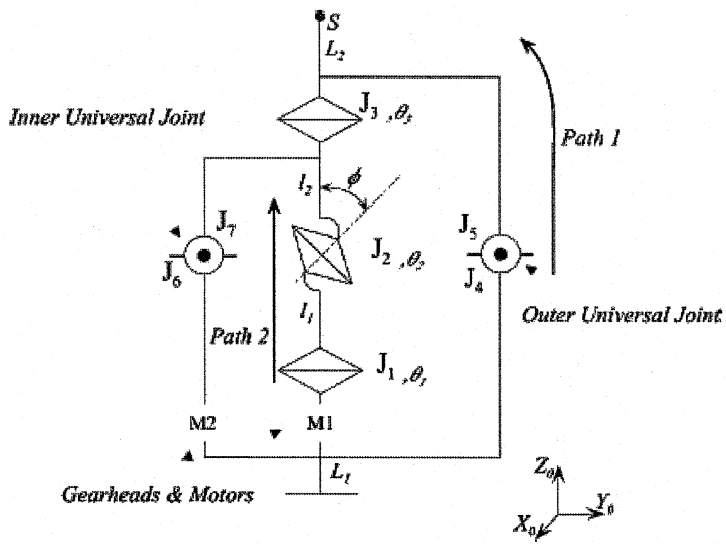

Figure 4-5: Kinematic diagram*

Figure 4-5 shows the simplified kinematic diagram of the anthropomorphic joint. J_i and θ_i denote the i-th joint and the joint angles, respectively. l_i is the distance between the joints. L_i represents the i-th link. In the proposed mechanism, the joints J_1 and J_3 are active joints. The outer and inner universal joints are passive joint couples J_4, J_5 and J_6, J_7, respectively. The joint J_2 is inclined at angle φ, and two passive universal joints around J_2 prevent the relative motions between link L_1 and L_2 from rolling along the link axis. DAUJ has two geared DC motors with reduction mechanisms. Also, two encoders are used for position measurement.

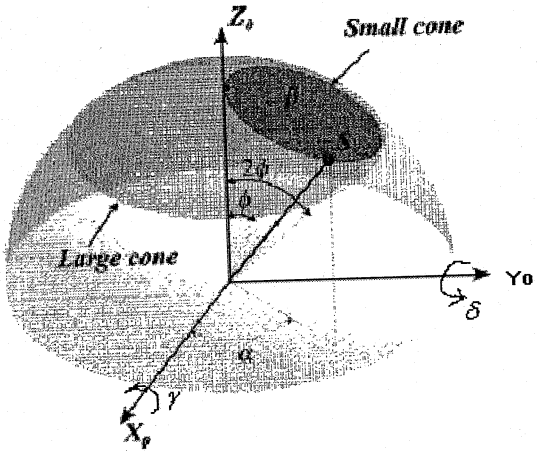

Figure 4-6: Workspace of DAUJ*

The proposed workspace is shown in Figure 4-6. The center of the sphere is the centre of the two degrees rotation, and S is the end of the second link. If θ_1 is fixed, only θ_2 is changed, a small cone is obtained. The large cone means the workspace obtained by varying θ_1. So the total workspace becomes the large cone generated by rotating the outer edge of the small cone slanted at the angle 2φ. In this figure, α and β denote longitudinal and latitudinal angles, respectively.

References [14] [24] and [25] prove the free of rolling characteristics and give the basic position analysis and force analysis about this DAUJ joint. But the provided formula can not be used directly and need to be modified for our application task: the force control of the manipulator. In the new manipulator, we need to know the direct forward kinematics (from the motor input angles θ_1 and θ_3 to the output angles δ (Pitch) and γ (Yaw) of the outer universal

joint link) and their inverse kinematics. Also we must know the direct force relationship between the motor torques τ_1 and τ_3 and the outer universal link torques τ_δ and τ_γ.

Reference [24] gives the forward kinematics (input: θ_1 θ_2 θ_3 output: δ γ) and their inverse kinematics. Since the structure of universal joint only allows two degree of freedom (δ and γ), the three joint variables θ_1, θ_2 and θ_3 are not independent and thus, θ_2 should be obtained as a function of θ_1 and θ_3. But the relationship is not provided. In the following published paper reference [14], it said this way is too complicated to get a solution.

Reference [25] uses a temporary variable θ_2' denotes the difference between the active rotations θ_3 and θ_1 ($\theta_2' = \theta_3 - \theta_1$). It gives the forward kinematics (input: θ_1 θ_2' θ_3 output: α and β) and their inverse kinematics. But the output α and β are not our needed variables δ and γ.

Reference [14] provides the forward kinematics (input: θ_1 θ_3 output: α and β) and their inverse kinematics. Similarly, the outputs are not our expected angles δ and γ. On the other hand, only reference [14] analyzes the force relationship. But it is the force relationship between the motor torques τ_1 and τ_3 and the torques τ_α and τ_β. We also need to derive the direct force relationship between the motor torques τ_1 and τ_3 and the outer universal link torques τ_δ and τ_γ.

In order to satisfy the application requirements, the following position analysis and force analysis provide a final complete solution.

4.2 DAUJ Wrist Position Analysis

DAUJ has an internal oblique joint which controls the joint rotation. It consist of an upper and a lower half sphere that meet each other in an inclined plane with angle φ as illustrated in Figure 4-5. Figure 4-7 describes the kinematic parameters and the frame assignments for the proposed mechanism. The coordinate frame Σ_2 is assigned to the internal oblique joint; the reference coordinate frame Σ_0 is fixed to the base of the mechanism. Because the inner universal joint just transmits the torque of the second motor to the joint 3, we can assign the coordinate frame Σ_3 to J_3 and the coordinate frame is attached to the rotation axis of the first motor.

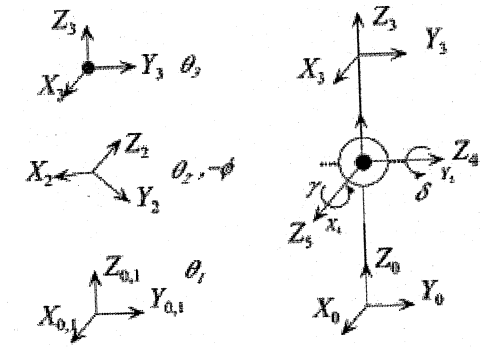

Figure 4-7: Kinematic parameters and frame assignments*

Also the outer universal joints output variables δ (pitch) and γ (yaw) are assigned coordinate frame Σ_4 and Σ_5, respectively. Then, the transformation matrix from Σ_0 and Σ_3 is able to be derived two different paths, path 1 and path 2 shown in Figure 4-5. And the results should satisfy the relation as follows:

$$ {}^0_3T(\delta,\gamma)={}^0_3T(\theta_1,\theta_2,\theta_3) \tag{4-1} $$

From (4-1) it can be assured that all the three joint variables θ_1, θ_2 and θ_3 are not independent and one of them typically θ_2 can be expressed as a function of θ_1 and θ_3. The followings are the results:

$$ {}^0_3T(\theta_1,\theta_2,\theta_3)=\begin{bmatrix} c_1c_2c_3-c_2c_\phi^2s_1s_3-c_3c_\phi s_1s_3-c_1c_\phi s_3s_2-s_1s_3s_\phi^2 \\ c_3c_2s_1+c_1c_2c_\phi^2s_3+c_1c_3c_\phi s_2-c_\phi s_1s_2s_3-c_1s_3s_\phi^2 \\ c_\phi s_3s_\phi-c_2c_\phi s_3s_\phi-c_3s_2s_\phi \\ 0 \end{bmatrix} $$

$$ \begin{bmatrix} -c_3c_2c_\phi^2s_1-c_1c_2s_3-c_1c_3c_\phi s_2+c_\phi s_1s_2s_3-c_3s_1s_\phi^2 & -c_\phi s_1s_\phi+c_2c_\phi s_1s_\phi+c_1s_2s_\phi & 0 \\ c_1c_2c_3c_\phi^2-c_3c_\phi s_1s_2-c_2s_1s_3-c_1c_\phi s_2s_3+c_1c_3s_\phi^2 & c_1c_\phi s_\phi-c_1c_2c_\phi s_\phi+s_1s_2s_\phi & 0 \\ c_3c_\phi s_\phi-c_3c_2c_\phi s_\phi+s_2s_3s_\phi & c_\phi^2+c_2s_\phi^2 & 0 \\ 0 & 0 & 1 \end{bmatrix} \tag{4-2} $$

=

$$ {}^{0}_{3}T(\delta,\gamma)={}^{0}_{4}T(\delta)\,{}^{4}_{5}T(\gamma)\,{}^{5}_{3}T(y,-\frac{\pi}{2}) \tag{4-3} $$

$$ = \begin{bmatrix} c_\delta & s_\delta s_\gamma & c_\gamma s_\delta & 0 \\ 0 & c_\gamma & -s_\gamma & 0 \\ -s_\delta & c_\delta s_\gamma & c_\delta c_\gamma & 0 \\ 0 & 0 & 0 & 1 \end{bmatrix} $$

From above Equations (4-1), (4-2) and (4-3) a constraint equation for the joint variable θ_1, θ_2 and θ_3 can be obtained as follows:

$$ \theta_2 = \frac{-s_{13}}{|s_{13}|}\arccos\left(\frac{|c_{13}|w_1 + c_{13}w_2}{c_{13}w_3}\right) \tag{4-4} $$

where

$$ w_1 = c_\phi c_{13}\sqrt{c_\phi^2 + (c_3^2 - c_1^2)s_\phi^2} $$
$$ w_2 = -c_1 s_3 s_\phi^2 (c_3 s_1 + c_1 c_\phi^2 s_3) $$
$$ w_3 = (c_1^2 c_\phi^2 + s_1^2)(c_3^2 + c_\phi^2 s_3^2) $$

The solution for forward kinematics becomes:

$$ \delta = \arctan 2(c_3 s_2 s_\phi - c_\phi s_3 s_\phi + c_2 c_\phi s_3 s_\phi, c_1 c_2 c_3 - c_3 c_\phi s_1 s_2 - c_2 c_\phi^2 s_1 s_3 - c_1 c_\phi s_2 s_3 - s_1 s_3 s_\phi^2) \tag{4-5} $$

$$ \gamma = \arctan 2(-c_1 c_\phi s_\phi + c_1 c_2 c_\phi s_\phi - s_1 s_2 s_\phi, c_1 c_2 c_3 c_\phi^2 - c_3 c_\phi s_1 s_2 - c_2 s_1 s_3 - c_1 c_\phi s_2 s_3 + c_1 c_3 s_\phi^2) \tag{4-6} $$

And the inverse kinematics becomes:

$$ \theta_2 = \pm\arccos\left(\frac{c_\delta c_\gamma - c_\phi^2}{s_\phi^2}\right) \tag{4-7} $$

$$ \theta_1 = -\frac{|s_\delta|}{s_\delta}\arccos\left(\frac{c_\gamma s_2 s_\delta s_\phi - s_\gamma\sqrt{c_\gamma^2 s_\delta^2 + s_\gamma^2 - s_2^2 s_\phi^2}}{c_\gamma^2 s_\delta^2 + s_\gamma^2}\right) \tag{4-8} $$

$$ \theta_3 = \arctan 2\left(\frac{-c_\phi s_\delta - c_\delta s_1 s_\phi}{s_\phi}, \frac{c_\delta c_\phi s_\gamma + c_1 c_\gamma s_\phi - s_1 s_\gamma s_\delta s_\phi}{s_\phi}\right) \tag{4-9} $$

Using a geometric approach, the above problem is easier to solve. Figure 4-8 depicts an equivalent kinematic diagram of the DAUJ by eliminating the inner universal joint. In the derivation Z-Y-Z Euler angle description is employed to exploit the characteristic of the mechanism. According to Z-Y-Z Euler angle representation, the rotation of the joint can be

considered to be performed in the following order: rotation about $\hat{Z}$ axis by α, rotation about negative $\hat{Y}'$ axis by β, and rotation about $\hat{Z}''$ axis by $-\alpha$.

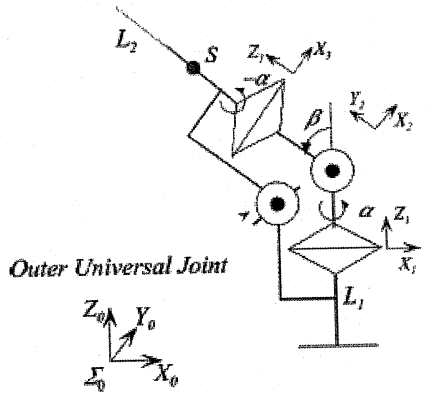

Figure 4-8 Generalized coordinate frame assignment for DAUJ*

The transformation matrix becomes

$$
\begin{aligned}
{}^{0}_{3}T_{ZY'Z''} &= T_Z(\alpha)T_{Y'}(\beta)T_{Z''}(-\alpha) \\
&= {}^{0}_{3}T(\alpha,\beta) \\
&= \begin{bmatrix}
c_\alpha^2 c_\beta + s_\alpha^2 & c_\alpha c_\beta s_\alpha - s_\alpha c_\alpha & -c_\alpha s_\beta & 0 \\
s_\alpha c_\beta c_\alpha - c_\alpha s_\alpha & s_\alpha^2 c_\beta + c_\alpha^2 & -s_\alpha s_\beta & 0 \\
s_\beta c_\alpha & s_\beta s_\alpha & c_\beta & L_1 \\
0 & 0 & 0 & 1
\end{bmatrix}
\end{aligned}
\tag{4-10}
$$

where the reverse rotation $-\alpha$ about $\hat{Z}''$ axis is due to the characteristics of the proposed mechanism that restricts rolling, and L_1 is zero because Σ_0 and Σ_1 have the same origin.

Consequently, we have

$$
{}^{0}_{3}T(\alpha,\beta) = {}^{0}_{3}T(\theta_1,\theta_2,\theta_3)
$$

The relationships between the variables θ_1, θ_3 and α, β are derived as follows:

$$
\alpha = \frac{\theta_1 + \theta_3}{2} + \pi \tag{4-11}
$$

$$
\beta = 2\arctan(\tan\phi\cos\frac{\theta_3 - \theta_1}{2}) \tag{4-12}
$$

The inverse kinematics can be solved by using (4-11) and (4-12),

$$\theta_1 = \alpha \pm \arccos(\cot\phi \tan\frac{\beta}{2}) - \pi \tag{4-13a}$$

$$\theta_3 = \alpha \mp \arccos(\cot\phi \tan\frac{\beta}{2}) - \pi \tag{4-13b}$$

To derive the required pitch and yaw angles in Figure 4-6, firstly, the orthogonal coordinates of S given by S (*Xs*, *Ys*, *Zs*), then we have,

$$\begin{aligned} X_s &= L\sin\beta\cos\alpha \\ Y_s &= L\sin\beta\sin\alpha \\ Z_s &= L\cos\beta \end{aligned} \tag{4-14}$$

From above Equation (14), the pitch δ and yaw γ become

$$\delta = \arctan 2(X_s, Z_s) \tag{4-15a}$$

$$\gamma = \arctan 2(Y_s, Z_s) \tag{4-15b}$$

For solving inverse kinematics, due to (14) and (15), we have,

$$\alpha = \arctan 2(Ys, Xs)$$

as

$$\alpha = \arctan 2(Ys/Zs, Xs/Zs)$$

so

$$\alpha = \arctan 2(\tan\gamma, \tan\delta) \tag{4-16a}$$

From Equation (4-15a),

$$\beta = \arctan 2(\tan\delta, \cos\alpha) \tag{4-16b}$$

Equations (4-11) to (4-16) provide the required forward kinematics (from variables θ_1 and θ_3 to link output δ and γ) and the inverse kinematics or future application.

4.3 DAUJ Wrist Force Analysis and Torque Relationship

For the force control of the mobile manipulator, References [14], [24] and [25] can not provide a proper force analysis for the application such as door opening task. The toques of pitch and yaw (τ_δ and τ_γ) should be analyzed.

Differentiating the above Equations (4-11) and (4-12), we have

$$\dot{\alpha} = \frac{\dot{\theta}_1 + \dot{\theta}_3}{2} \tag{4-17a}$$

$$\dot{\beta} = -\Omega \bullet (\dot{\theta}_1 - \dot{\theta}_2) \tag{4-17b}$$

where

$$\Omega = \frac{\sin\frac{\theta_1 - \theta_3}{2}\tan\phi}{1 + \cos^2\frac{\theta_1 - \theta_3}{2}\tan^2\phi} \tag{4-17c}$$

Thus, the angular velocity relationship becomes,

$$\omega_1 = J_1 \cdot \dot{\theta} \tag{4-18}$$

or
$$\begin{bmatrix} \dot{\alpha} \\ \dot{\beta} \end{bmatrix} = J_1 \begin{bmatrix} \dot{\theta}_1 \\ \dot{\theta}_2 \end{bmatrix}$$

where $\dot{\theta} = [\dot{\theta}_1, \dot{\theta}_3]^T$, $\omega_1 = [\dot{\alpha}, \dot{\beta}]^T$ and the Jacobian J_1 expressed in the frame Σ_0 is derived by

$$J_1 = \begin{bmatrix} \frac{1}{2} & \frac{1}{2} \\ -\Omega & \Omega \end{bmatrix} \tag{4-19}$$

Force analysis is derived as below. The torque relationship can be expressed by the above Jacobian between ω_1 and $\dot{\theta}$. From the virtual work principle, we have

$$\tau_{13} = J_1^T \bullet \tau_{\alpha\beta} \tag{4-20a}$$

or
$$\begin{bmatrix} \tau_1 \\ \tau_3 \end{bmatrix} = J_1^T \begin{bmatrix} \tau_\alpha \\ \tau_\beta \end{bmatrix} \tag{4-20b}$$

where $\tau_{\alpha\beta} = [\tau_\alpha, \tau_\beta]^T$ and $\tau_{13} = [\tau_1, \tau_3]^T$. Also the inverse torque equation yields,

$$\tau_{\alpha\beta} = (J_1^T)^{-1} \cdot \tau_{13} \tag{4-21}$$

The above Equations (4-20) and (4-21) have theoretical meaning. In practice, they should be extended to the toques of Pitch and Yaw (τ_δ and τ_γ) acting on the output link of the outer universal joint.

According to the definition of Jacobian, define the following:

$$\begin{bmatrix} \dot{\delta} \\ \dot{\gamma} \end{bmatrix} = J_2 \begin{bmatrix} \dot{\alpha} \\ \dot{\beta} \end{bmatrix} \tag{4-22}$$

$$\text{or} \qquad \omega_2 = J_2 \omega_1 \tag{4-23}$$

where $\omega_2 = [\dot{\delta}, \dot{\gamma}]^T$ and $\omega_1 = [\dot{\alpha}, \dot{\beta}]^T$ while Jacobian is

$$J_2 = \begin{bmatrix} \frac{\partial \delta}{\partial \alpha} & \frac{\partial \delta}{\partial \beta} \\ \frac{\partial \gamma}{\partial \alpha} & \frac{\partial \gamma}{\partial \beta} \end{bmatrix} \tag{4-24}$$

From Equations (4-15a) and (4-15b), we know,

$$\frac{\partial \delta}{\partial \alpha} = \frac{-\tan\beta \sin\alpha}{1+\tan^2\beta\cos^2\alpha} \tag{4-25a}$$

$$\frac{\partial \delta}{\partial \beta} = \frac{\sec^2\beta\cos\alpha}{1+\tan^2\beta\cos^2\alpha} \tag{4-25b}$$

$$\frac{\partial \gamma}{\partial \alpha} = \frac{\tan\beta\cos\alpha}{1+\tan^2\beta\sin^2\alpha} \tag{4-25c}$$

$$\frac{\partial \gamma}{\partial \beta} = \frac{\sec^2\beta\sin\alpha}{1+\tan^2\beta\sin^2\alpha} \tag{4-25d}$$

Thus, Jacobian J_2 becomes,

$$J_2 = \begin{bmatrix} \frac{-\tan\beta\sin\alpha}{1+\tan^2\beta\cos^2\alpha}, & \frac{\sec^2\beta\cos\alpha}{1+\tan^2\beta\cos^2\alpha} \\ \frac{\tan\beta\cos\alpha}{1+\tan^2\beta\sin^2\alpha}, & \frac{\sec^2\beta\sin\alpha}{1+\tan^2\beta\sin^2\alpha} \end{bmatrix} \tag{4-26}$$

From Equation (4-23), the torque relationship between τ_α, τ_β and the outer universal link torques τ_δ and τ_γ becomes,

$$\begin{bmatrix} \tau_\alpha \\ \tau_\beta \end{bmatrix} = J_2^{\,T} \begin{bmatrix} \tau_\delta \\ \tau_\gamma \end{bmatrix} \tag{4-27}$$

From Equations (4-20b) and (4-27), we have,

$$\begin{bmatrix} \tau_1 \\ \tau_3 \end{bmatrix} = J_1^T J_2^T \begin{bmatrix} \tau_\delta \\ \tau_\gamma \end{bmatrix} \tag{4-28}$$

Also the inverse torque equation yields,

$$\begin{bmatrix} \tau_\delta \\ \tau_\gamma \end{bmatrix} = (J_1^T J_2^T)^{-1} \begin{bmatrix} \tau_1 \\ \tau_3 \end{bmatrix} \tag{4-29}$$

Thus, the final result is,

$$\begin{bmatrix} \tau_\delta \\ \tau_\gamma \end{bmatrix} = (J_2^T)^{-1} (J_1^T)^{-1} \begin{bmatrix} \tau_1 \\ \tau_3 \end{bmatrix} \tag{4-30}$$

Equations (4-28) and (4-30) provide the force relationship between the motor torques τ_1 and τ_3 and the outer universal link torques τ_δ and τ_γ. They can be directly used in practice.

The typical example is that a force control of manipulator is used for door opening in next Chapter 5.

Figure 4-9 shows the assembled wrist for the final experiment. The compact size is ideal for the dexterous mobile manipulation and wrist motors & electronics in its link.

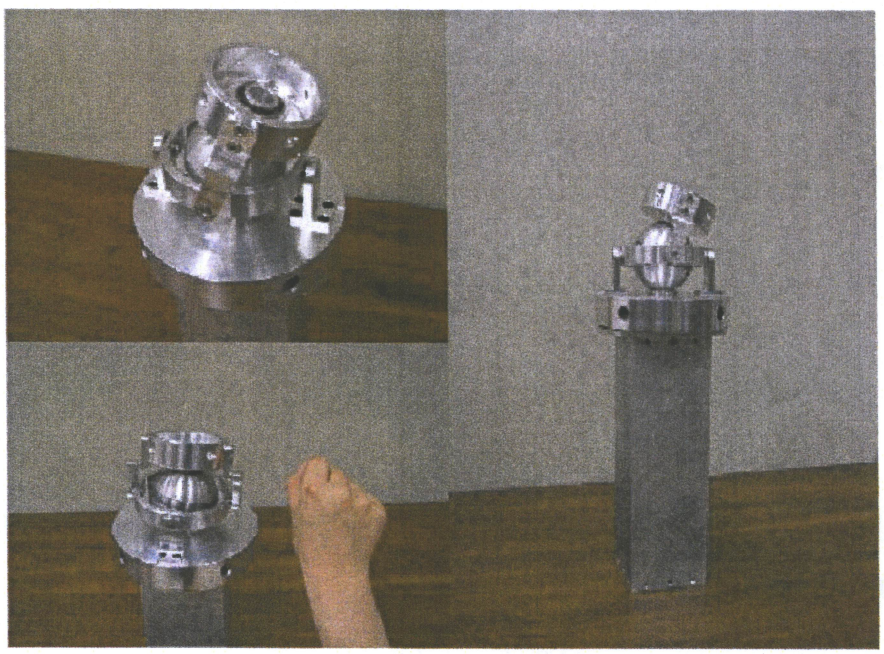

Figure 4-9: Assembled DAUJ Wrist

Chapter 5

Robot Manipulation and Door Opening Case Study

The new designed mobile manipulator aims at the manipulation in an uncontrolled environment or human being living environment. The above chapters proposed a manipulator with multiple working modes to tackle with this problem. Different from the industrial manipulator working in a controlled environment where a task can only be finished in active mode, the door opening task needs more dexterous manipulation like a human being does. These challenges need us rethinking them in a different way [1]. In this chapter, door opening task as a typical example is studied. Using our designed manipulator with multiple modes, a new manipulation method is provided and researched through simulations.

5.1 Door Opening Task Study

5.1.1 Literature Review and Research Status

In the past decade, this topic about mobile robot for opening a door has been attracting some researchers in different countries. These research groups include:

1. University of Tsukuba, 1994
2. The University of Electro-Communications, 1995
3. Massachusetts Institute of Technology, 1997
4. Technische Universität München, 1997
5. Royal Institute of Technology, 2000
6. Katholieke Universiteit Leuven, 2003
7. Korea Institute of Science and Technology (two groups), 2004

Mobile robot for opening a door is one of the typical service robots in human being living environment. Many service robots are now spreading their applications areas to our daily life [26]. However, the development of robots under the coexistence with people will depend largely

on the full integration of mobility and manipulation [27]. In the published papers on the door-opening issue by a mobile manipulator, the conventional approaches to do this task are mainly dependent upon the combination of position and compliance control. At a start, the robot gripper holds a door knob or handle, and then the robot arm tracks the pre-defined trajectory for door opening.

Nagatani and Yuta proposed general approach of the door-opening strategy [28]. It assumed that the position and radius of the door are known in order to push and open a door safely. Compliance control algorithm was applied by implementing 6 axis force/ torque sensor attached to the wrist of the manipulator [29]. They applied the concept of action primitives in order to open a door and move to other place. A vision camera was mounted on the wrist, images were obtained though it. Hough transformation algorithm calculated the principle axis and shape information of the knob [30]. The experiment is implemented on a mobile robot "YAMABICO type-TEN" with a light weight 6 degree of freedom manipulator. The vision camera is used for confirming the exact position of the knob [31].

Ohwi did research on the algorithm to determine the initial position of the mobile robot in front of a door and path the planning of the manipulator trajectory for opening a door. They gave the simulation results of a 5 DOF manipulator on a mobile robot [32].

Niemeyer and Slotine at MIT presented a simple method to follow the path of least resistance that the trajectory of the door assumes enough smooth above the least curvature. This approach requires high resolution of velocity on the wrist. If there exit a large amount of backlash, it is difficult to be implemented [33]. This approach was demonstrated on the four degree of freedom 'Whole Arm Manipulator'.

Hanebeck, Fischer and Schmidt presented another door opening performance by a mobile robot called ROMAN [34], which had a 6 DOF manipulator on a mobile platform and presented overview of service robot and module representation.

Peterson, Austin and Kragic proposed high-level control of a mobile manipulator by using compliant motion control [15]. Furthermore, the use of a hybrid dynamic system is proposed for the complicated tasks such as opening a door. They demonstrated the intelligent control architecture from finding the doorknob by visual tracking to estimating the parameters to opening door [35] [36]. The radius and the centre of rotation of the door are estimated online.

In 2004, Waarsing, Nuttin and Brussel researched the possibilities that the behavior-based paradigm has to offer when it comes to mobile manipulator. They have implemented a demo application for opening a door [37]. The robot is called LiAS which is constructed from a Router commercial platform and a CRS A465 industrial manipulator.

In 2004, two groups in Korea Institute of Science and Technology built two different mobile robots for opening a door. Rhee designed a multi-fingered robotic hand for the indoor service robot PSR-1[38]. The robot is a mobile platform and a 6 DOF robotic manipulator equipped with a multi-fingered hand. There is a CCD mono vision camera mounted on the wrist of the multi-fingered hand for finding the location of a door handle.

The most recent advance was made by Kim, Kang, Hwang and Park. They developed a special mobile robot called Hombot for opening a door [39]. Hombot has the following advantages:

First, the manipulator is a special designed anthropomorphous manipulator, and the manipulator joint mechanism is double active universal joint (DAUJ) for compact size of the manipulator [40], which was designed by other Korea researchers at Sungkyunkwan University, Korea.

Second, the vision system for the object recognition is driven by a pair of stereo camera which is mounted on the locomotion system (not on the manipulator or the hand wrist). The visual servoing is for the end-effector to grasp the doorknob and aligning the gripper with doorknob. The visual system is also used for the mobile robot navigation at KIST [41].

Moreover, cheap force sensors are employed for the information of door opening task instead of expensive JR3 sensor to effectively reduce the cost in robot [16]. They presented a simple control method for opening a door from the viewpoint of the mobile manipulation. From three components of applied forces which was directly obtained by the three-axis force sensor and three components of applied forces which was indirectly estimated by the joint-torque sensors, all of joint-torques that will exactly balance forces at the end-effector in the static situation can be found. It is more practical method than using a six-axis force sensor in a wrist . Experimental results has shown that the opening a door can be more effectively from the suggested control method of mobile manipulation.

Finally compliant control is used in the door opening process. The mobile platform moves in the door opening process and needs path planning. Figure 5-1 shows the whole process.

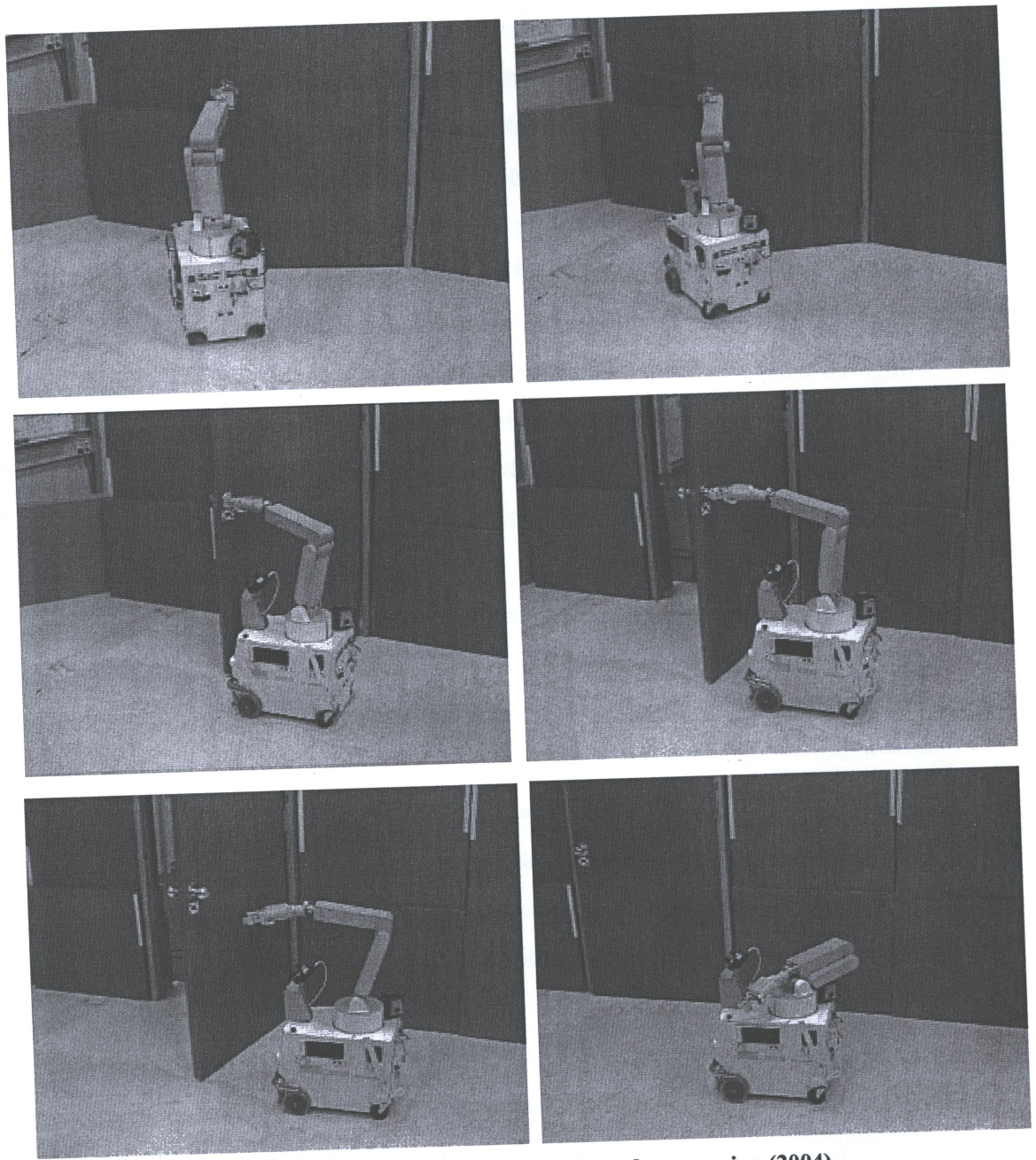

Figure 5-1: Service robot HomBot for door opening (2004)

Compliant control of the manipulator is important for the door opening task. When the robot moves on the planned path while pulling the door, position and orientation errors of the robot may result in large forces in the end-effector. Therefore, we have to control the end-effector compliantly along the vertical plane axis of the doorknob using the force sensor on the wrist. The relaxation of the end-effector is performed by the compliant control. The compliant control is

realized as follows. The force sensor located at the gripper of the manipulator detects force of the end-effector; the reference position of the end-effector is shifted to detected force direction.

In summary, first, the above publications used position control combined with force compliant control. The door parameters such as the radius are known [28] or should be estimated [15]. Compliant control can relax the gripper to shift to the direction of detected force; second, the manipulators are either industrial commercial manipulator or special designed manipulator. The vision cameras are used to detect the position for gripper holding the knob [15] [16] [38] or for robot navigation [41]; third, the mobile platform needs a path planning [16]. Even using a behavior-based control, the basic idea is still based on normal manipulator plus mobile platform. When the environment is changed, such as different radius of the door, the position control will be difficult to get precise points and the compliant force control is limited to a small shift distance.

5.1.2 Door Opening Requirement and Process Analysis

The basic requirement for door opening is to provide a minimum moment to balance the friction on the pivot of the door.

$$J_d \ddot{\theta}_d = F \bullet r - M_f \tag{5.1}$$

where J_d – The moment of inertia of the door

θ_d – The rotated angle of the door

r – The radius of the door between the pivot and the knob

M_f – The minimum moment caused by friction

F – The required force acting on the knob and vertical to the surface

If the door opening process is very slow, the acceleration of the door can be considered as small or zero. And then the required force is close to a constant value:

$$F = M_f / r \tag{5.2}$$

During the door opening process, the direction of the pulling force F is always changed, and the gripper of the manipulator is on the circle with radius (r). Consider the gripper length known as a, the wrist centre is on the bigger circle with radius ($\sqrt{r^2 + a^2}$).

If the position control of the manipulator is used in the door opening, the gripper position must fellow the circle as the target trace, so the radius must be known for the robot. But online

estimation of the radius is not an easy job. If the error of the tracing is not small enough, the caused internal force of the gripper and manipulator will damage the manipulator, so a compliant force control or a mechanical RCC must be used. The published papers used this method. This method comes from the manipulation in a controlled environment such as workshop or a production assembly line. In a controlled environment, the important trace parameters are known or easy identified by measuring, and then the position controls are successfully used. But for an uncontrolled environment, the trace parameters become difficult to get, door opening job is still a challenge [1].

After carefully observing the door opening operation process of human beings, we find that the whole process can be divided into two stages: First, human beings use vision system to detect the knob and direction of the trend of the door movement. The visual guided position control of the manipulator is used to close the knob and hold the knob.

Second, after rotated the knob and holding it, the door is pulled open, the wrist is relaxed and even the elbow is also relaxed, the compliance is greatly increased, and the trace of the knob circle does not need to be estimated. Human beings can close their eyes. The vision system does not work. They can try a force to let the door move. The pulling process should be a force control of the manipulator.

From the viewpoint of the manipulator, the gripper always suffers a pulling force during the process. Although the direction is changed in the spatial frame which is attached to the platform base, but in the tool frame attached on the gripper, the direction is always along the roll axis of gripper and vertical to the door surface. In the tool frame, the forces and moments around other axes (yaw axis and pitch axis) can be null. In wrench description, it means $F_b = [0, F, 0, 0, 0, 0]$. This will be used in the simulations in the next section.

How to use the force control in our mobile MRR manipulator and how to run the proposed multiple working modes are in the following section.

5.2 Passive Mode Control and Force Control

Firstly, let us simplify the problem in planar manipulator. The gravity compensation problem is ignored. But it unveils the nature of the force control. During opening a door, the manipulator should provide a desired pulling force to replace position control. The parameters of

the door radii are not necessary to estimate, and then the manipulation can adapt to the uncontrolled environment. The pulling force can be preset for different doors.

Figure 5-2 shows a planar model of the door opening process. The door opening motion is assumed to be planar and follow an arc trajectory in the x-y plane with a centre of rotation at (x0, y0) and a radius r. Assume that the gripper holds the door handle or knob firmly, and the handle position (x, y) during the door opening process forms the gripper's trajectory. The following relation has to hold:

$$r^2 = (x - x_0)^2 + (y - y_0)^2 \tag{5.3}$$

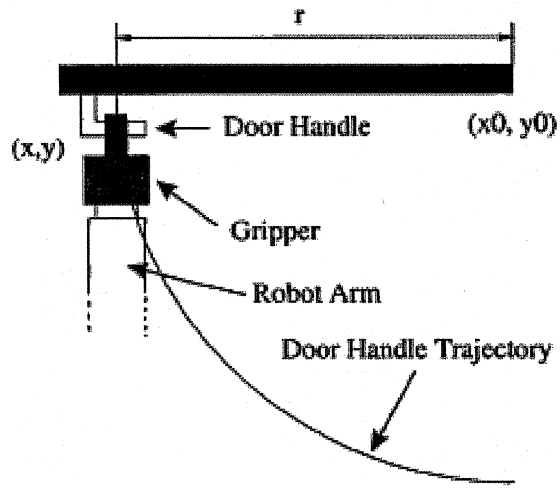

Figure 5-2: A planar model of door opening

With only active working mode, the mobile platform needs to move continually in the whole door opening process while all joints of the manipulator are under active control. The disadvantages associated with such a door opening approach include: 1) complicated control techniques such as compliant motion control and predictive control are required [19]; 2) a precise path or motion planning is required for the mobile platform and all joints of the manipulator, which involves accurate kinematics models and solving complex matrix equations [20]; and 3) the door parameters such as the rotation center and the distance between the pivot and the knob have to be estimated on-line.

Figure 5-3 illustrates the process of opening a door using a three joints planar manipulator. After the gripper opens the door lock, the second joint and the third joint are switched to passive

mode, and only the first joint is still in active mode and under position control. In Figure 5-3, the three links are assumed rigid. As assumed, the gripper has held the door handle or knob firmly. At this point, Joint 1 remains in an active control mode, but Joints 2 and 3 are switched to passive mode. After Joint 1 moves to, the two passive joints will rotate to and move to, respectively, due to external torques. The door is rotated from the initial OA position to the OA' position:

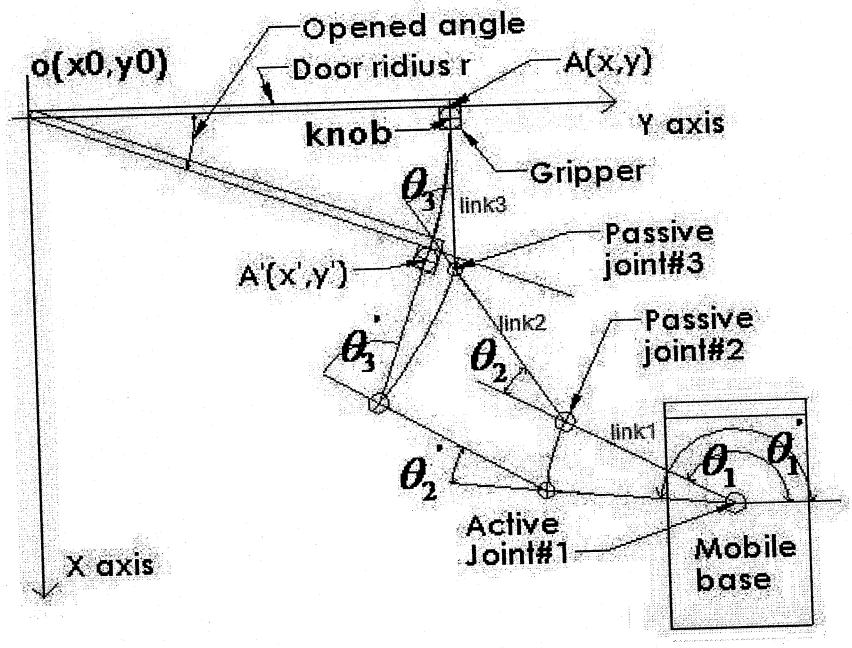

Figure 5-3: Door opening procedure with two passive joints and one active joint

During this process, only the trend of the door's rotation is known to the robot controller. After the door is opened to a certain angle, the mobile platform moves to next position, and the manipulator repeats the above process until the door is fully opened. The path planning for the mobile platform is greatly simplified as there is no need for a continuous path. The mobile platform needs only to stop at a proper area (not a point), which is similar to what human being does.

From this simple case study, we can see that mobile manipulators with the proposed multiple mode control create behaviors closer to those of human being, leading to substantial improvement in abilities to adapt to complicated human environments.

In nature, the passive mode control is one of the situations of force control. The torque output of the robot joint is zero. When the manipulation is in 3D space, the following force control of a 6 DOF manipulator will be applied.

5.3 Six DOF Manipulator Door Opening Process

5.3.1 Process Analysis and Force Control

The Figure5-4 shows the mobile manipulator used for door opening process and coordinate relationship between spatial frame and tool frame.

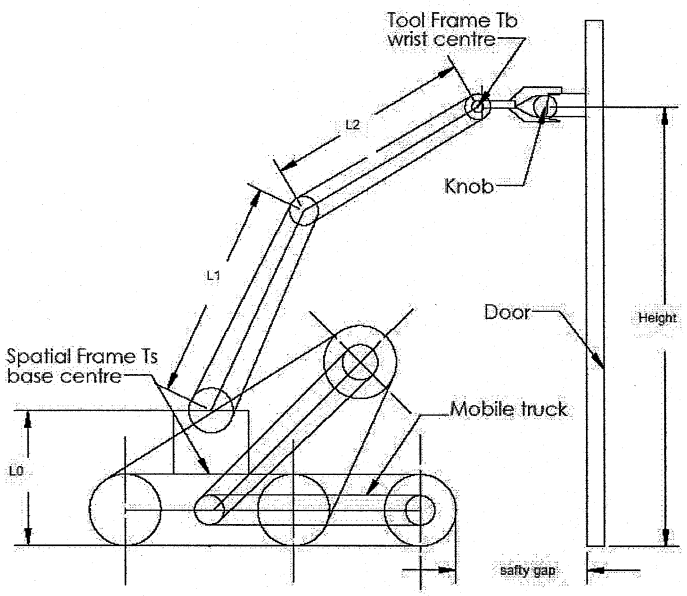

Figure 5-4: Door opening process and coordinate relation

The manipulator model is demonstrated in former chapter 3 and the description of the wrist model is given in former chapter 4. In this section, the above models especially the torque relationship of DAUJ wrist and the Jacobian Matrix will be used in the force control of the proposal manipulator. When using the multi proposal manipulator in door opening process, we have,

Stage 1: Motion Control

As the mobile robot platform moves in front of the door at a proper position, because the mobile manipulator needs to hold the knob, all the modular joints are in the active mode and the control method is motion control (position control), each joint's rotation angle or position can be measured while a camera or other method such as a laser sensor, or an indoor GPS can be used for the feedback signal. All these methods have been studied and published in the past decade.

Stage 2: Force control

After the mobile manipulator holds the door knob, the position of the end-effecter is fixed and perpendicular to a door, the control strategy of each modular joint is force control, the torque should be measured.

Stage 3: Passive mode

After the door is opened at an angle such 15~20 degrees, the mobile robot platform begins to move to the next position. (The position becomes an area but a point, the restrict path planning does not need.) Each joint of the manipulator such as the waist, the shoulder, the elbow and the wrist joint should be switched in a passive mode, so the mobile platform can move freely. This greatly improves the range and makes it easy for the mobile manipulator movement and operation. A proper posture of the mobile manipulator is easy to find for next manipulation.

From the above analysis, the new designed modular joint has multi-proposal functions, which greatly enhance the dexterous application in practice.

In the force control, the relationship between static forces and the corresponding joint torques is defined by the Jacobian matrix. Generally, the transformation of the forces and torques acting on the end-effector into corresponding each manipulator's joint torque is described as follows:

$$\tau = J^T f \tag{5.4}$$

where τ is the vector of joint torques of the manipulator;

f is the vector of force acting on the end-effector; and

J^T is the transpose of Jacobian matrix of the manipulator

The above Equation (5.4) is in the spatial frame. When using the wrench (force) in tool frame, the relationship is in former section 3.2.1. That is the following:

If B is a coordinate frame attached to a rigid body, then we write $F_b = (f_b, \tau_b)$ for a wrench applied at origin of B, with f_b and τ_b specified with respect to the B coordinate frame. If C is a second coordinate frame, then we can write $F_b = (f_b, \tau_b)$ as an equivalent wrench applied at C:

$$F_c = Ad^T_{g_{bc}} F_b \,. \tag{5.5}$$

For a rigid body with configuration g_{ab}, $F^{s} := F_{a}$ is called the spatial wrench and $F^{b} := F_{b}$ is called the body wrench.

From Equations (5.4), (5.5) and the Jacobian Matrix Equations (3.63) ~ (3.70), we can get the torques of each joints. For DUAJ joint, the torques of the 4th joint and 5th joint can be converted to the torques of the two motors in DUAJ wrist though Equations (4-28) and (4-30), which provide the force relationship between the motor torques τ_1 and τ_3 and the outer universal link torques τ_δ and τ_γ. They can be directly used in practice.

For the simulation of the whole process, we must firstly solve the inverse kinematics of the manipulator, and then use the above force relations. In solving the inverse kinematics the origin of the coordinate is at the intersection of the pivot axis and the ground. The wrist centre and the gripper (holding the knob) are on a horizontal plane and the traces are two circles.

The above calculations are attached in Appendix B. Inverse kinematics and force control simulations. File name: elbowink2.m and elbow2.m.

5.3.2 Door Opening Simulation

1. Inverse kinematics MATLAB simulation result (Filename: elbowink2.m)

Simulation Parameters:

Mobile base cart (yellow):

Type: L-LMA (ESI Inc. Toronto)

Length: 700 (mm)

Height: 170 (mm)

Width: 510 (mm)

Manipulator: Modular Multi-proposal Manipulator (blue)

Height: (to 2nd joint axis) L0 = 450 (mm)

Length of link: L1 = L2 = 380 (mm)

Length of the gripper: 200 (mm)

Door: Regular office door (red)

Height of the knob: 1010 (mm)

Width of the door: 900 (mm)

Distance between the door pivot and the knob (Radius): 800 (mm)

The origin of coordinate is at the intersection of the door pivot and the ground. The results are shown in Figure 5-5, Figure 5-6 and Figure 5-7.

2. Mobile Manipulator Simulation

The origin of above coordinate is on the mobile cart and at the intersection of 1st joint axis and the ground. Using Force Control to provide a pull force which is along the gripper handle and always vertical to the door surface. The pull force gives the minimum moment to open a door. Normally the required pull force is from 20~30 N. And the required moment is about 16~24Nm.

The results are shown in Figure 5-8 and Figure 5-9.

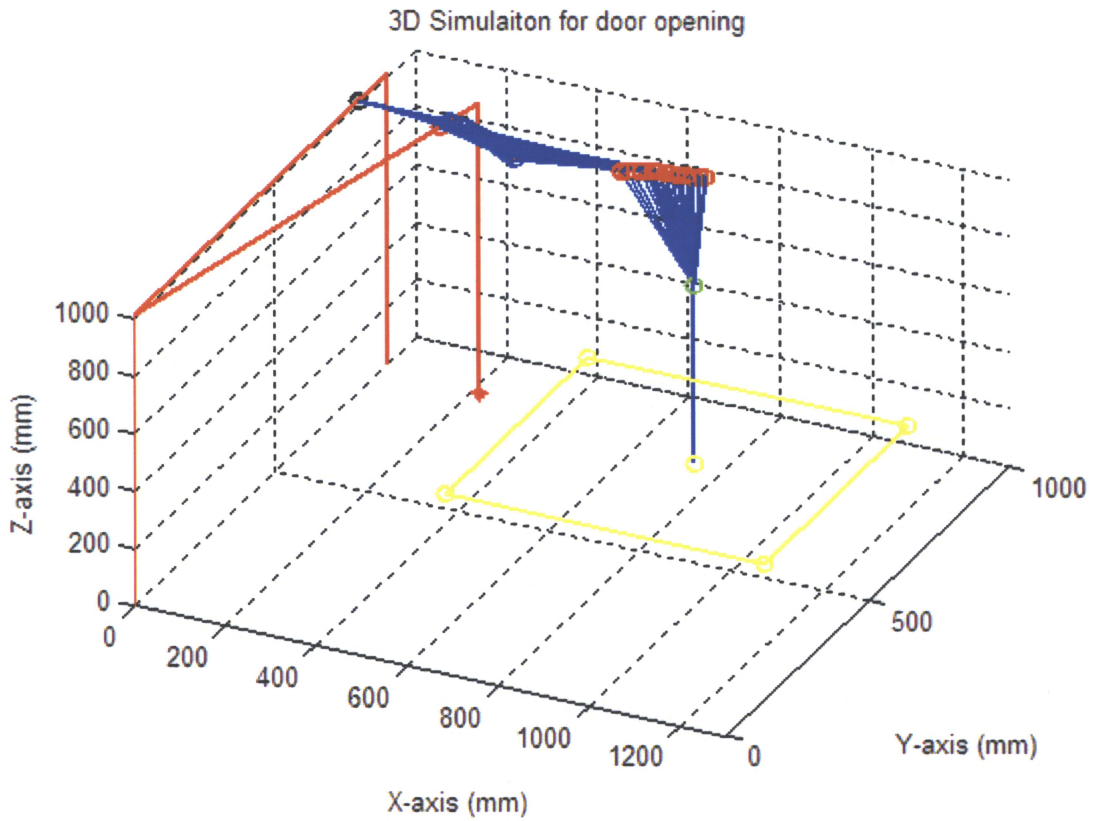

Figure 5-5: Simulation for door opening process (T1=0)

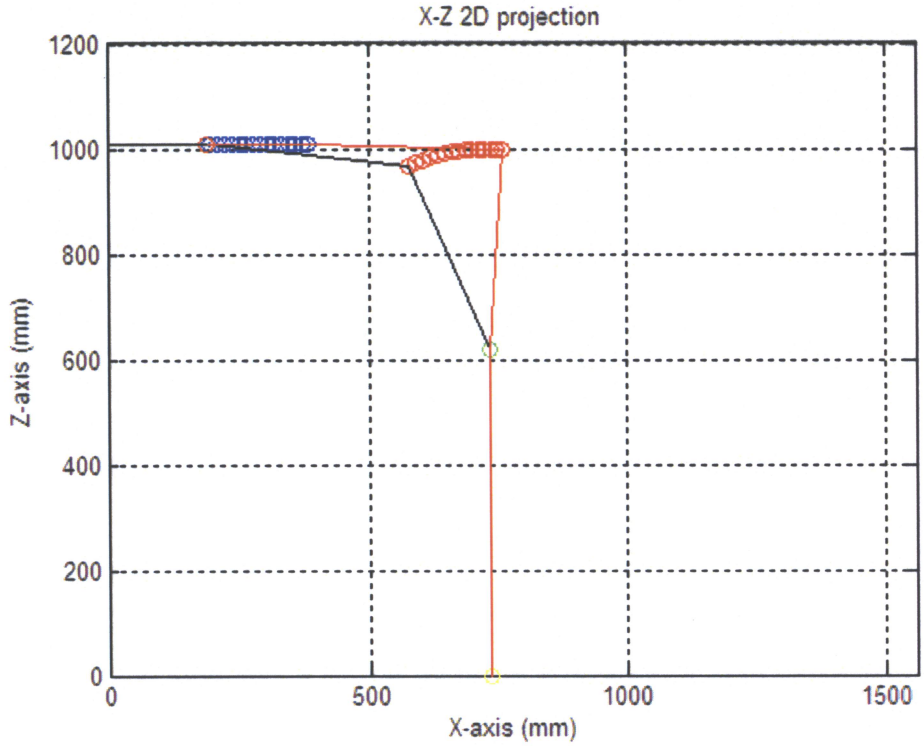

Figure 5-6: X-Z Projected Vision (T1=0)

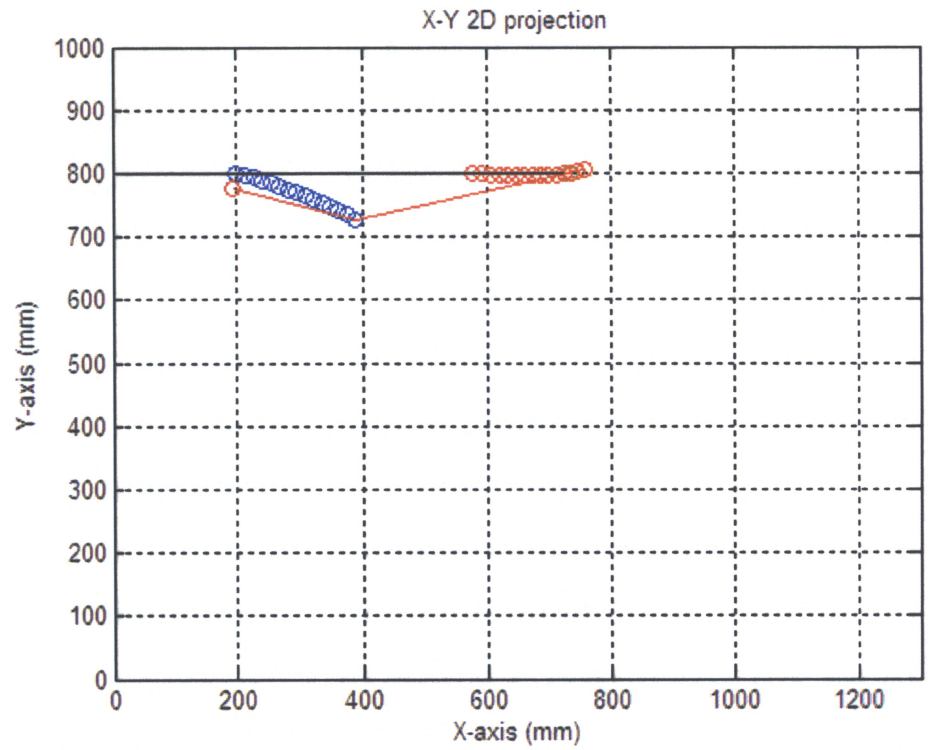

Figure 5-7: X-Y Projected Vision (T1=0)

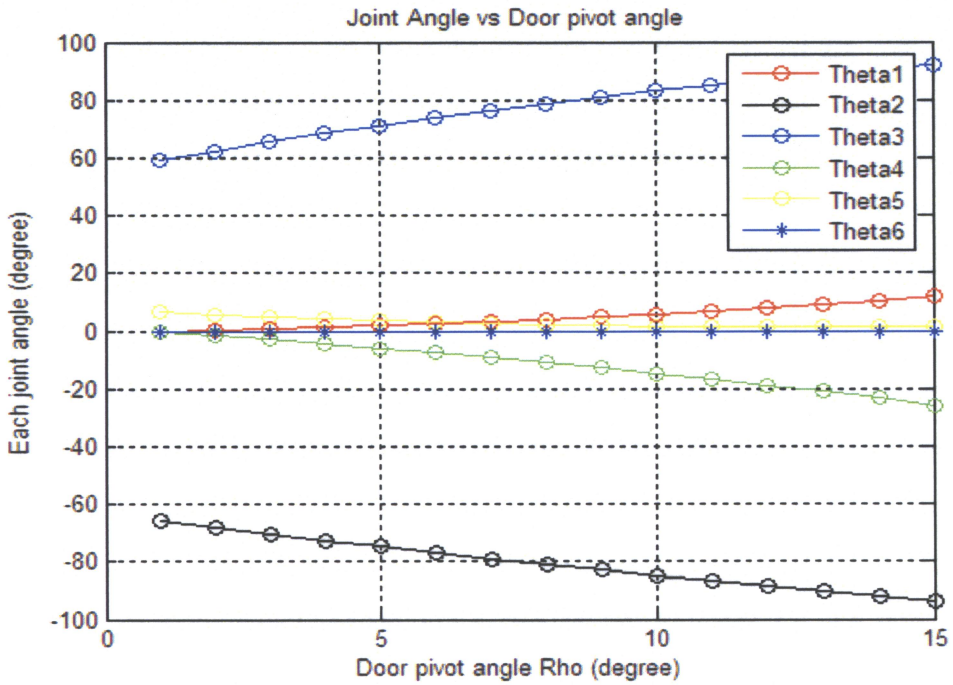

Figure 5-8: Joint angles in door opening process (T1=0)

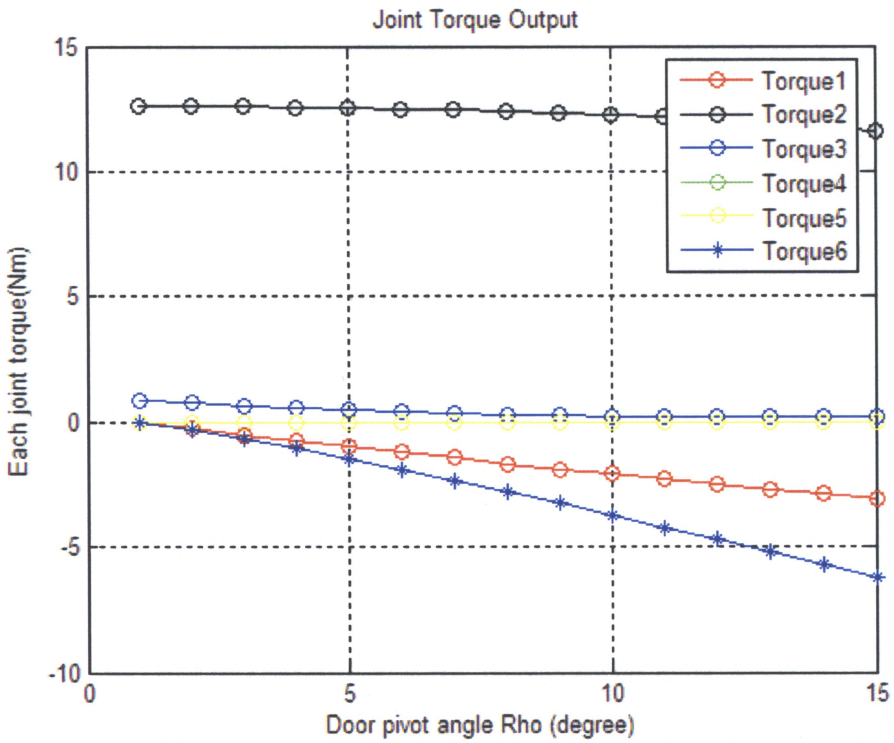

Figure 5-9: Torque output of each joint without gravity compensation (T1=0)

5.4 Initial Position Effects and Gravity Compensation

The gravity and initial positions have effects on the final force control of each joint. Considering these effects, we have following analysis and results.

5.4.1 Gravity Compensation

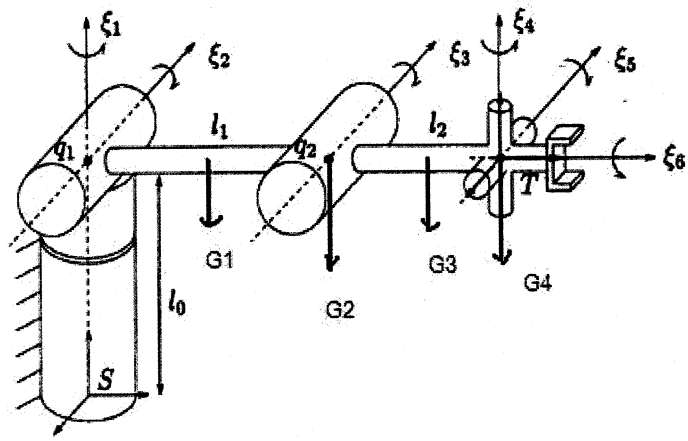

Figure 5-10: Gravity compensation for the elbow manipulator

In Figure 5-10, the weights of links and joints are considered. For the elbow manipulator, the origin of the spatial frame is at the intersection of the first joint axis and the ground. The direction of the gravity is always on the opposite of the Z axis in the spatial frame. The actual gravity of each component is as:

The weight of the MMR2 link is 0.5 kg (G1)

The weight of the MRR2 joint is 1.5kg (G2)

The weight of the wrist tube is 1.3kg (G3)

The weight of the spherical wrist is 1.2kg (G4)

The equivalent gravity on the third joint centre as,

$$Ge1 = 0.5 * G1 + G2 \tag{5.6}$$

The equivalent gravity on the spherical wrist centre as,

$$Ge2 = G_4 + \frac{G3 * (1 + 0.5 * C23 / C2)}{1 + C23 / C2} \tag{5.7}$$

where, $C23 = \cos(\theta_2 + \theta_3)$, $C2 = \cos\theta_2$.

Using the equivalent gravity, we can get the torques of joint#2 and joint#3.

$$\tau_2 = -l_1 c_2 (G_{e1} + G_{e2}) \tag{5.8}$$

$$\tau_3 = -l_2 c_{23} G_{e2} \tag{5.9}$$

The result is programmed in MATLAB file elbow3e.m.

MATLAB File name: elbow3e.m; elbowink3.m

Compared with Figure 5-9, after gravity compensation, the torque of each joint becomes the value in Figure 5-11.

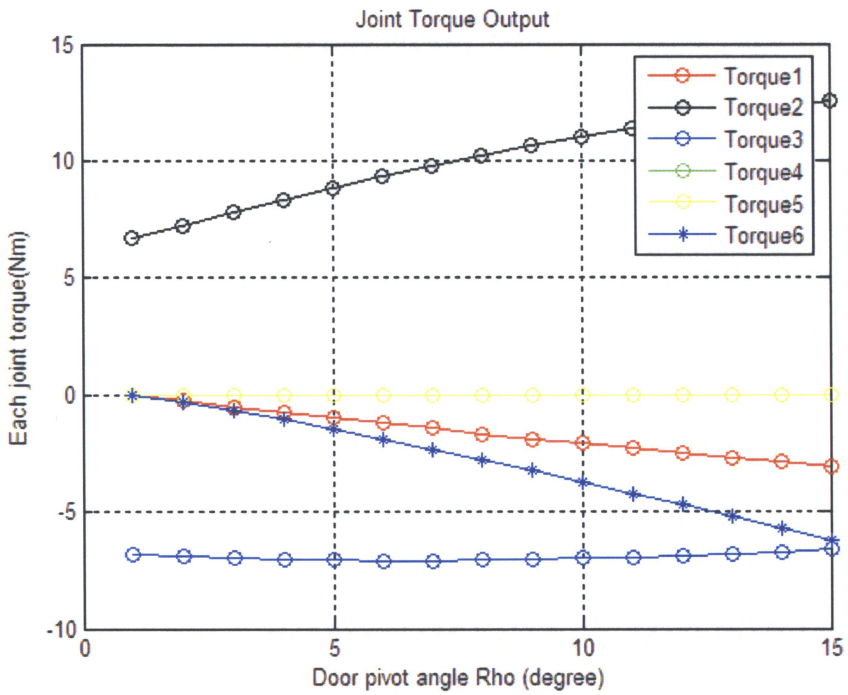

Figure 5-11: Torque output of each joint with gravity compensation (T1=0)

5.4.2 Initial Position Effects

It is not easy for the mobile platform to obtain a proper initial position in front of the door knob, the effects of different initial position is analyzed here. After comparing the required

torque of each joint, we would like to find the most reasonable initial potion. The expectation is its fluctuating value is less than others. The opening movement will be smooth.

The T1 is the initial angle of the first joint angle. It is set to -30 and +30 degrees

MATLAB File name: elbowink3.m (T1 is changed) eblbow3e1.m

A. T1=+30: the results are shown in Figure 5-12 ~ Figure 5-16

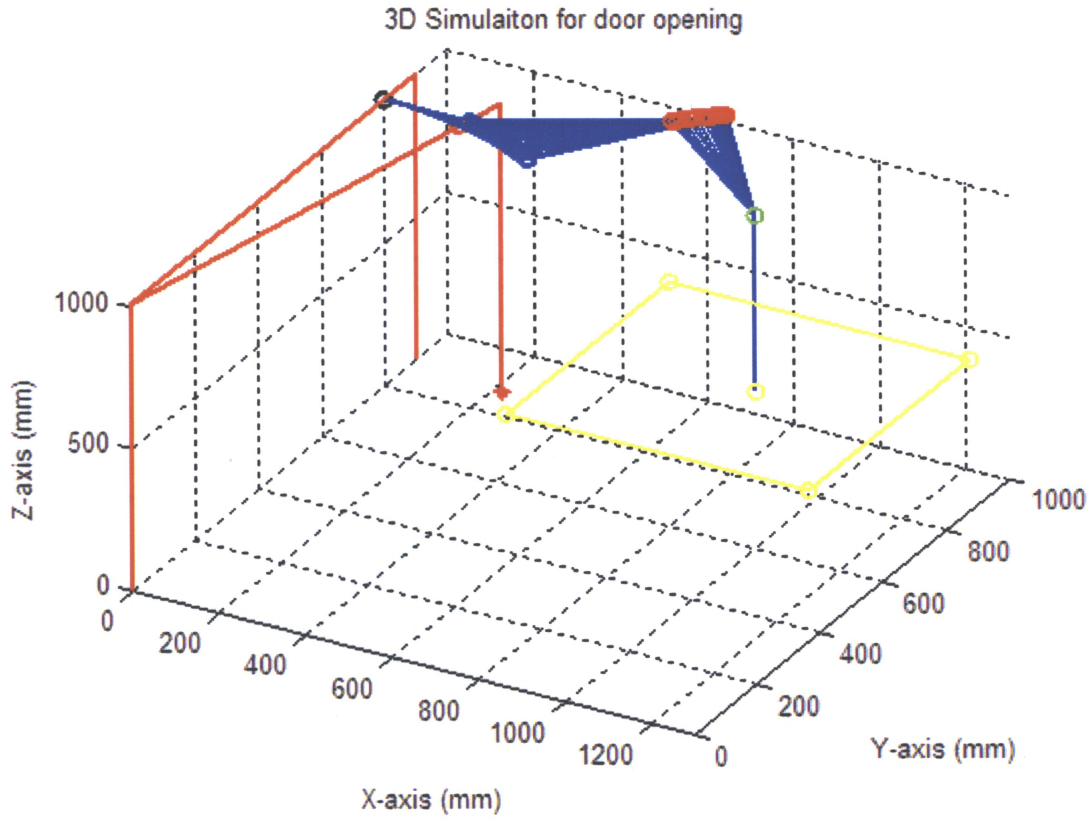

Figure 5-12: Different initial condition and its effect in door opening (T1=+30)

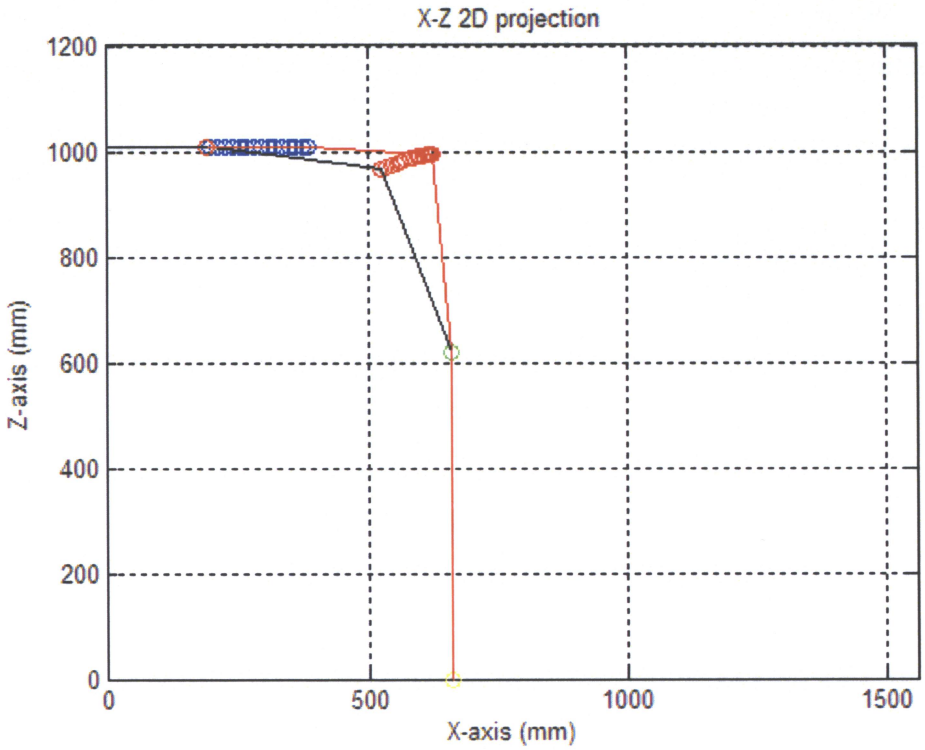

Figure 5-13: X-Z Projected Vision (T1=+30)

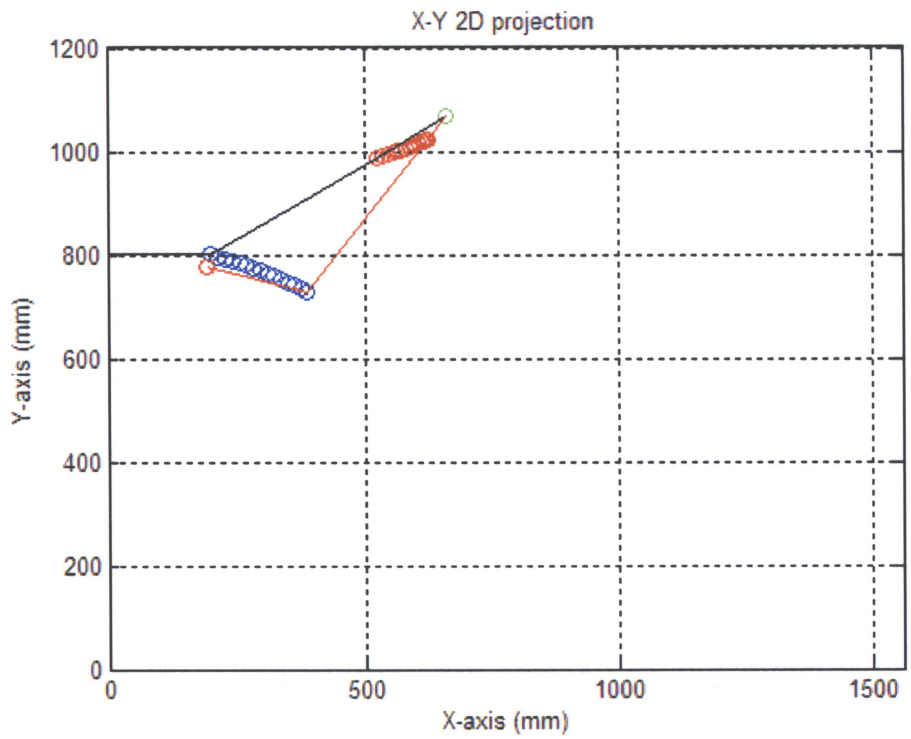

Figure 5-14: X-Y Projected Vision (T1=+30)

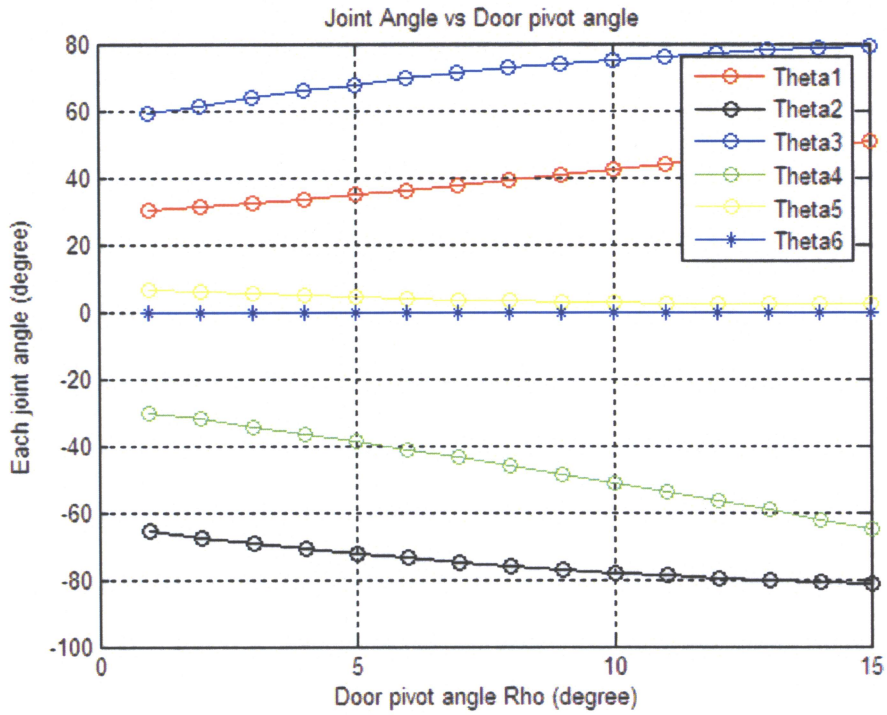

Figure 5-15: Joint angles in door opening process (T1=+30)

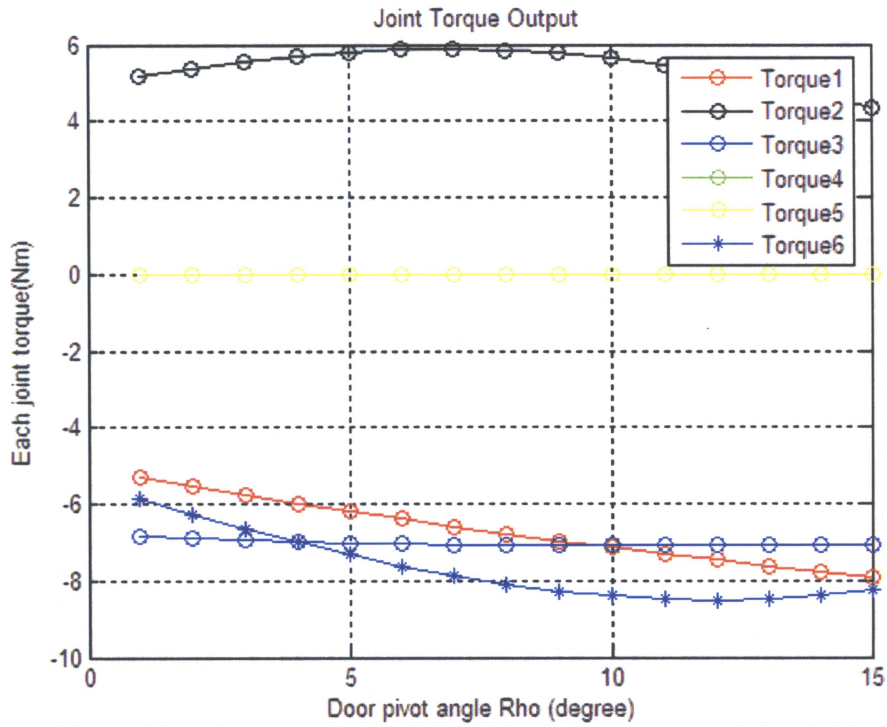

Figure 5-16: Torque output of each joint in door opening process (T1=+30)

B. T1=-30: the results are shown in Figure 5-17 ~ Figure 5-21.

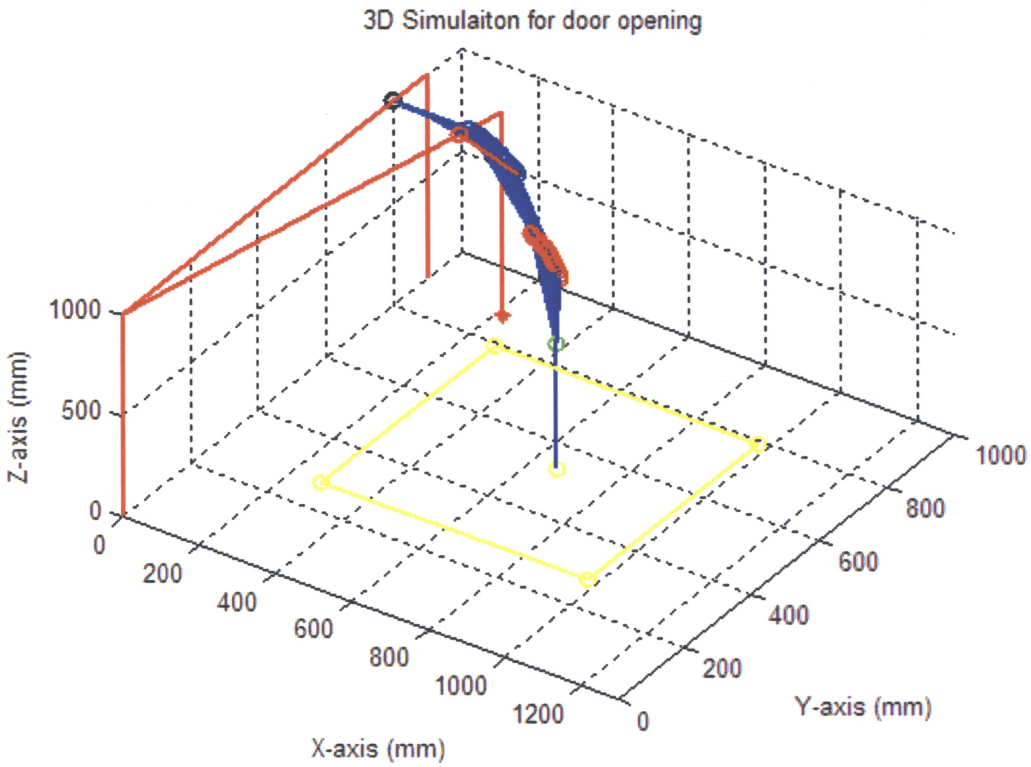

Figure 5-17: Different initial condition and its effect in door opening (T1=-30)

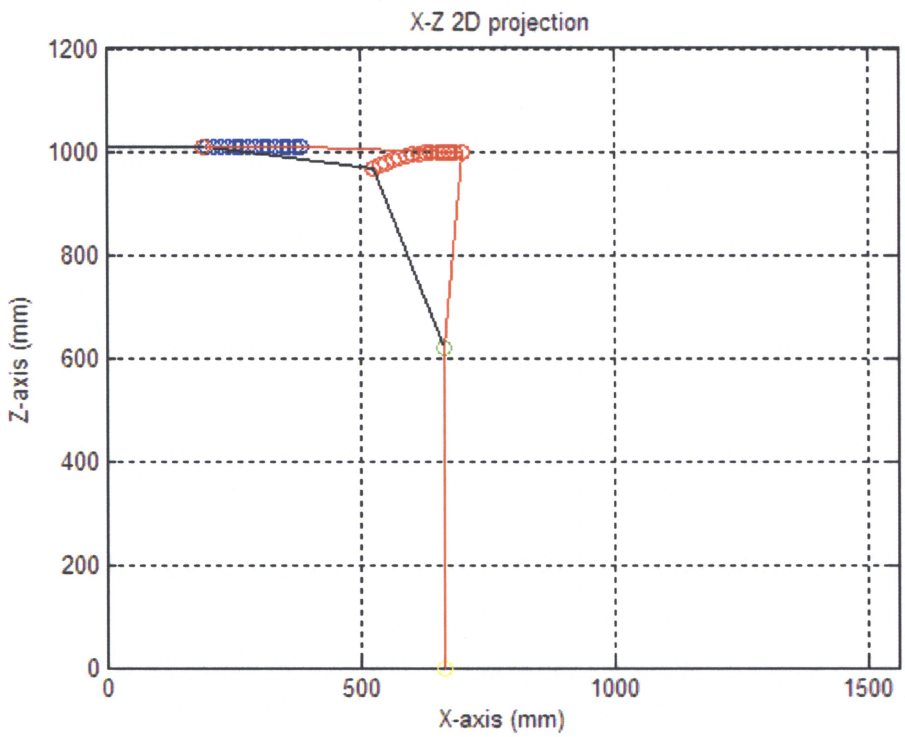

Figure 5-18: X-Z Projected Vision (T1=-30)

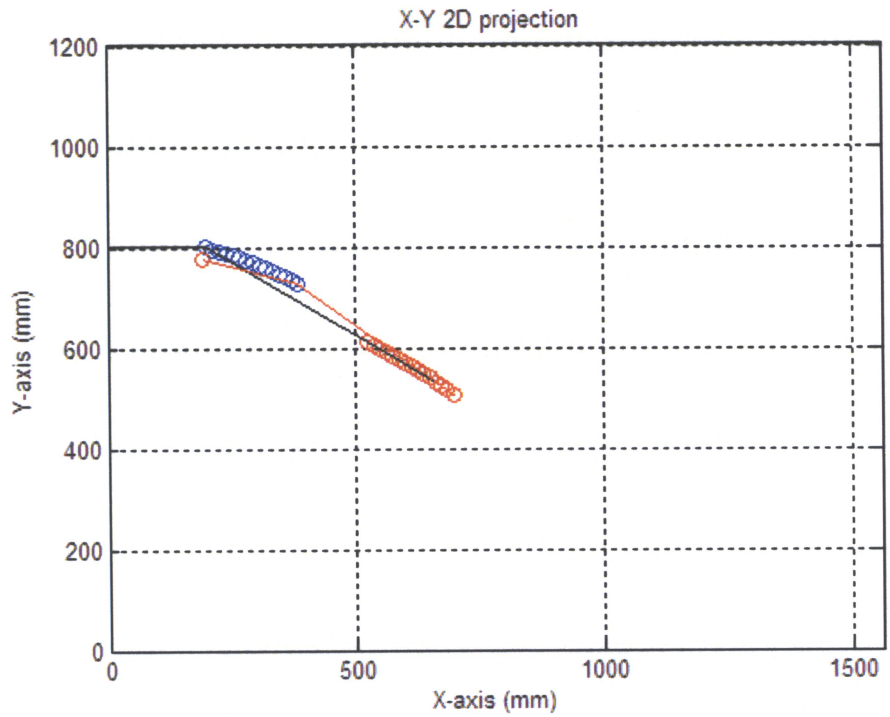

Figure 5-19: X-Y Projected Vision (T1=-30)

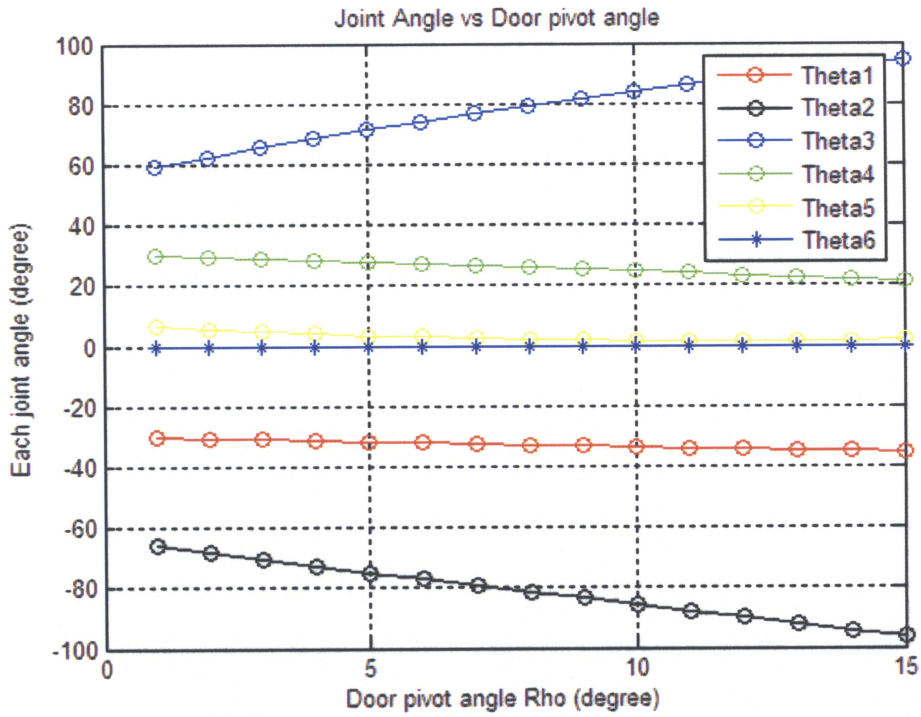

Figure 5-20: Joint angles in door opening process (T1=-30)

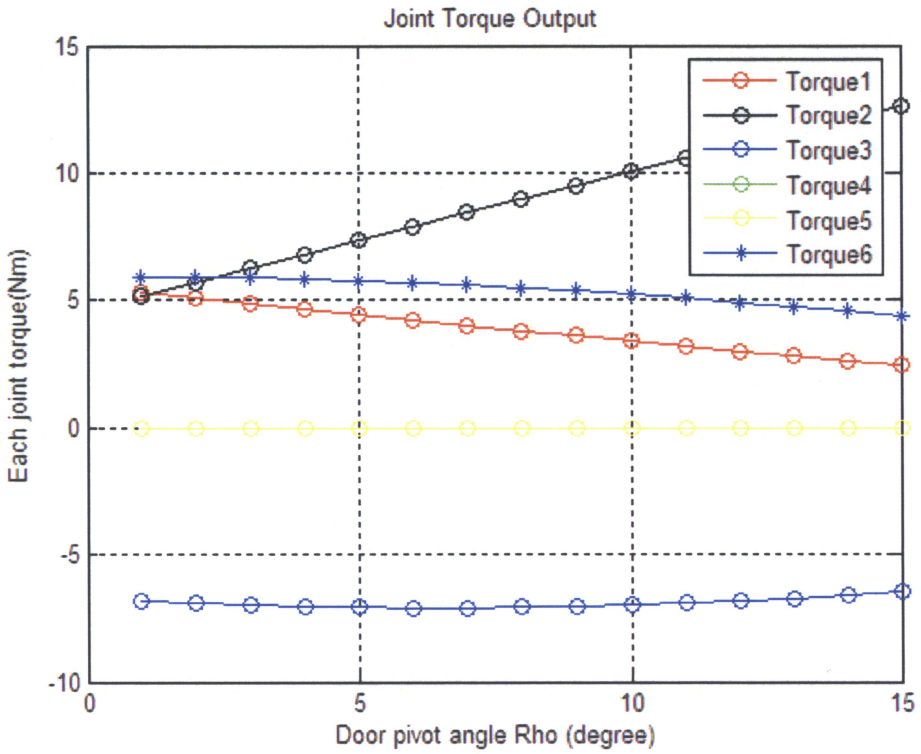

Figure 5-21: Torque output of each joint in door opening process (T1=-30)

When the torques are compared, the output is the best when T=0. And the output of the B (T=-30) is better than that of A (T=+30).

When the angles are compared, the result is the best when T=0. And the varied range of the B (T=-30) is still better tan that of B (T= -30).

So the situation when T=0 is the best. That means the mobile cart should rightly stop in front of the door knob. Or the mobile cart on the left side of the knob position is better than on the right side of the knob. The result consists with the door opening action of human beings.

Chapter 6

Dexterous Manipulation Experiment

The designed manipulator consists of the electronics control system and mechanical system. The setup of the dexterous manipulation experiment is introduced as follows.

6.1 Experiment Setup

6.1.1 Experiment Setup and Software Platform

The manipulator consists of three MRR joints and a spherical wrist. The three MRR joints have both position and torque sensors, with the 2nd and 3rd MRR joint axes being parallel and vertical to the 1st joint axis. The wrist has the pitch and the yaw rotation movements, and two position sensors are installed in the wrist. The experiment manipulator is shown in Figure 6-1.

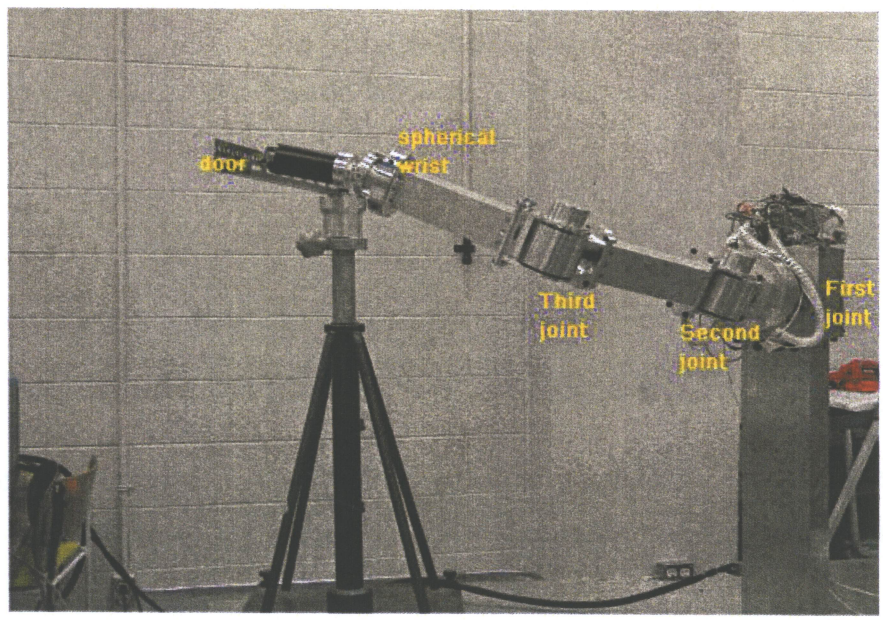

Figure 6-1: MRR2 module manipulator with spherical wrist

For the manipulation experiments, a real time operation system QNX is used. The distributed control platform is RT_LAB. The control algorithm for each DC motor is coded in C.

6.1.2 Experimental Control System

Three DSP Boards are employed to control the three MRR joints, and the communication among the three joints is accomplished by CAN bus. In Chapter 2, Figure 2-2 and Figure 2-3 provide the architecture. Figure 6-2 shows the facilities of the control system and connection environment.

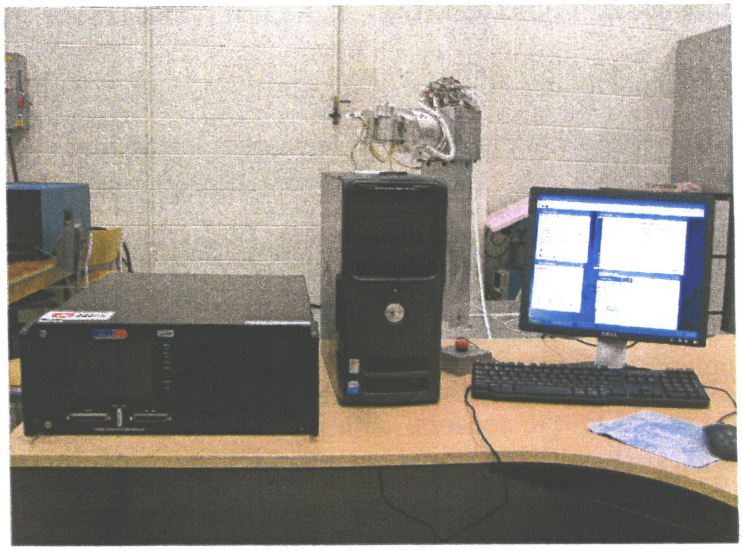

Figure 6-2: Experimental System

6.1.3 Sensors and Power System

Each modular joint needs three cables for connection. They are CAN bus cable, sensors cable and power cable.

The sensors cable has all of the torque sensors, the joint angle sensors and their amplifiers, and DSP drivers installed in the links or connectors to make it compact and suitable for the future mobile manipulator.

The power system used in this experiment is able to provide three different powers as 70V, 24V and 5V to meet multiple power requirements for different parts, such as DC motors, relay & brakes, logic and signal amplifier boards. In the future, rechargeable batteries should be available for the mobile manipulator.

6.2 Position Control Manipulation

In the designed manipulator the position ranges of each joint are as follows:

For the arm,

The 1st waist joint: 0 ~ 360 degrees;

The 2nd elbow joint: -120 ~ +120 degrees;

The 3rd elbow joint: -120 ~ + 120 degrees;

For the wrist,

The pitch joint: -30 ~ +30 degrees;

The row joint: -30 ~ +30 degrees;

Figure 6-3 shows the joint angle position of three DOF motion control, and Figure 6-4 is the demonstration.

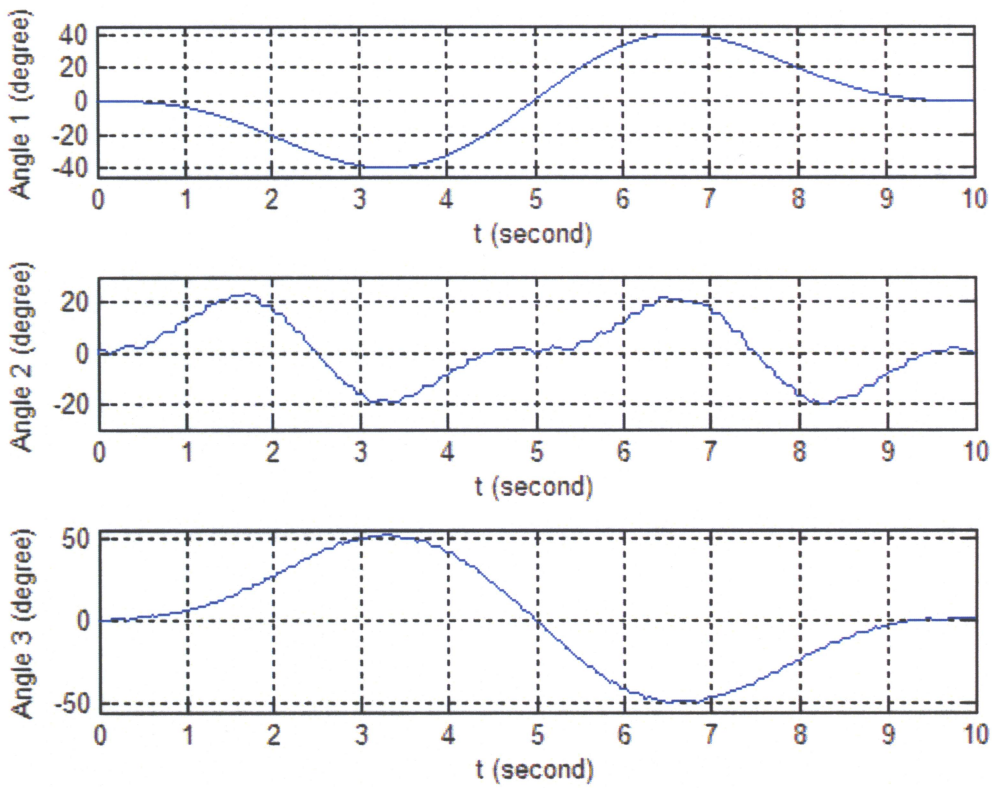

Figure 6-3: The joint angle position in a three DOF motion control

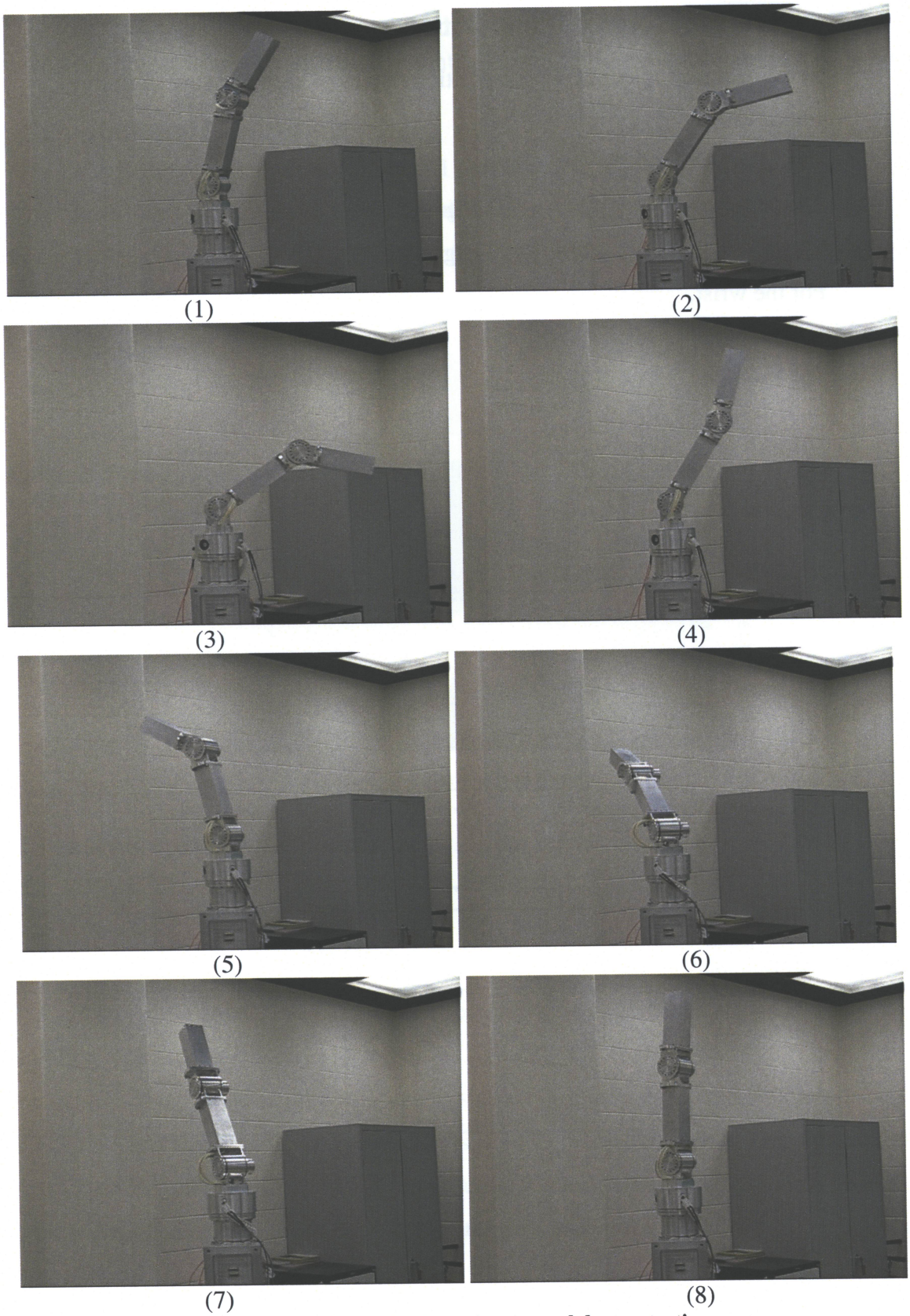

Figure 6-4: Three MRR motion control demonstration

6.3 Friction Compensation and Passive Joint Experiment

If the friction of MRR joint is compensated, the MRR joint will become a passive joint making it easy to rotate.

In Chapter 2, the friction model is provided. In this experiment, the decomposition-based friction compensation method proposed by Liu [16] is employed. By using this compensation algorithm, it is not necessary to know the motion trend, which makes it much easier to use in practice. In Table 6-1, with and without friction compensation, the external torques required to rotate the MRR joint in the passive mode in two different directions are measured and about 85% of the friction is reduced.

Table 6-1: External Torque for MRR Joint in Passive Mode with friction model

Rotate Direction	**Positive** (0~360 deg)	**Negative** (0 ~ -360 deg)
Torque without compensation(a)	15.0 Nm	19.6 Nm
Torque with compensation(b)	1.53 Nm	3.0 Nm
Ratio (b/a)	10.2 %	15.3 %

In the experiment, when an external torque acts on the MRR joint and the direction of the external torque is alternatively switched, the torque sensor output is recorded as in Figure 6-5.

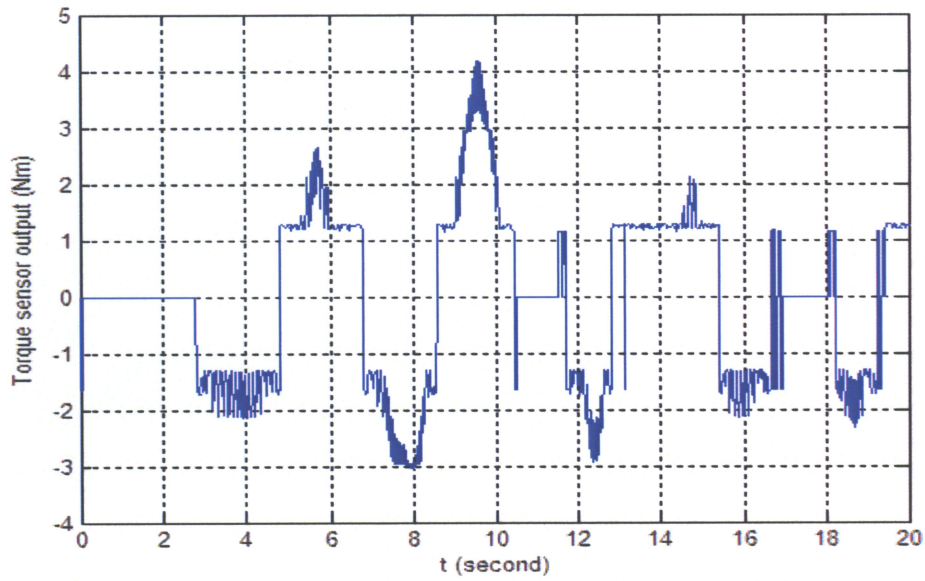

Figure 6-5: Torque sensor output in passive joint experiment

6.4 Door Opening Experiment

In this experiment, only one joint is in active mode, the elbow and wrist joints are in passive mode. The elbow passive mode is implemented by the friction compensation method.

Figure 6-6 (1) shows a mimic door. The torque to rotate the door can be adjusted to 12Nm ~18Nm. A scale is used for measuring the pulling force. The radius of the door is also adjustable. Figure 6-6 (2) to (6) shows the door opening process. The door opening video is also recorded.

During the door-opening process, only one joint is actively controlled, which simplifies the control strategy and reduces the expenses for the sensors and other devices. For the reason that there is no RCC device or compliance control needed, no torque sensor on the gripper and no online radius estimation for the calculation.

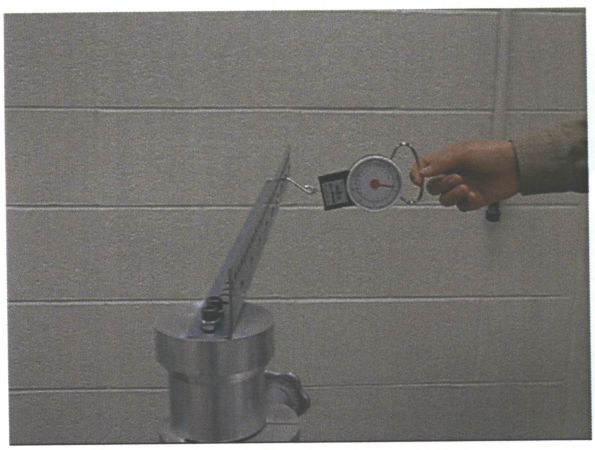

(1)

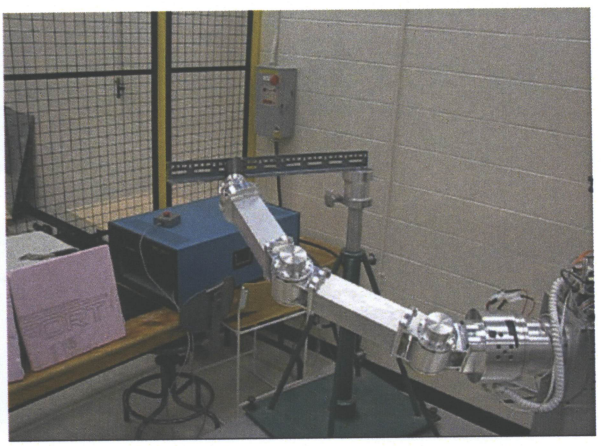

(2)

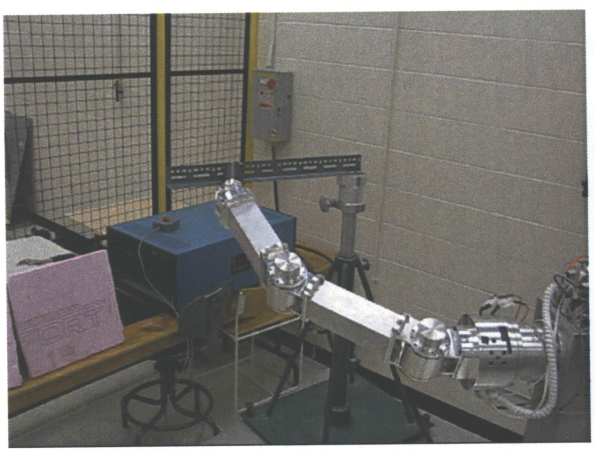

(3)

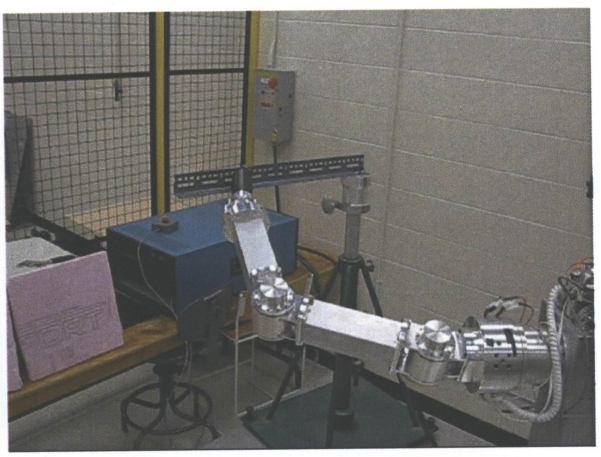

(4)

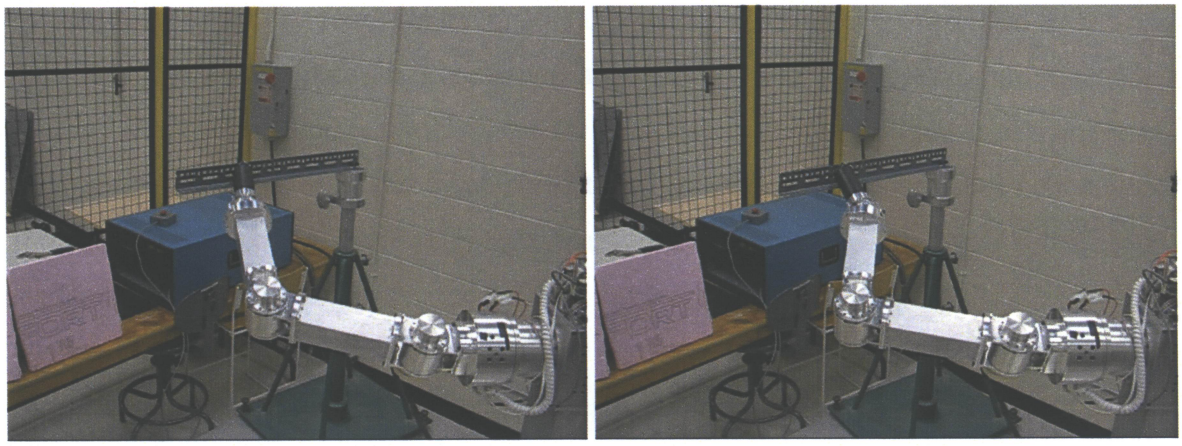

(5) (6)

Figure 6-6: Door opening experiment with multiple working modes

Chapter 7

Conclusions and Future Work

The purpose of this thesis is to develop a modular reconfigurable robot manipulator with multiple working modes, aiming to meet the challenges of manipulation in uncontrolled environments. The typical application of the manipulator is to open a door.

The development of an MRR manipulator is a complex task involving the integration of mechanical design, electronics design, and control system design. MRR has been investigated at Ryerson University for several years. In order to improve the performance of MRR, new features to the MRR manipulator are proposed and developed in this research study. A main focus of this research is to implement multiple working modes for the MRR to work in uncontrolled environments.

The newly designed MRR manipulator has multiple working modes: active mode and passive mode. In the active mode, there are two control strategies: position control and force control. For the force control issue, the model of the whole manipulator and the torque relationship of the DUAJ wrist are analyzed. All of these are aimed at the manipulation in an uncontrolled environment. The door opening case is studied as an application.

The main contributions of this thesis include the following:

A passive joint mode using friction compensation is proposed. The new method does not need a clutch or other added physical device, and the original mechanical structure of the joint does not need to change. It is a simple and effective method to implement the switch between active and passive modes. It is implemented through experiment validation and used in the door opening process. MRR joint with multiple working modes plays an important role in uncontrolled environments.

In order to use the force control mode, the MRR manipulator is modelled and analyzed. The task consists of the forward kinematics analysis, inverse kinematics analysis and Jacobian matrix. The D-H method is widely used for modeling a traditional industrial manipulator. If the D-H method is used to get the Jacobian matrix, it is tedious and complicated. In addition, when the number of robot's DOF is greater than five, it becomes difficult to obtain an accurate Jacobian matrix. In this thesis, the twist & wrench method is used instead. The two significant advantages of this new method are: the first is to avoid the sophisticated differential calculation; the second is that the correct result can be easily checked.

To build a manipulator, an anthropomorphic wrist is employed. The DAUJ wrist has a compact size and is suitable for dexterous mobile manipulation. The spherical wrist can rotate in two movements: pitch and yaw. The output link is prepared for the future roll movement. In order to use force control, the force analysis must be done for practical use. In this thesis, not only the position analysis is given, but also the force/torque relationship between the torques of the pitch & yaw and the torques of the applied two motors is provided. All the above results can be used for the final force control mode. The design task includes wrist motion simulation, position kinematics algorithm simulation, concept and subsystem design. The DUAJ wrist is successfully assembled and tested.

Door opening is a typical manipulation task in an uncontrolled environment. Using the above results and analyzing the door opening process of human beings, the door opening process is analyzed and divided into two stages: (A) The gripper searches the door knob and holds it. This stage needs position control to let the gripper close the door knob. During this position control, the feedback could be vision signal or others. (B) The gripper holds the knob and pulls the door open. This stage should be a force control. Most published papers used the position control in this stage. They need to know the radius of the door or online estimation of the door radius. Although a compliance control is employed in the process, which still made the control system design complicated and very difficult to implement. This thesis simulated the manipulation of a 6-DOF mobile manipulator to open a door in the force control active mode. The simulations combine the inverse kinematics analysis of the manipulator and the door's position analysis. The final force control of each joint of the manipulator is provided. The gravity compensation and initial position of the mobile platform are considered and discussed in the

simulation. From this case study, the thesis would like to consider a new path to meet the challenge in an uncontrolled environment.

In the final experiments, first, the MRR manipulator position control is demonstrated. Second, the passive mode of an MRR joint is implemented by using a friction compensation method. Third, a door opening process using multiple working modes is done, where only one MRR joint is actively controlled, another MRR joint and the spherical wrist are in passive mode. It successfully shows how to use multiple modes to open a door in a 3D space uncontrolled environment.

Development of a robot is a long-time task which needs much redesign work and improvements. The future work will include the following:

For the DUAJ wrist, it is necessary to develop the position kinematics algorithm and install a torque sensor at the wrist for the pitch and the yaw force control. Friction compensation for the wrist to implement the passive mode is an issue to be addressed.

For the manipulator, a gripper is needed. A six degree of freedom force sensor should be mounted onto it and a real time force control would be implemented. For visually guided position control, a stereo vision system is required.

A mobile platform mounted with the above manipulator is the final solution to perform mobile dexterous manipulations in an uncontrolled environment.

Appendix A. Jacobian Matrix Check

The following equation can be used for checking the Jacobian Matrix

$$(J^{s}_{st}\dot{\theta})^{\wedge}\, p(\theta) = \dot{p}(\theta) \tag{A1.0}$$

From Equations (3-69) and (3-70)

$$J^{s}_{st}\dot{\theta} = \begin{bmatrix} l_0 s_1 \dot{\theta}_2 + (l_0 s_1 - l_1 s_1 s_2)\dot{\theta}_3 + \xi'_{4_1}\dot{\theta}_4 + \xi'_{5_1}\dot{\theta}_5 + \xi'_{6_1}\dot{\theta}_6 \\ -l_0 c_1 \dot{\theta}_2 - (l_0 c_1 - l_1 c_1 s_2)\dot{\theta}_3 + \xi'_{4_2}\dot{\theta}_4 + \xi'_{5_2}\dot{\theta}_5 + \xi'_{6_2}\dot{\theta}_6 \\ l_1 c_2 \dot{\theta}_3 + \xi'_{4_3}\dot{\theta}_4 + \xi'_{5_3}\dot{\theta}_5 + \xi'_{6_3}\dot{\theta}_6 \\ -c_1 \dot{\theta}_2 - c_1 \dot{\theta}_3 + \omega'_{4_1}\dot{\theta}_4 + \omega'_{5_1}\dot{\theta}_5 + \omega'_{6_1}\dot{\theta}_6 \\ -s_1 \dot{\theta}_2 - s_1 \dot{\theta}_3 + \omega'_{4_2}\dot{\theta}_4 + \omega'_{5_2}\dot{\theta}_5 + \omega'_{6_3}\dot{\theta}_6 \\ \dot{\theta}_1 + \omega'_{4_3}\dot{\theta}_4 + \omega'_{5_3}\dot{\theta}_5 + \omega'_{6_3}\dot{\theta}_6 \end{bmatrix} = \begin{bmatrix} J_1 \\ J_2 \\ J_3 \\ J_4 \\ J_5 \\ J_6 \end{bmatrix} \tag{A1.1}$$

where,

$$\xi'_{4_1} = -c_1 s_{23} l_0 + (c_1 s_2 s_{23} + c_1 c_2 c_{23}) l_1 + c_1 l_2$$
$$\xi'_{4_2} = -s_1 s_{23} l_0 + (s_1 c_2 c_{23} + s_1 s_2 s_{23}) l_1 + s_1 l_2$$
$$\xi'_{4_3} = 0$$

$$\xi'_{5_1} = (s_1 c_4 + c_1 s_4 c_{23}) l_0 - (s_1 s_2 c_4 + c_1 s_2 s_4 c_{23} - c_1 c_2 s_4 s_{23}) l_1 - s_1 c_4 s_{23} l_2$$
$$\xi'_{5_2} = -(c_1 c_4 - s_1 s_4 c_{23}) l_0 + (c_1 s_2 c_4 - s_1 s_2 s_4 c_{23} + s_1 c_2 s_4 s_{23}) l_1 + c_1 c_4 s_{23} l_2$$
$$\xi'_{5_3} = c_2 c_4 l_1 + c_4 c_{23} l_2$$

$$\xi'_{6_1} = \begin{matrix} -(c_1 c_4 c_5 c_{23} - s_1 s_4 c_5 - c_1 s_5 s_{23}) l_0 - (c_1 s_5 + s_1 s_4 c_5 s_{23}) l_2 \\ -(c_1 c_2 c_4 c_5 s_{23} - c_1 s_2 c_4 c_5 c_{23} + s_1 s_2 s_4 c_5 + c_1 c_2 s_5 c_{23} + c_1 s_2 s_5 c_{23}) l_1 \end{matrix}$$

$$\xi'_{6_2} = \begin{matrix} -(s_1 c_4 c_5 c_{23} + c_1 s_4 c_5 - s_1 s_5 s_{23}) l_0 - (s_1 s_5 - c_1 s_4 c_5 s_{23}) l_2 \\ -(s_1 c_2 c_4 c_5 s_{23} - s_1 s_2 c_4 c_5 c_{23} + c_1 s_2 s_4 c_5 + s_1 c_2 s_5 c_{23} - s_1 s_2 s_5 s_{23}) l_1 \end{matrix}$$

$$\xi'_{6_3} = c_2 s_4 c_5 l_1 + s_4 c_5 c_{23} l_2$$

$$\omega'_{4_1} = -s_1 s_{23}$$
$$\omega'_{4_2} = c_1 s_{23}$$

$$\omega'_{4\,3} = c_{23}$$

$$\omega'_{5\,1} = -c_1 c_4 + s_1 s_4 c_{23}$$
$$\omega'_{5\,2} = -s_1 c_4 - c_1 s_4 c_{23}$$
$$\omega'_{5\,3} = s_4 s_{23}$$

$$\omega'_{6\,1} = -c_1 s_4 c_5 - s_1 c_4 c_5 c_{23} + s_1 s_5 s_{23}$$
$$\omega'_{6\,2} = -s_1 s_4 c_5 + c_1 c_4 c_5 c_{23} - c_1 s_5 s_{23}$$
$$\omega'_{6\,3} = -c_4 c_5 s_{23} - s_5 c_{23}$$

because

$$(J^s_{st}\dot{\theta})^{\wedge} = \begin{bmatrix} \hat{\omega} & \upsilon \\ 0 & 0 \end{bmatrix} = \begin{bmatrix} \begin{bmatrix} 0 & -J_6 & J_5 \\ J_6 & 0 & -J_4 \\ -J_5 & J_4 & 0 \end{bmatrix} & \begin{matrix} J_1 \\ J_2 \\ J_3 \end{matrix} \\ \begin{matrix} 0 & 0 & 0 \end{matrix} & 0 \end{bmatrix} \tag{A1.2}$$

$$(J^s_{st}\dot{\theta})^{\wedge} p(\theta) = \begin{bmatrix} \hat{\omega} & \upsilon \\ 0 & 0 \end{bmatrix} \begin{bmatrix} \begin{bmatrix} p_1 \\ p_2 \\ p_3 \end{bmatrix} \\ 1 \end{bmatrix} = \begin{bmatrix} \begin{bmatrix} 0 & -J_6 & J_5 \\ J_6 & 0 & -J_4 \\ -J_5 & J_4 & 0 \end{bmatrix} & \begin{matrix} J_1 \\ J_2 \\ J_3 \end{matrix} \\ \begin{matrix} 0 & 0 & 0 \end{matrix} & 0 \end{bmatrix} \begin{bmatrix} \begin{bmatrix} p_1 \\ p_2 \\ p_3 \end{bmatrix} \\ 1 \end{bmatrix}$$

$$= \begin{bmatrix} \begin{bmatrix} -J_6 p_2 + J_5 p_3 + J_1 \\ J_6 p_1 - J_4 p_3 + J_2 \\ -J_5 p_1 + J_4 p_2 + J_3 \end{bmatrix} \\ 1 \end{bmatrix} = \begin{bmatrix} \begin{bmatrix} J_{d1} \\ J_{d2} \\ J_{d3} \end{bmatrix} \\ 1 \end{bmatrix} \tag{A1.3}$$

and,

$$\begin{bmatrix} p_1 \\ p_2 \\ p_3 \end{bmatrix} = \begin{bmatrix} -s_1(l_1 c_2 + l_2 c_{23}) \\ c_1(l_1 c_2 + l_2 c_{23}) \\ l_0 - l_1 s_2 - l_2 s_{23} \end{bmatrix}$$

In the Equation (A1.3), we have

$$J_{d1} = -J_6 p_2 + J_5 p_3 + J_1$$

$$=-(\dot{\theta}_1+\omega'_{4_3}\dot{\theta}_4+\omega'_{5_3}\dot{\theta}_5+\omega'_{6_3}\dot{\theta}_6)\ c_1(l_1c_2+l_2c_{23})+$$
$$(-s_1\dot{\theta}_2-s_2\dot{\theta}_3+\omega'_{4_2}\dot{\theta}_4+\omega'_{5_2}\dot{\theta}_5+\omega'_{6_3}\dot{\theta}_6)\ (l_0-l_1s_2-l_2s_{23})+$$
$$l_0s_1\dot{\theta}_2+(l_0s_1-l_1s_1s_2)\dot{\theta}_3+\xi'_{4_1}\dot{\theta}_4+\xi'_{5_1}\dot{\theta}_5+\xi'_{6_1}\dot{\theta}_6 \qquad \text{(A1.4)}$$

From Equation (A1.4), we obtain,

$$J_{d1}=-c_1(l_1c_2+l_2c_{23})\dot{\theta}_1+((l_0-l_1s_2-l_2s_{23})(-s_1)+l_0s_1)\dot{\theta}_2$$
$$+((l_0-l_1s_2-l_2s_{23})(-s_1)+(l_0s_1-l_1s_1s_2))\dot{\theta}_3$$
$$+[-c_1(l_1c_2+l_2c_{23})\omega'_{4_3}+(l_0-l_1s_2-l_2s_{23})\omega'_{4_2}+\xi'_{4_1}]\dot{\theta}_4$$
$$+[-c_1(l_1c_2+l_2c_{23})\omega'_{5_3}+(l_0-l_1s_2-l_2s_{23})\omega'_{5_2}+\xi'_{5_1}]\dot{\theta}_5$$
$$+[-c_1(l_1c_2+l_2c_{23})\omega'_{6_3}+(l_0-l_1s_2-l_2s_{23})\omega'_{6_2}+\xi'_{6_1}]\dot{\theta}_6$$

$$=-c_1(l_1c_2+l_2c_{23})\dot{\theta}_1+((l_0-l_1s_2-l_2s_{23})(-s_1)+l_0s_1)\dot{\theta}_2$$
$$+((l_0-l_1s_2-l_2s_{23})(-s_1)+(l_0s_1-l_1s_1s_2))\dot{\theta}_3$$
$$+(-c_1(l_1c_2+l_2c_{23})c_{23}+(l_0-l_1s_2-l_2s_{23})c_1s_{23}+-c_1s_{23}l_0+(c_1s_2s_{23}+c_1c_2c_{23})l_1+c_1l_2)\dot{\theta}_4$$
$$+[-c_1(l_1c_2+l_2c_{23})s_4s_{23}+(l_0-l_1s_2-l_2s_{23})(-s_1c_4-c_1s_4c_{23})$$
$$+(s_1c_4+c_1s_4c_{23})l_0-(s_1s_2c_4+c_1s_2s_4c_{23}-c_1c_2s_4s_{23})l_1-s_1c_4s_{23}l_2]\dot{\theta}_5$$
$$+[-c_1(l_1c_2+l_2c_{23})(-c_4c_5s_{23}-s_5c_{23})+(l_0-l_1s_2-l_2s_{23})(-s_1s_4c_5+c_1c_4c_5c_{23}-c_1s_5s_{23})$$
$$-(c_1c_4c_5c_{23}-s_1s_4c_5-c_1s_5s_{23})l_0-(c_1s_5+s_1s_4c_5s_{23})l_2$$
$$-(c_1c_2c_4c_5s_{23}-c_1s_2c_4c_5c_{23}+s_1s_2s_4c_5+c_1c_2s_5c_{23}+c_1s_2s_5c_{23})l_1]\dot{\theta}_6$$

$$=-c_1(l_1c_2+l_2c_{23})\dot{\theta}_1+(l_1s_1s_2+l_2s_1s_{23})\dot{\theta}_2+l_2s_1s_{23}\dot{\theta}_3+0\cdot\dot{\theta}_4+0\cdot\dot{\theta}_5+0\cdot\dot{\theta}_6$$
$$=-c_1(l_1c_2+l_2c_{23})\dot{\theta}_1+(l_1s_1s_2+l_2s_1s_{23})\dot{\theta}_2+l_2s_1s_{23}\dot{\theta}_3=\dot{p}_1 \qquad \text{(A1.5)}$$

Similarly, we also get

$$J_{d2}=-s_1(l_1c_2+l_2c_{23})\dot{\theta}_1-(l_1c_1s_2+l_2c_1s_{23})\dot{\theta}_2-l_2c_1s_{23}\dot{\theta}_3=\dot{p}_2 \qquad \text{(A1.6)}$$

$$J_{d3}=-(l_1c_2+l_2c_{23})\dot{\theta}_2-l_2c_{23}\dot{\theta}_3=\dot{p}_3 \qquad \text{(A1.7)}$$

From Equations (A1.5), (A1.6) and (A1.7), we obtain,

$$(J_{st}^{s}\dot{\theta})\hat{}\, p(\theta)=\begin{bmatrix}\begin{bmatrix}J_{d1}\\ J_{d2}\\ J_{d3}\end{bmatrix}\\ 1\end{bmatrix}=\begin{bmatrix}\dot{p}_1\\ \dot{p}_2\\ \dot{p}_3\\ 1\end{bmatrix}=\dot{p}(\theta) \tag{A1.8}$$

Finally Equation (A1.0) and Equation (3-70) have been checked.

Appendix B. Inverse kinematics and force control simulations.

MATLAB File name: elbowink2.m and elbow2.m

```
% elbowink2.m
% Manipulator Inverse Kinematics for Door Opening
%
% The 1st joint revolute angle: Phi(i)
% The 2nd and 3rd joint angles: Theta1(i) and Theta2(i)
% Input door angle Rho(i) and cart initial position Xc_0, Yc_0 and Phi_0
% Output: Manipulator joint angles saved in elbowdat.mat for elbow2.m
% Theta1e, Theta2e, Theta3e, Theta4e, Theta5e
% reviewed on Feb-6-2008
% By Xiaojia He



ci=15;
for i=1:ci                  % 1~10 degree
    Rho_d(i)=(i-1)*1;         % door pivot angle called Rho(i) <<INPUT>>
    Rho(i)=Rho_d(i)*pi/180;   % Rho(i)is in rad unit

Rho_max=(ci-1)*pi/180;
a=800;  %the distance between the pivot line O to Knob K |OK|
b=900;  %door width  |OE| door edge to pivot
c=200; %300 %the length of the door handle (knob K to point H)|KH|          !!!
d=sqrt(a^2+c^2); %pivot to handle point H (the wrist)

Alpha_0=atan(c/a);  %0.1853;  %atan(c/a)=0.1853                      (new)
%the fixed angle between Pivot Axis with handle/Knob
%Assume the handle is horizontal and perpendicular to the door at knob K

%============= Design Parameters ==============
Theta1_0d=63;  %54;   %Initial Theta1 (63 degree) DESIGN PARAMETERS    !!!!!!!!!
Theta2_0d=-45;  %20;   %Initial Theta2 (-45 degree)                     !!!!!!!!!
Phi_0d=0;      %Initial Phi (the links on a revolute base of robot)!!
Theta4_0d=-10;


Theta1_0=Theta1_0d*pi/180;
Theta2_0=Theta2_0d*pi/180;
Phi_0=Phi_0d*pi/180;

L1=380; %520;     %length of Link #1          DESIGN PARAMETERS
L2=380; %480;     %length of link #2
H=1010;      %height of the door knob
h=620;  %170 + 450;      %height of the base of the mobile cart/ joint position
dH=H-h;     %difference between the knob and the link base

%-----------------------------------------------------------
%The center of the revolute axis on mobile robot
%Initial robot arm conditions C(Xc_0,Yc_0)

LL=L1*cos(Theta1_0) + L2*cos(Theta1_0+Theta2_0);
            %On the XOY plant, the projection of the length of  Link#1, #2
Xc_0=c + LL*cos(Phi_0); %At beginning, the start point is H_0(c,a)
Yc_0=a + LL*sin(Phi_0); % H_0 is the hand end point
            % Here the handle is assumed the link #3 which is planned
            % (horizontal and perpendicular to the door at knob K)

%-----------------------
%For any angle Rho(i)  Here, 0<= Rho(i) <= 10 degree
%Calculation of the handle point H(Xh, Yh)
Xh(i)=d*sin(Alpha_0 + Rho(i));  %The handle point H_i(Xh(i),Yh(i))
Yh(i)=d*cos(Alpha_0 + Rho(i));
Zh(i)=H;

%-----------------------
%For any angle Rho(i), the knob's position
X_knob(i)=a*sin(Rho(i));
Y_knob(i)=a*cos(Rho(i));
Z_knob(i)=H;

%-----------------------
num1=Yc_0-Yh(i);     % for calculation of Phi
den1=Xc_0-Xh(i);     % triangular relationship
Phi(i)=atan(num1/den1);     % the relvolute angle Phi
Phi_d(i)=Phi(i)*180/pi;     % degree (Unit)
```

```
%----------------------
num2=den1;           % for calculation of angle Theta1 and Theta2
den2=cos(Phi(i));
ff1=num2/den2;

%--------------Calculation of Theta1
num3=L1^2 + ff1^2 + dH^2 - L2^2;
den3=2*L1*ff1;
ff3=num3/den3;   %show the temporary result for programing

b2=dH/ff1;       %show the temporary result
% Using Symbolic toolbox for equations solving
%%eqs1='cos(Theta1(i))+ b2*sin(Theta1(i))=ff3'
%Theta1(i)=solve(eqs1)
%But it's not a numerical solution

% --------------Calculation of Theta1 using function2
% details see the book <<Foundations of Robotics>> Appendix1 pp261
%
% k1*sin(Theta)+ k2*cos(Theta)=k3
% Theta=atan2(k1,k2)+/- atan2(sqrt(k1^2+k2^2-k3^2),k3)
% Here k1=b2, k2=1, k3=ff3
k1=b2;
k2=1;
k3=ff3;
Theta1p(i)=atan2(k1,k2)+ atan2(sqrt(k1^2+k2^2-k3^2),k3); %the sign is plus
Theta1m(i)=atan2(k1,k2)- atan2(sqrt(k1^2+k2^2-k3^2),k3); %the sign is minus

T1(i)=Theta1p(i)*180/pi; % Select the reasonable result +/- sign
T1r(i)=T1(i)*pi/180;     % T1r(i) is the rad unit of T1(i)

%--------------Calculation of Theta2
% Equation  L1*sin(Theta1)+L2*sin(Theta1+Theta2)=dH
% then      sin(Theta1+Theta2)=(dH-L1*sin(Theta1))/L2 = ff4
% so the angle Theta2=asin(ff4)-Theta1
num4=dH-L1*sin(T1r(i));
den4=L2;
ff4(i)=num4/den4;
T2r(i)=asin(ff4(i))-T1r(i); % T2r(i) is the T2(i)in rad unit
T2(i)=T2r(i)*180/pi;

%==== for calculating joint points C(Xc,Yc), A(Xa,Ya), B(Xb,Yb), H(Xh,Yh)
Xc(i)=Xc_0;
Yc(i)=Yc_0;
Zc(i)=0.0;

Xa(i)=Xc(i);
Ya(i)=Yc(i);
Za(i)=h;

Xb(i)=Xa(i)- L1*cos(T1r(i))*cos(Phi(i));
Yb(i)=Ya(i)- L1*cos(T1r(i))*sin(Phi(i));
Zb(i)=h + L1*sin(T1r(i));

%Xh(i)=Xb(i)- L2*cos(T1r(i)+T2r(i))*cos(Phi(i)) %!!! These equations are
%Yh(i)=Yb(i)- L2*cos(T1r(i)+T2r(i))*sin(Phi(i)) %only for deriving Theta1
%Zh(i)=Zb(i)+ L2*sin(T1r(i)+T2r(i))             %and Theta2

%In the above program, Xh(i), Yh(i) and Zh(i) have been calculated

Xt=[Xc(i) Xa(i) Xb(i) Xh(i) X_knob(i)]; %show links, joints of robot arm
Yt=[Yc(i) Ya(i) Yb(i) Yh(i) Y_knob(i)];
Zt=[Zc(i) Za(i) Zb(i) Zh(i) Z_knob(i)];

Xt_1=[Xc(1) Xa(1) Xb(1) Xh(1), 0]; %for 3D plotting /including start point
Yt_1=[Yc(1) Ya(1) Yb(1) Yh(1), a]; %plus the knob Initial position K(0,a,H)
Zt_1=[Zc(1) Za(1) Zb(1) Zh(1), H];

%figure
plot3(Xt,Yt,Zt,'linewidth',2);     %plotting the links'lines
axis([0,1300,0,1000,0,1000]);
hold on
plot3(Xc,Yc,Zc,'yo',Xa,Ya,Za,'go',Xb,Yb,Zb,'ro',Xh,Yh,Zh,'bo','linewidth',2);
                                   %plotting the joints
title('3D Simulaiton for door opening');
xlabel('X-axis (mm)'),ylabel('Y-axis (mm)'),zlabel('Z-axis (mm)')
grid;

Xd_0=[0,0,0,0];Yd_0=[b,b,0,0];Zd_0=[0,H,H,0];%door edges (Initial)
plot3(Xd_0,Yd_0,Zd_0,'r-','linewidth',2)     %3D line plotting
Xk_0=[0,c];Yk_0=[a,a];Zk_0=[H,H];            %Knob's position
```

```
plot3(Xk_0,Yk_0,Zk_0,'ko-','linewidth',2)    %color k means black

%---for plotting the front position of the cart
length_cart=700;        % Cart parameters  total length
length_base=620;        % length of the truck base
width_base=510;         % width of the truck base
Xf_r=Xc_0 -(length_cart-length_base/2); % front right X axis dimensions
Xf_l=Xf_r;                              % front left X axis dimensions
Yf_r=Yc_0+width_base/2; %front right Y axis dim
Yf_l=Yc_0-width_base/2; %front left Y dim
Zf_l=0;                 %front left Z
Zf_r=0;                 %front right Z

Xr_l=Xc_0+length_base/2; % rear left X dim
Xr_r=Xr_l;               % rear right X dim
Yr_l=Yf_l;               % rear left Y
Yr_r=Yf_r;               % rear right Y
Zr_l=0;                  % rear left Z
Zr_r=0;                  % rear right Z

X_cart=[Xr_l,Xf_l,Xf_r,Xr_r,Xr_l];     % plotting the cart area
Y_cart=[Yr_l,Yf_l,Yf_r,Yr_r,Yr_l];
Z_cart=[Zr_l,Zf_l,Zf_r,Zr_r,Zr_l];
plot3(X_cart,Y_cart,Z_cart,'yo-','linewidth',2);

%for watching the collision with the above front position of the cart
%-----------------------------------
X_door=b*sin(Rho_max); %Calculation of the door edge at final pivot angle
Y_door=b*cos(Rho_max); %Door edges' position (Final)
Z_door=0;
plot3(X_door,Y_door,Z_door, 'r*','linewidth',2); % on XoY plant

X_dr(i)=b*sin(Rho(i));
Y_dr(i)=b*cos(Rho(i));
Z_dr(i)=0;
%plot3(X_dr(i),Y_dr(i),Z_dr(i), 'r*','linewidth',2); the continuing point

%Xd_f=[X_dr(i),X_dr(i),0,0]; % show the whole door opening process
%Yd_f=[Y_dr(i),Y_dr(i),0,0];
%Zd_f=[0,H,H,0];
%plot3(Xd_f,Yd_f,Zd_f,'r-','linewidth',2);

Xd_f=[X_door,X_door,0,0];   %door edges' 3D lines at final position
Yd_f=[Y_door,Y_door,0,0];
Zd_f=[0,H,H,0];
plot3(Xd_f,Yd_f,Zd_f,'r-','linewidth',2);

%-----------------------------------
Xk_f=a*sin(Rho_max);     % The final Knob point K1(Xk_f,Yk_f)
Yk_f=a*cos(Rho_max);
Zk_f=H;

Xh_f=d*sin(Alpha_0 + Rho_max); %The final handle point H1(Xh_f,Yh_f)
Yh_f=d*cos(Alpha_0 + Rho_max);
Zh_f=H;

Xhh_f=[Xk_f, Xh_f];Yhh_f=[Yk_f, Yh_f];Zhh_f=[H,H]; % the handle line K1H1
plot3(Xhh_f,Yhh_f,Zhh_f,'ro-','linewidth',2); %k means black color
%================ for payload or force calculation ===========Feb 4,2007
G1=10;
G2=30;
G3=10;
Mj=35;
Ls1=L1/1000;
Ls2=L2/1000;
Ma=G1*(Ls1/2)*cos(T1r(i))+G2*Ls2*cos(T1r(i));
M1(i)=Ma + G3*Ls2*cos(T1r(i)+T2r(i))/2 + G3*Ls1*cos(T1r(i));
M(i)=Mj-M1(i);
denm=Ls1*cos(T1r(i))+ Ls2*cos(T1r(i)+ T2r(i));
G(i)=M(i)/denm;

Theta1e(i)=Phi_d(i);
Theta2e(i)=-T1(i);
Theta3e(i)=-T2(i);
Theta4e(i)=-(Phi_d(i)+Rho_d(i));
Theta5e(i)=(T1(i)+T2(i));

end
T1r;
T2r;
M1;
```

```
M;
G;
%=================================================================
Rho; %show the temporary results

Xk_f=a*sin(Rho_max);     % The final Knob point K1(Xk_f,Yk_f)
Yk_f=a*cos(Rho_max);
Zk_f=H;

Xt_ci=[Xc(ci) Xa(ci) Xb(ci) Xh(ci), Xk_f]; %for 3D plotting
Yt_ci=[Yc(ci) Ya(ci) Yb(ci) Yh(ci), Yk_f];
Zt_ci=[Zc(ci) Za(ci) Zb(ci) Zh(ci), H];

Phi_d;    % The revolute angle(degree)
T1=-90+T1;       % Theta1 (degree) new the axis is the phi center
T2;       % Theta2 (degree)
T3=-90+T1-T2; %-(T1+T2);
T4=-(Phi_d + Rho_d);    % NEW


dPhi=Phi_d-Phi_0d;
dT1=T1-Theta1_0d;
dT2=T2-Theta2_0d;
dT3=T3+(Theta1_0d + Theta2_0d);
dT4=T4 + Phi_0d; %NEW


%Xh, Yh; % for temporary results
%Xa, Ya;
%Xb, Yb;
%Xc, Yc;

%-------- 2D graphic XoY --------
figure;
plot(Xc,Yc,'yo',Xa,Ya,'go',Xb,Yb,'ro', Xh,Yh,'bo',Xk_f,Yk_f,'ro');
axis([0,1300,0,1000]);
xlabel('X-axis (mm)'),ylabel('Y-axis (mm)');
grid;
hold on
plot(Xt,Yt); title('X-Y 2D projection')
hold on
plot(Xt_1,Yt_1,'k');
hold on
plot(Xt_ci,Yt_ci,'r');

%-------- 2D graphic XoZ --------
figure;
plot(Xc,Zc,'yo',Xa,Za,'go',Xb,Zb,'ro',Xh,Zh,'bo',Xk_f,Zk_f,'ro');
axis([0,1560,0,1200]);
xlabel('X-axis (mm)'),ylabel('Z-axis (mm)');
grid;
hold on
plot(Xt,Zt); title('X-Z 2D projection');
hold on
plot(Xt_1,Zt_1,'k');
hold on
plot(Xt_ci,Zt_ci,'r');

%-------- 2D graphic YoZ --------
figure;
plot(Yc,Zc,'yo',Ya,Za,'go',Yb,Zb,'ro',Yh,Zh,'bo',Yk_f,Zk_f,'ro');
axis([0,1560,0,1200]);
xlabel('Y-axis (mm)'),ylabel('Z-axis (mm)');
grid;
hold on
plot(Yt,Zt); title('Y-Z 2D projection');
hold on
plot(Yt_1,Zt_1,'k');
hold on
plot(Yt_ci,Zt_ci,'r');

%-------- 3D graphic XYZ ---------
figure;
plot3(Xc,Yc,Zc,'yo',Xa,Ya,Za,'go',Xb,Yb,Zb,'ro',Xh,Yh,Zh,'bo',Xk_f,Yk_f,Zk_f,'r+');
axis([0,1560,0,1200,0,1200]);
title('3D Simulation for door opening');
xlabel('X-axis (mm)'), ylabel('Y-axis (mm)'), zlabel('Z-axis (mm)');
grid;
hold on
plot3(Xt,Yt,Zt);
hold on
```

```
plot3(Xt_1,Yt_1,Zt_1,'k');
hold on
plot3(Xt_ci,Yt_ci,Zt_ci,'r');
%========== END ==========
save elbowdata  Phi_d T1 T2 T3 T4  %% for force control

figure;
%subplot(2,1,1),
plot(Rho_d,Phi_d,'ro-',Rho_d,T1,'ko-',Rho_d,T2,'bo-',Rho_d,T3,'go-', Rho_d,T4,'yo-');
legend('Phi','Theta1','Theta2','Theta3','Theta4');
title('Joint Angles vs Door pivot angle Rho'); grid; axis([0,ci,-100,50]);
xlabel('Door pivot angle Rho (degree)');ylabel('Phi,Theta1 and Theta2(degree)');

figure;
%subplot(2,1,2),
plot(Rho_d,dPhi,'y*-',Rho_d,dT1,'k*-',Rho_d,dT2,'b*-',Rho_d,dT3,'r*-',Rho_d,dT4,'g*-');
legend('dPhi','dT1','dT2','dT3','dT4');
title('dPhi, dT1, dT2, dT3 vs Rho'); grid; axis([0,ci,-100,50]);
xlabel('Door pivot angle Rho (degree)');ylabel('dT1,dT2,dT3(degree)');

figure;
subplot(2,1,1),plot(Rho_d,M,'r*'), title('Rho--M(Nm)');
xlabel('Rho(degree)');ylabel('Torque M(Nm)');grid;
subplot(2,1,2),plot(Rho_d,G,'ko'), title('Rho--G(N)');
xlabel('Rho(degree)');ylabel('Payload force G(N)');grid;
%subplot(3,1,3),plot(Rho_d,T1,'r-',Rho_d,T2,'k-'), title('Rho--Theta1,Theta2');
%xlabel('Rho(degree)');ylabel('T1,T2(degree)');grid;
```

```
ELbow manipulator kinematics

Forward Kinematics and Jacobian Matrix
Force control using Jacobian
By Xiaojia HE
Feb-6-2008
file name: elbow2.m
%Theta1,...,Theta6, come from inverse kinematiccs
%Input angle parameters Theta1 to Theta6
%Load Data from other inverse kinematics result

load elbowdata  %created by elbowink.m

for i=1:1:15

L0=0.620;  % Link parameters
L1=0.380;  % length of the 2nd link
L2=0.380;

% Initial Conditions or INPUT of each joint angle
Theta1=Theta1e(i)*pi/180;   %the initial position
Theta2=Theta2e(i)*pi/180;   %the sign is correct!!! Feb5 2:30pm
Theta3=Theta3e(i)*pi/180;   %the sign is correct!!!
Theta4=Theta4e(i)*pi/180;
Theta5=Theta5e(i)*pi/180;
Theta6=0;                   %for 5DOF manipulator
Ft=[0, 40, 0, 0, 0, 0]'  %For door opening Always a constant force 3kg=30N not zero
%For Ft: [1,0,0,0,0,0]' means Fx4=1,Fy4=Fz4=0,Mx4=My5=Mz5=0

TTheta1(i)=Theta1*180/pi; TTheta2(i)=Theta2*180/pi; TTheta3(i)=Theta3*180/pi;
TTheta4(i)=Theta4*180/pi; TTheta5(i)=Theta5*180/pi; TTheta6(i)=Theta6*180/pi;
% Calculation of each revoluted joint
c1=cos(Theta1);
s1=sin(Theta1);
c2=cos(Theta2);
s2=sin(Theta2);
c3=cos(Theta3);
s3=sin(Theta3);
c4=cos(Theta4);
s4=sin(Theta4);
c5=cos(Theta5);
s5=sin(Theta5);
c6=cos(Theta6);
s6=sin(Theta6);

c23=cos(Theta2+Theta3);
```

```
s23=sin(Theta2+Theta3);

%*** For orientaion matrix R and position vector P ***

    q1=c1*c4-s1*s4*c23;
    q2=s1*c5*s23+s5*(c1*s4+s1*c4*c23);
r11=c6*q1+s6*q2;      %% For Eq(39)
    q3=c1*s4+s1*c4*c23;
r12=-c5*q3+s1*s5*s23;
r13=s6*q1-c6*q2;

    q7=s1*c4+c1*s4*c23;
    q8=c1*c5*s23+s5*(-s1*s4+c1*c4*c23);
r21=c6*q7-s6*q8;
    q9=-s1*s4+c1*c4*c23;
r22=c5*q9-c1*s5*s23;
r23=s6*q7+c6*q8;

    q10=(c5*c23-c4*s5*s23);
r31=-s4*c6*s23-s6*q10;
r32=-s5*c23-c4*c5*s23;
r33=-s4*c6*s23+c6*q10;

    q11=L1*c2+L2*c23;
p1=-s1*q11;         %% For wrist centre position
p2=c1*q11;
p3=L0-L1*s2-L2*s23;
Position=[p1,p2,p3]'    % Wirst centre vector
pp1(i)=p1; pp2(i)=p2; pp3(i)=p3; %save for 3D plotting

R=[r11 r12 r13; r21 r22 r23; r31 r32 r33];  % Orientation matrix


pcap=[0 -p3 p2; p3 0 -p1; -p2 p1 0];
PcapR=pcap*R;

Adg=[r11, r12, r13, PcapR(1,1), PcapR(1,2), PcapR(1,3);
     r21, r22, r23, PcapR(2,1), PcapR(2,2), PcapR(2,3);
     r31, r32, r33, PcapR(3,1), PcapR(3,2), PcapR(3,3);
     0,  0,  0,  r11,     r12,     r13;
     0,  0,  0,  r21,     r22,     r23;
     0,  0,  0,  r31,     r32,     r33 ];

% The followings are used for verifing the inv(Adg) function
RT=R';                % Transpose
MRTpcap=-RT*pcap;     % MinusRTpcap
InvAdg=[RT(1,1), RT(1,2),RT(1,3),MRTpcap(1,1),MRTpcap(1,2),MRTpcap(1,3);
        RT(2,1), RT(2,2),RT(2,3),MRTpcap(2,1),MRTpcap(2,2),MRTpcap(2,3);
        RT(3,1), RT(3,2),RT(3,3),MRTpcap(3,1),MRTpcap(3,2),MRTpcap(3,3);
        0,     0,    0,   RT(1,1), RT(1,2),RT(1,3);
        0,     0,    0,   RT(2,1), RT(2,2),RT(2,3);
        0,     0,    0,   RT(3,1), RT(3,2),RT(3,3) ];

    %compare inv(Adg)
    %inv(Adg)       observe this result and the above InvAdg

%********** Jacobian Matrix ***********
Ksi_1=[0, 0, 0, 0, 0, 1]'; %!!! corrected
    ks21=L0*s1;
    ks22=-L1*c1;
Ksi_2=[ks21, ks22, 0, -c1, -s1, 0]';

    ks31=s1*(L0-L1*s2);
    ks32=-c1*(L0-L1*s2);
    ks33=L1*c2;
Ksi_3=[ks31, ks32, ks33, -c1, -s1, 0]';

    ks41=-c1*s23*L0+(c1*s2*s23+c1*c2*c23)*L1+c1*L2; %new correct!
    ks42=-s1*s23*L0+(s1*c2*c23+s1*s2*s23)*L1+s1*L2;
    ks43=0;
    ks44=-s1*s23;
    ks45=c1*s23;
    ks46=c23;
Ksi_4=[ks41, ks42, ks43, ks44, ks45, ks46]';

    ks51=(s1*c4+c1*s4*c23)*L0-(s1*s2*c4+c1*s2*s4*c23-c1*c2*s4*s23)*L1-s1*c4*s23*L2;
    ks52=-(c1*c4-s1*s4*c23)*L0+(c1*s2*c4-s1*s2*s4*c23+s1*c2*s4*s23)*L1+c1*c4*s23*L2;
    ks53=c2*c4*L1+c4*c23*L2;
    ks54=-c1*c4+s1*s4*c23;      % correct
    ks55=-s1*c4-c1*s4*c23;      % correct
    ks56=s4*s23;
```

```
Ksi_5=[ks51, ks52, ks53, ks54, ks55, ks56]';

    ks61=-(c1*c4*c5*c23-s1*s4*c5-c1*s5*s23)*L0-(c1*s5+s1*s4*c5*s23)*L2;
    ks61=ks61-(c1*c2*c4*c5*s23-c1*s2*c4*c5*c23+s1*s2*s4*c5+c1*c2*s5*c23+c1*s2*s5*c23)*L1;

    ks62=-(s1*c4*c5*c23+c1*s4*c5-s1*s5*s23)*L0-(s1*s5-c1*s4*c5*s23)*L2;
    ks62=ks62-(s1*c2*c4*c5*s23-s1*s2*c4*c5*c23+c1*s2*s4*c5+s1*c2*s5*c23-s1*s2*s5*s23)*L1;

    ks63=c2*s4*c5*L1+s4*c5*c23*L2;

    ks64=-c1*s4*c5-s1*c4*c5*c23+s1*s5*s23;
    ks65=-s1*s4*c5+c1*c4*c5*c23-c1*s5*s23;
    ks66=-c4*c5*s23-s5*c23;
Ksi_6=[ks61, ks62, ks63, ks64, ks65, ks66]';

Jst=[Ksi_1, Ksi_2, Ksi_3, Ksi_4, Ksi_5, Ksi_6];   %% Jacobian Matrix
Jst';

Fsg=[0, 0, -30, 0, 0, 0]'    %%Gravity Compensation 2kg=20N %% Spatial frame
    %Ft=Adg'*Fs               %% Body frame

%*********************************************************************
% Input the Ft and Verify the Fs
%Ft=[0, 1, 0, 0, 0, 0]' %[1,0,0,0,0,0]' means Fx4=1,Fy4=Fz4=0,Mx4=My5=Mz5=0

Adg_T=Adg';
InvAdg_T=inv(Adg_T);
Fs=InvAdg_T*Ft          % Verified  It's OK

    %JBst=inv(Adg)*Jst;
    %JBst2=InvAdg*Jst
    %JBst';
    %Torque=JBst'*Ft;

Fss=Fs+Fsg                      %With Gravity Compensation!!!
Torque=Jst'*Fss;                %%Torque of each joint

Tq1(i)=Torque(1);
Tq2(i)=Torque(2);
Tq3(i)=Torque(3);
Tq4(i)=Torque(4);
Tq5(i)=Torque(5);
Tq6(i)=Torque(6);
Angle(i)=i;

end

Tq1
Tq2
Tq3
Tq4
Tq5
Tq6     % used for test or verifing

figure;
plot(Angle,Tq1,'ro-',Angle,Tq2,'ko-',Angle,Tq3,'bo-',Angle,Tq4,'go-',Angle,Tq5,'yo-
',Angle,Tq6,'b*-');
legend('Torque1','Torque2','Torque3','Torque4','Torque5','Torque6');
title('Joint Torque Output'); grid; %axis([0, 15, -3,3]);
xlabel('Door pivot angle Rho (degree)');ylabel('Each joint torque(Nm)');

figure;
plot3(pp1,pp2,pp3,'*');
title('3D plot of wrist center');
grid on ;
axis square; %([0,1,-0.5,0.5,0,1]);
xlabel('p1(m)');ylabel('p2(m)');zlabel('p3(m)');

figure;
plot(Angle,TTheta1,'ro-',Angle,TTheta2,'ko-',Angle,TTheta3,'bo-',Angle,TTheta4,'go-
',Angle,TTheta5,'yo-',Angle,TTheta6,'b*-');
legend('Theta1','Theta2','Theta3','Theta4','Theta5','Theta6');
title('Joint Angle vs Door pivot angle'); grid;
xlabel('Door pivot angle Rho (degree)');ylabel('Each joint angle (degree)');
```

References

[1] C. C. Kemp, A. Edsinger, E. Torris-Jara, Challenges for Robot Manipulation in Human Environments, IEEE Robotics & Automation Magazine, March 2007, 20-29.

[2] D. Wang, A.A. Goldenberg, G. Liu, Development of Control System Architecture for Modular and Re-configurable Robot Manipulators, IEEE International Conference on Mechatronics and Automation, Harbin, China, Aug.2007, 20-25.

[3] G. Liu, S. Abdul, A. A. Goldenberg, Distributed Control of Modular and Reconfigurable Robot with Torque Sensing, Robotica, vol. 26, no. 1, 2008, 75-84.

[4] M. Adamson, G. Liu, S. Abdul, Control of Modular Robot with Parameter Estimation Using Genetic Algorithms, 2007 IEEE International Conference on Mechatronics and Automation, Harbin, China, 2007, 1-6.

[5] Z. Li, A. Ming, N. Xi, J. Gu, M. Shimojo, Development of Hybrid Joint for the Complaint Arm of Human-Symbiotic Mobile Manipulator, International Journal of Robotics & Automation, vol. 20, no. 4, 2005, 260-270.

[6] A. Ming, M. Satou, T. Kamimura, Y. Hasegawa, T. Jinnai, C. Kanamori, M. Kajitani, Automatic insertion of a long-pipe by a mobile manipulator with exchangeable active/passive joints, IEEE International Conference on Systems, Man, and Cybernetics, vol. 1, 2001, 359 – 64.

[7] Y.H. Liu, Y. Xu, M. Bergerman, Cooperation Control of Multiple Manipulators with Passive Joints, IEEE Transaction on Robotics and Automation, vol.15, Issue 2, 1999, 258 – 267.

[8] K. F. Laurin-Kovitz, J.E. Colgate, S.D.R. Carnes, Design of components for programmable passive impedance, IEEE International Conference on Robotics and Automation, vol.2, 1991, 1476-81.

[9] K. Suita, Y. Yamada, N. Tsuchida, K. Imai, H. Ikeda, N. Sugimoto, A Failure-to-safety "Kyozon" System with Simple Contact Detection and Stop Capabilities for Safe Human-autonomous Robot Coexistence, IEEE International Conference on Robotics and Automation, vol. 3, 1995, 3089 – 96.

[10] H. Iwata, H. Hoshino, T. Morita, S. Sugano, A Physical Interference Adapting Hardware System Using MIA Arm and Humanoid Surface Covers, IEEE/RSJ International Conference on Intelligent Robots and Systems, vol. 2, 1999, 1216–21.

[11] T. Morita, S. Sugano, Development of 4-DOF Manipulator Using Mechanical Impedance Adjuster, IEEE International Conference on Robotics and Automation, Volume 4, Minneapolis, Minnesota, 1996, 2902 – 07.

[12] Z. Li, A. Ming, N. Xi, M. Shimojo, M. Kajitani, Mobile Manipulator Collision Control with Hybrid Joints in Human-Robot Symbiotic Environments, IEEE/RSJ International Conference on Intelligent Robots and Systems, Sendal, Japan, 2004, 154-161.

[13] J. Luo, Z. Li, A. Ming, S. Ge, Robust Motion/Force Control of Holonomic Constrained Nonholonomic Mobile Manipulators using Hybrid Joints, the Sixth World Congress on Intelligent Control and Automation, Volume 1, Dalian, China, 2006, 408 – 412.

[14] S. Ryew, H. Choi, Double active universal joint (DAUJ): robotic joint mechanism for human-like motions, IEEE Transactions on Robotics and Automation, Volume 17, Issue 3, June 2001, 290 – 300.

[15] L. Peterson, D. Austin, D. Kragic, High-level Control of a Mobile Manipulator for Door Opening, 2000 IEEE/RSJ International Conference on Intelligent Robots and System, Volume 3, 2000, 2333–38.

[16] J. Kang, C. Hwang, G. Park, A Simple Control Method of Opening a Door with Mobile Manipulator, ICCAS, Gyeongju, Korea, 2003, 1593-97.

[17] B. Armstrong-Helouvry, P. Dupont, A Survey of Models, Analysis Tools and Compensation methods for the Control of Machines with Friction, Automatica, vol. 30, no. 7, 1994, 1083–1138.

[18] E. Papadopoulos and G. Chasparis, Analysis and Model-based Control of Servomechanisms with Friction, IEEE/RSJ International Conference on Intelligent Robots and System, Volume 3, Lausanne, Switzerland, 2002, 2109 – 14.

[19] T. Morita and S. Sugano, Development and Evaluation of Seven DOF MIA ARM, IEEE International Conference on Robotics and Automation, Volume 1, New Mexico, 1997, 462 – 467.

[20] G. Liu, Decomposition-based Friction Compensation of Mechanical Systems, Mechatronics, Volume 12, 2002, 755 – 69.

[21] G. Liu, A. A. Goldenberg, Y. Zhang, Precise Slow Motion Control of a Direct-drive Robot arm with Velocity Estimation and Friction Compensation, Mechatronics, Volume 14, 2004, 821–34.

[22] T. R. Kurfess, Robotics and Automation Handbook, CRC Press, 2005.

[23] R. M. Murray, Z. Li, S. S. Sastry, A Mathematical Introduction to Robotic Manipulation, CRC Press, 1994.

[24] H. R. Choi, S. M. Ryew, Anthropomorphic joint mechanism with two degrees of freedom, 2000 IEEE International Conference on Robotics and Automation (ICRA '00), Volume 2, April 24-28, 1525 – 1530.

[25] M. Ryew, H. R. Choi, W. K. Chung, Robotic finger mechanism with new anthropomorphic metacarpal joint, 26th Annual Conference of the IEEE Industrial Electronics Society (IECON 2000), Volume 1, 2000, 416 – 421.

[26] O. Khatib, Mobile manipulation: The robotic assistant, Journal of Robotics and Autonomous Systems, Vol.26, 1999, 175-183.

[27] O. Khatib, K. Yokoi, O. Brock, K. Chang, A. Casal, Robotics in Human Environment: Basic Autonomous Capabilities, International Journal of Robotics Research, Vol.18, No.7, July 1999, 684-696

[28] K. Nagatani and S. Yuta, Designing a behavior to open a door and to pass through a door-way using a mobile robot equipped with a manipulator, 1994 IEEE/RSJ/GI International Conference on Intelligent Robots and Systems, Volume 2, Sept.12-16, 1994, 847 – 853.

[29] K. Nagatani and S. Yuta, An experiment on opening-door-behavior by an autonomous mobile robot with a manipulator, 1995 IEEE/RSJ International Conference on Intelligent Robots and Systems, Volume 2, Aug 5-9, 1995, 45–50.

[30] K. Nagatani and S. Yuta, Designing strategy and implementation of mobile manipulator control system for opening door, 1996 IEEE International Conference on Robotics and Automation, Volume 3, April 22-28, 1996, 2828-2834.

[31] K. Nagatani and S. Yuta, Designing a behavior of a mobile robot equipped with a manipulator to open and pass through a door, Robotics and Autonomous systems, Volume 7, Issue:1-2, April, 1996.

[32] J. Ohwi, S.V. Ulyanov, K. Yamafuji, GA in continuous space and fuzzy classifier system for opening of door with manipulator of mobile robot: new benchmark of evolutionary intelligent computing, 1995 IEEE International Conference on Evolutionary Computation, Volume 1, Nov.29 - Dec.1, 1995, 251-257.

[33] G. Niemeyer, J. E. Slotine, A simple strategy for opening an unknown door, IEEE International Conference on Robotics and Automation, Volume 2, April 20-25, 1997, 1448 – 1453.

[34] U. D. Hanebeck, C. Fischer, G. Schmidt, ROMAN: a mobile robotic assistant for indoor service applications, 1997 IEEE/RSJ International Conference on Intelligent Robots and Systems (IROS'97), Volume 2, Sept 7-11, 518 – 525.

[35] L. Peterson, D. Austin, D. Kragic, DCA: A Distributed Control Architecture for Robotics, 2001 IEEE/RSJ International Conference on Intelligent Robots and Systems (IROS' 2001), Hawii, USA, Oct 29- Nov 3, 2361-2368.

[36] D. Kragic, L. Peterson, H. Christensen, Visually guided manipulation tasks, Robotics and Autonomous Systems, v 40, n 2-3, Aug 31, 2002, 193-203.

[37] B. J. W. Waarsing, M. Nuttin and H. V. Brussel, Behaviour-based mobile manipulation: the opening of a door, 1st International Workshop on Advances in Service Robotics(ASER2003), Bardolino, Italy, March 13-15, 2003, 170-175.

[38] C. Rhee, W. Chung, M. Kim, Y. Shim, H. Lee, Door opening control using the multi-fingered robotic hand for the indoor service robot, 2004 IEEE International Conference on Robotics and Automation (ICRA '04),Volume 4, April 26-May 1, 2004, 4011-4016.

[39] D. Kim, J. Kang, C. Hwang, G. Park, Mobile robot for door opening in a house, Lecture Notes in Artificial Intelligence, 596-602, Springer-Verlag, Berlin, 2004.

[40] S. Ryew, H. Choi, Double Active Universal Joint (DAUJ): Robotic Joint Mechanism for Humanlike Motions, IEEE Transactions on Robotics and Automation, Vol. 17, No. 3, June 2001, 290-300.

[41] S. Park, M. Kim, C. Lee, Mobile Robot Navigation Based on Direct Depth and Color-based Environment Modeling, 2004 IEEE International Conference on Robotics and Automation, New Orleans, LA, April 2004, 4253-4258.